An Introduction to the Digital Protection of Power Systems

By

Dr.Eng.Yesri Zaki AL-Harbawi

Ph.D. , M.Sc,B.Sc. in Electrical Engineering

WROCLAW UNIVERSITY OF TECHNOLOGY
INSTITUTE OF ELECTRICAL
POWER ENGINEERING

2013

AN INTRODUCTION TO THE DIGITAL PROTECTION OF POWER SYSTEMS

By

DR. YESRI ZAKI MOHAMMAD

Ph.D., M.Sc. in Electrical Engineering

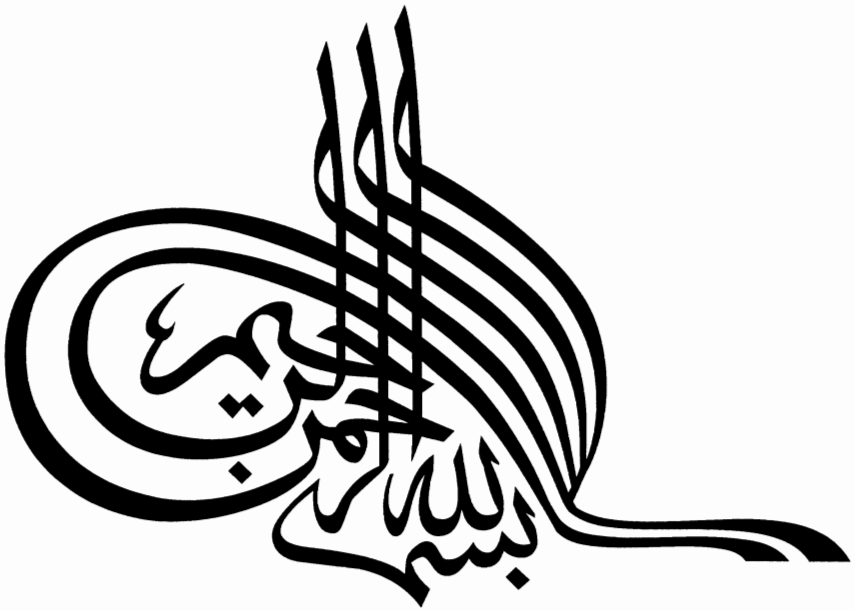

IN THE NAME OF

ALLAH

MOST GRACIOUS,M0ST MERCIFUL

Wroclaw University of Technology

Institute of Electrical Power Engineering

Wroclaw, November 5th, 2013

Dr Yesri Zaki Mahammad

I appreciate very much receiving from you the drafts of the books:

1. An Introduction to the Digital Protection of Power Systems, 162 pages
2. An Advance Course in Power System Protection, 5 lectures.

After careful studying of them I would like to say that those are very good materials which are suitable for use by our students studying at the M.Sc. specialisations: Control in Electrical Power Engineering and Renewable Energy Systems. The teachers in our Institute including myself will recommend this two drafts as the literature for the courses: Power System Protection, Digital Signal Processing for Power System Protection, Power System Faults and M.Sc. theses related to those subjects. Therefore those two drafts will be sent to our Faculty Library to be available for all interested students. Also I will appreciate receiving from you the pdf files of the books to include them on the web sites with materials for students.

Thank you very much for nice and fruitful cooperation.

Yours sincerely

DYREKTOR INSTYTUTU
Prof. dr hab. inż. Jan IŻYKOWSKI

Prof. dr. Jan Iżykowski
Director of Institute of Electrical Power Engineering
Wroclaw University of Technology
Wroclaw, Poland
e-mail: jan.izykowski@pwr.wroc.pl

Postal address:

Wybrzeze Wyspiańskiego 27
50-370 Wrocław
POLAND

Building: D-20

Tel: 0-71 3202655
Tel/fax: 0-71 3202656

Email: Inst.Energ@pwr.wroc.pl
Http://www.ie.pwr.wroc.pl

CONTENTS

PREFACE

The applications of digital techniques in power system protection have been established in 1969, and since then, those applications have been received accelerating interest. The growing abilities of the digital computers and hence the digital relays, make them to be more powerful and cheaper than the analog relays. The advance development in hardware engineering has been followed by a rapid protection engineering studies to create new digital protection algorithms. The main goal of these studies is to reduce the operation time, and to increase both security and selectivity of the proposed algorithms.

Digital protection developments have been published in scientific and technical literatures, such as the proceedings of transactions, the proceedings of conferences, the publications of the various manufacturers, and in a limited number of books in this field. Any researcher or professional engineer, who is interesting in studying a special problem in the digital protection field, finds himself surrounded by many references that he has to dive in.

Therefore, books which can be regarded as an adequate introduction to the digital power system protection, become more than necessary. I was thinking in this book to include most of what a student, a researcher, or an engineer needs to go deeper in this field. It was difficult task but I found it important. Thank God, this book comes true, and it can be developed in the future. In a world becomes day by day more digitally, I have the wish that through this book, I have been giving a hand to those who start the first step.

Dr. Yesri Zaki Mohammad

CHAPTER ONE

INTRODUCTION

In the recent years, there has been considerable interest in the area of using digital techniques in power systems protection. The main features which have encouraged many researchers to investigate the feasibility of designing digital relays for power system protection are its economy, reliability, flexibility, improved performance over conventional relays and the possibility of integrating a digital relay into the hierarchical computer system. In this chapter those features are illustrated and the advantages of using digital techniques are pointed.

1-1:DIGITAL AGAINST ANALOG PROCESSING TECHNIQUES

It is necessary to recall some basic differences between digital technique and the well-known electromechanical and static analog technique, in order to understand the characteristics and the related possibilities of microprocessor-based (digital) protection. A digital relay is understood as an equipment that contains a microcomputer or microprocessor to detect a fault condition in the electrical apparatuses.

The main difference between digital and analog relays will be clearer by studying the following features;

1. Filtering
2. Stability
3. Memorizing
4. Functionality
5. Algorithms
6. Man-Machine Communication (MMC)
7. Communication
8. Self-monitoring and Self-diagnosis

1- FILTERING

In electromechanical relay, inherent filtering takes place due to the mass and corresponding inertia involved. An example is when the

restraint torque is proportional to the harmonic signal components and noise. A certain degree of adaptability can also be observed. If the measuring quantity is close to the set value, the measuring time automatically increases.

In static relays with analog signal processing, filtering is performed with passive and/or active electronic circuits. Furthermore, some natural filtering occurs due to the limited bandwidth of the electronic circuits.

Filtering in a microprocessor- based relay takes place first in the analog to digital (A/D) converter part. Band limiting is performed by analog means in order to prevent aliasing (i.e., more details will be in section 2-2). Anyhow, additional filtering with numerical techniques is quite complex and requires a substantial processing capability.

In digital filtering, inputs and outputs are quantitised and the system function (i.e. transfer or filter function) is realized numerically. The basic elements of such a filter are delays (i.e. sample intervals), constant multipliers and summers. When a filter is only dependent on inputs and not on previous outputs, it is called non-recursive filter. Non-recursive filter circuit diagram is shown in figure (1-1).

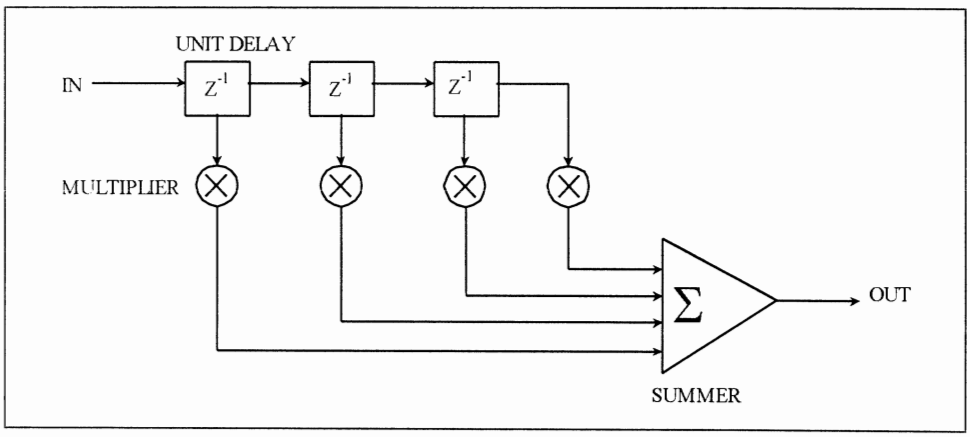

Figure 1- 1: NON-RECURSIVE DIGITAL FILTER

The transfer equation of the non-recursive filter may be expressed as;

$$Y(n) = \sum_{k=0}^{\infty} a_k x(n-k) \quad \text{..... (1-1)}$$

which states that the present output sample Y(n) is found by the summation of the input samples x(n-k) scaled with a factor a(k).

Recursive filters have a certain feedback from the output to the input. A recursive filter circuit diagram is shown in figure(1-2).

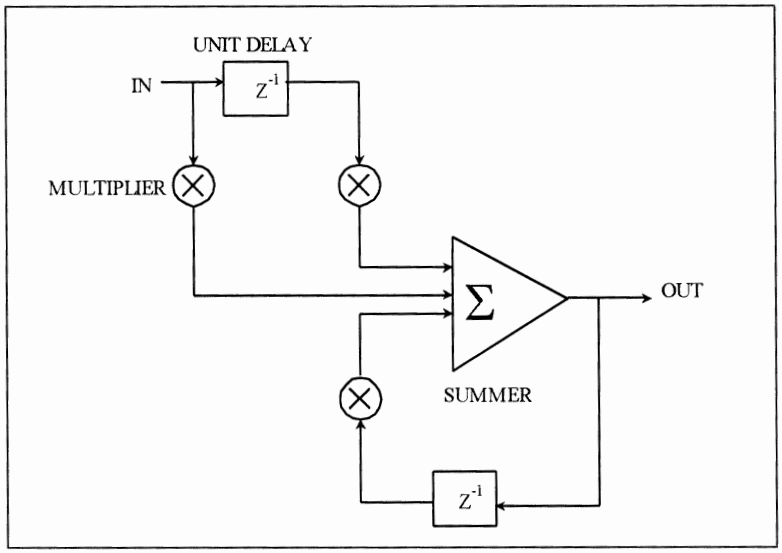

Figure 1-2 : RECURSIVE DIGITAL FILTERS

The transfer equation of the recursive filter may be expressed as;

$$Y(n) = \sum_{k=0}^{\infty} a_k x(n-k) + \sum_{k=1}^{\infty} b_k y(n-k) \qquad \text{..... (1-2)}$$

which states that the present output sample Y(n) is found by the summation of the input samples x(n-k) scaled with a factor a(k) then adding them to the summation of the output samples y(n-k) scaled with a factor b(k).

Digital filters can process signals with an accuracy and stability that is difficult to achieve with an analog device. Simply changing some scaling and/or summing coefficients may change the filter characteristics.

2- **STABILITY**

The electromechanical or static electronic relays are by nature not stable in the long term. Mechanical friction, wear and/or component

degradation, temperature and humidity, etc. eventually affect the accuracy and the performance of the equipment.

In digital relays, far fewer components are influenced by environmental factors. Due to the high accuracy found in digital signal processing, the performance is constant as long as a certain level of degradation is not exceeded. Practically, using modern methods and automatic calibration, all these effects can be eliminated.

3- **MEMORIZING**

It is too difficult and an expensive task to store data over a long time with analog means. The same is true with respect to transmitting analog data to distant locations. Great efforts are necessary to ensure an acceptable degree of noise immunity and accuracy.

Using digital techniques, storing data over long periods of time is possible. Transmitting such data to various users is simple and can be afforded at moderate cost. Utilizing optical fibers and efficient transmission protocols, excellent security and accuracy can be achieved even at high data transfer rates.

4- **FUNCTIONALITY**

The function of a device using analog techniques is governed by the hardware design. Only minor changes of is characteristics are possible with adjustments or settings.

With digital techniques, very different functions can be realized with the same hardware. The functionality of digital devices is mainly determined by software and processing power. *It is important to mention that the functionality itself can be changed as a function of the System State or as a function of results from previous calculations or even on a command received from some remote station.*

5- **ALGORITHMS**

Talking about relaying, the term *algorithm* refers mainly to measuring. For conventional analog relays, this task is performed with different means. The simplest are single input relays (i.e.; detectors). For multiple input relays, the signal processing quit often requires vector operation. In static relays, the corresponding analog signals are changed to binary sequences. Phase comparators then carry out the vectorial computation and allow different characteristics to be realized.

In digital protection relays, complex measuring function can be executed. Digital algorithms can be extracted with the aid of well-known filtering techniques. Digital techniques requires a substantial processing power, since high resolution and time consuming operations (i.e.; multiplication, division, square roots, etc.) are to be performed.

It has to be mentioned that there is no ideal or perfect algorithm. Each approach has its merits and limitations. A good design of an algorithm when it meets the desired protection function under all possible fault or healthy conditions.

6- MAN-MACHINE COMMUNICATION (MMC)

The MMC elements for electromechanical and static relays are simple and direct. They could be pointers, knobs, or labels, ... etc.

In digital techniques, MMC based on a dialog between the user and the protection equipment.

7- COMMUNICATION

Analog techniques offered very limited communications. Usually only on/off informations from contacts are available. Information regarding settings or events must be obtained on site.

Digital techniques carry out communication tasks, which are necessary to match protection and control activities.

8- SELF-MONITORING AND SELF-DIAGNOSIS

Self-monitoring and self-diagnosis are features which are very difficult and expensive to fulfill in analog equipment. With microprocessor-based equipment, those tasks are easy to achieve. A certain processing time can periodically be assigned to perform selected checks and verifications. Results can be viewed, stored, and compared with previous results. Any abnormal detected results can initiate corrective algorithms or restrain certain functions or the whole equipment.

With Self-monitoring and self-diagnosis the following tasks can possibly utilized;

- Initialization after start-up
- Memory checks (RAM, ROM, read, write, etc.)
- A/D converter and multiplexer supervision.

- Supply voltage supervision.
- Verification of the setting values before issuing a trip command.
- Man-Machine display and operation.
- Programs execution with supervision.

1-2: ADVANTAGES OF USING DIGITAL TECHNIQUES IN POWER SYSTEMS PROTECTION

1- IMPROVED PERFORMANCE

Relay performances can be seen from different perspectives. Some of these important aspects are;

- More complex and hence improved signal processing.
- Higher selectivity and accuracy leading.
- Improved security and availability through self-monitoring.
- Shorter response time.
- Faster and more accurate localization of faults.
- Greater flexibility due to the fact that functionality is determined by software rather than hardware.
- Less different parts simplified maintenance and spare parts management.

2- LONG-TERM STABILITY

Long-term stability of the equipment influences maintenance and routine testing and therefore strongly reduces the total lifetime cost for that equipment. Digital protection and control systems offer the following advantages;

- No, or only very few adjustment points within the equipment.
- Performance largely unaffected by component aging.
- Possibility of automatic calibration and adjustment.
- Abnormality can be detected by self-monitoring, reducing risk for malfunction.
- Higher availability.

4- SECURITY AND AVAILABILITY

Protection relays based digital techniques can fully utilize Self-monitoring and self-diagnosis elements with approximately 5-10 % of

the processing power. As a gain, both the availability and security are increased at the same time.

The availability increases as all major functional units are tested periodically and in short intervals. Those intervals are usually milliseconds versus 1 to 2 years when testing manually. Owing to the comprehensive diagnosis possible, faulty parts are identified and are replaced conveniently with little effort. Consequently, the availability of the protection equipment increases considerably. With self-monitoring and self-diagnosis, security is improved as abnormal doing is detected and blocked automatically. In addition, digital relay components and interconnections failures can be detected soon after the occurrence, and could be repaired before the have a chance to misoperate. However, software has to be designed to ensure reliability and security.

In analog schemes, security is improved by series connection of protections at the cost of availability. On the other hand, availability may be increased with protection in parallel, but only at the cost of security.

5- SUPPLEMENTARY AND/OR ASSOCIATED FUNCTIONS

One of the important aspects of the supplementary and/or associated functions is communication. It is to simplify monitoring the entire system and to utilize stored information and capabilities.

In case of disturbance, fault location and trouble shooting can be simplified much easier and in a shorter time if information about the operation of the individual protection and control devices is available in time. This reduces the down time of the power system and improves availability. With bi-directional communication, settings may be read out or new settings may be entered. Furthermore, the status of each relay may be monitored. Stored data and sequences of events may be transferred to a control room for analysis and printout. Other supplementary functions such as circuit supervision load monitoring, metering... etc. are only a matter of available processing power and memory space.

6- COST

All other things being equal, the cost of a relay is the main consideration in its acceptability. Over the years, the cost of digital computers has steadily declined, at the same time their computational power has increased substantially. The cost of the analog relays has steadily increased over the same period mainly because of some design improvements. It is estimated that the cost of the most sophisticate digital relays with all its abilities and features including software costs, would be the same as that of analog relay or even cheaper.

REFERENCES

(1.1) O. LANZ and B. LUNDAUIST " THE APPLICATION OF NUMERICAL TECHNIQUES IN PROTECTION AND STATION CONTROL SYSTEMS", ABB LECTURE No. L000-934E-1, MAY, 1989.

(1.2) "COMPUTER-AIDED RELAY PROTECTION COORDINATION", EPRI, EL-6145, PROJECT 2444-2, FINAL REPORT, DEC. 1988.

(1.3) "DIGITAL PROTECTION TECHNIQUES AND SUBSTATION FUNCTIONS", REPORT BY WORKING GROUP 34.01 OF STUDY COMMITTEE 34, CIGRE`, 16 MAY, 1989.

(1.4) E. A. UDREN and M. SACKIN, " RELAYING FEATURES OF AN INTEGRATED MICROPROCESSOR-BASED SUBSTATION CONTROL AND PROTECTION SYSTEM", IEE CONFERENCE PUBLICATIONS, No.185, LONDON 1980.

CHAPTER TWO

STRUCTURE AND OPERATION OF THE DIGITAL PROTECTION SYSTEM

2-1: DIGITAL RELAY STRUCTURE

Digital relays consist of subsystems with well-defined functions. The block diagram in figure (2-1) shows the principle subsystems of a digital relay.

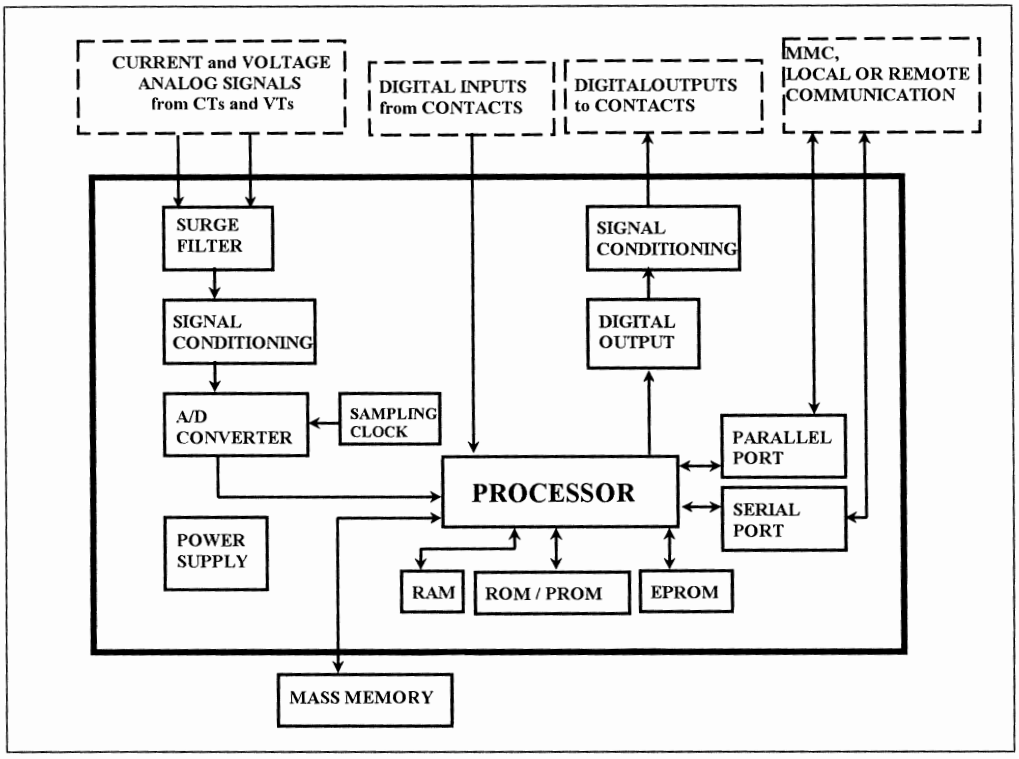

Figure 2- 1: Digital relay structure.

The *processor* is the main brain of the organization. It is responsible for the execution of relay programs, maintenance of various timing functions, and communicating with its outer equipment.

The scheme consists of several types of *memories* each of them serves a specific need. The Random Access Memory (RAM) holds the input sample data as they are brought in and processed. It may also be

used to buffer data for later storage in a more permanent medium. In addition, RAM is needed as a scratch pad to be used during relay algorithm execution.

The Read Only Memory (ROM) or Programmable Read Only Memory (PROM) is used to store the programs permanently. In some cases, the programs may execute directly from the ROM if its read time is short enough. Otherwise, the programs must be copied from the ROM into the RAM during an initialization stage, and then the real-time execution would take place from the RAM.

The Erasable PROM (EPROM) is needed for storing certain parameters (such as relay settings) which may be changed from time to time, but once set must remain fixed even if the power supply to the computer is interrupted. Either a core type memory or an on board battery backed RAM may be suitable for this function.

A large capacity EPROM is likely to become a desirable feature of a computer relay. Such a memory would be useful as an archival data storage medium, for storing data tables of related faults, event logs, and checking trails of investigations and setting changes made in the relay. The main consideration her is the cost of such a memory. If it becomes sufficiently low, it could be used as a container of such data until they can be sent to remote and more permanent data storing facility.

The *relay inputs* are analog current and voltage signals or digital signals indicating contacts status. It is common to use conventional current and voltage transformers (i.e.; CTs and VTs). If electronic CTs and CVTs are used, the input circuits may be mainly different and data are to be entered directly in processor memory. The analog signals have to be converted to voltage signals suitable for conversion into digital form.

The current inputs must be converted to voltages by resistive shunts to produce the desire voltage for the *Analog to Digital Converters* (A/D`s). An alternative arrangement would be to use an auxiliary current transformer to reduce the current to a lower level. However, any inaccuracies in the auxiliary current transformer would contribute to the total error of conversion process, and must be kept as low as possible. The auxiliary CT also provides electrical isolation between the main CT secondary and the computer inputs system. In this case, the shunt may be grounded at its midpoint in order to provide a balanced input. These considerations are illustrated in figure (2-2).

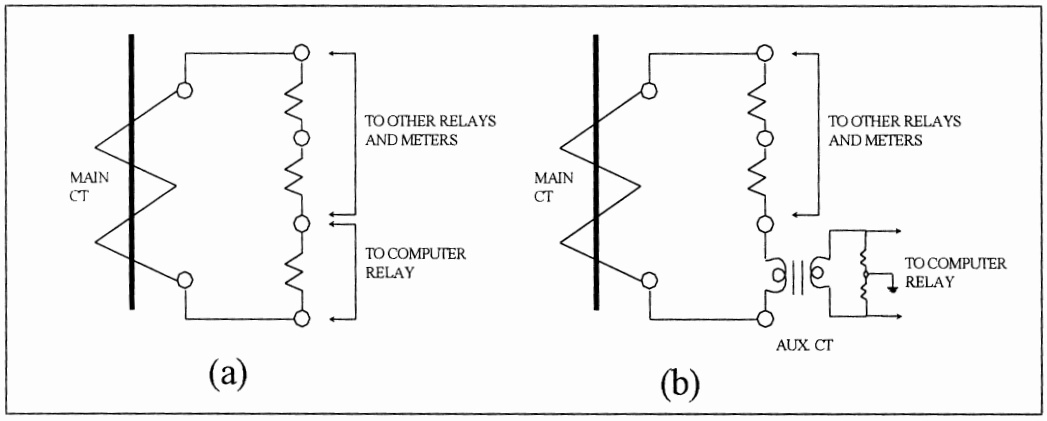

Figure 2- 2: Scaling of current signals for input to digital relays. (a) direct connection in the main CT secondary. (b) Use of auxiliasry CT.

Figure (2-3) shows connections to the voltage transformer. A fused circuit is provided for each instrument or relay, and a similar circuit may be provided for the computer relay as well. The normal voltage at the secondary of a voltage transformer can be reduced to desired level by a resistive potential divider sized to provide adequate source impedance to drive the following stages of a filters and amplifiers. Although an auxiliary voltage transformer may be used in this case to provide additional isolation, it is not a necessity.

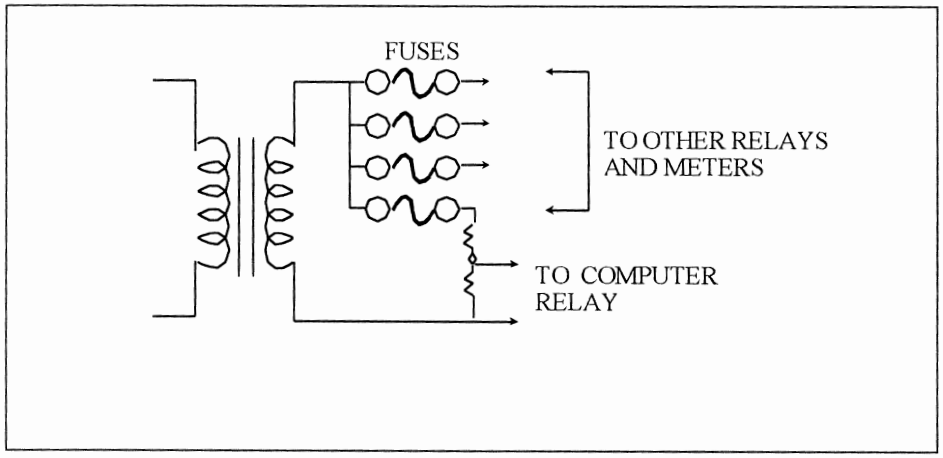

Figure 2- 3: Scaling of voltage signals for input to digital relays by potential divider.

Conversion of signals into digital form is done by the *Analog to Digital Converter* (A/D). The current and voltage signals (i.e., which are obtained from current and voltage transformer secondary windings) must be *conditioned* accordingly. The largest possible signal levels must be anticipated, and the relation between the root mean square value of the signal and its peak must be considered. In most cases, the high frequency transient components of the signal are removed by *anti-aliasing* filters, which have a low cut-off frequency. The anti-aliasing filters are low-pass analog filters designed to suit a specific choice of sampling rate used. The sampling instants are determined by the *sampling clock*, which must produce pulses at a fixed rate. At each instant defined by the clock, a conversion from the instantaneous value of an analog input signal to a digital form is performed by the A/D, and made available to the processor. More details about signal conditioning and conversion will be discussed later.

Suppression of surges from wiring connected to any protection system is done by *surge filters*. High voltage and high-energy content surges are merged into the wiring that connects current, voltage, and digital inputs to the protection system. The surges are created by faults and switching operations on the power system, or by certain types of switching operations within the control house. For example, sparking contacts in inductive protection and control circuits within the control house have been found to be a source of very serious disturbances. Suppression of these surges requires very careful grounding and shielding of leads and equipment, as well as low-pass filtering. Surge filters are necessary for input and output wiring, as well as for the power supply leads.

The *power supply* is usually a single dc input multiple dc output converter powered by the station battery. The output is generally 5 volts dc to power the logic circuits, and ±15 volts for the analog circuits.

2-2: ANTI-ALIASING FILTERS

Input analog signals contain not only fundamental and dc components, but also higher frequency and oscillatory unwanted components which affect the accuracy of digital relays operation. By means of low-pass analog filtering, unwanted oscillatory components

can be omitted. This preferred done by analog and not by digital filter because the high frequency of the oscillatory components bring incorrect doing to the digital filtering. Those filters are called the anti-aliasing filters. They are so designed to suit a specific choice of sampling rate used. The cut-off frequency (f_c) of the anti-aliasing filters is less than or equal to one half the sampling frequency (f_s) used by the A/D;

$$fc \leq \frac{1}{2} fs \qquad \text{..... (2- 1)}$$

An ideal anti-aliasing filter characteristic is shown in figure (2-4). The practical characteristic of the filter is shown too.

Anti-aliasing filters could be passive, consisting of resistors and capacitors exclusively, or active ones utilizing operational amplifiers. As some buffering between the filters and the A/D is generally necessary, an operational amplifier is needed in any case, and one could use the active filter design, which leads to smaller component sizes. The transfer function for the filter in any case is determined from considerations of sharpness of cut-off in the stop band, and the transient response of the filter.

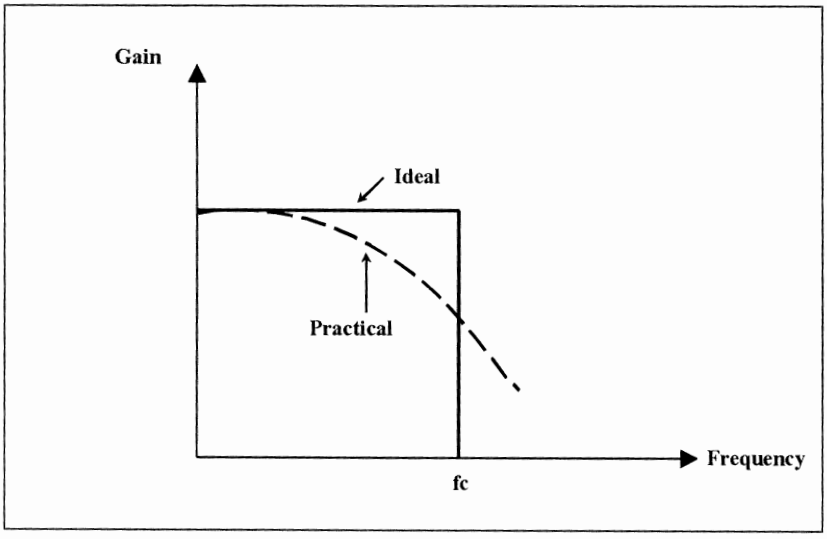

Figure 2- 4: Ideal and practical characteristics of the anti-aliasing filter.

In general, if filters with very sharp cut-off are employed, they produce longer time delays in their step function response. In most applications of digital relaying, two-stage RC filters are found to

provide an acceptable compromise between sharpness of the cut-off characteristic in the stop band, and the time delay in their step input response.

Two-stage RC filters are quite popular because of their simplicity, passive components, and a reasonable frequency response. Their main drawback is that they produce a rounded characteristic at the beginning of the stop band. A two-stage RC filter achieves a 12 dB per octave attenuation rate when it is well into its stop band (i.e., which is rather high). In fact, this is a property of second order filters. Figure (2-5) shows the circuit diagram of a two-stage RC filter. The transfer function of a two-stage RC filter is given by;

$$H(j\omega) = \frac{1}{1 + j\,\omega\,(R_1C_1 + R_2C_2 + R_1C_2) - \omega^2(R_1C_1R_2C_2)} \qquad \text{.....(2- 2)}$$

The gain of the filter (i.e., G(ω)) is obtained by taking the magnitude of H(ω);

$$G(\omega) \equiv \left|H(\omega)\right| =$$

$$= \sqrt{\frac{1}{\left\{1 - \omega^2(R_1C_1R_2C_2)\right\}^2 + \omega^2(R_1C_1 + R_2C_2 + R_1C_2)^2}} \qquad \text{.....(2- 3)}$$

The phase shift of the filter is obtained by taking the phase angle of H(ω);

$$F(\omega) \equiv \angle H(\omega) = -\arctan\left[\frac{\omega\,(R_1C_1 + R_2C_2 + R_1C_2)}{1 - \omega^2(R_1C_1R_2C_2)}\right] \qquad \text{.....(2- 4)}$$

where; R1,C1,R2 and C2 are the components of the two-stage filter.

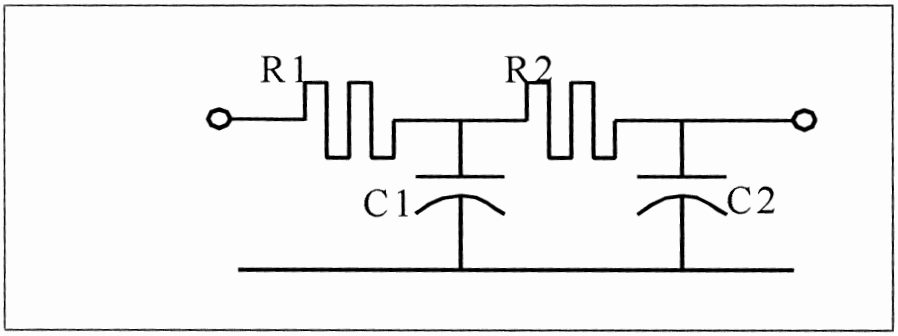

Figure 2- 5: Two-stage RC filter circuit diagram

As an example, the design of a two-stage RC filter suitable for sampling process, as that of figure (2-5), will be considered. For a 50 Hz power system and a sampling rate (f_s) of 600 Hz, the filter must be of cut-off frequency (f_c) of 300 Hz. A dc gain of unity is specified to make either an active or a passive design possible. The filter can naturally be designed to provide any other reasonable gain. Filter components are selected to provide the necessary attenuation at a desired cut-off frequency. Figure (2-6) shows the frequency response and step wave response of the desired filter calculated using equations (2-3) and (2-4) [2.1].

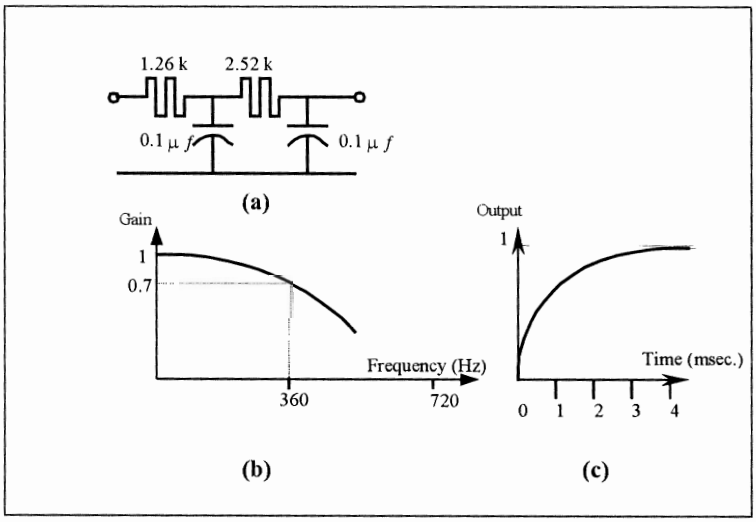

Figure 2- 6: Two-stage RC filter with cut-off frequency of 360 Hz. (a) Circuit diagram. (b) Frequency response. (c) Step-wave input response.

As can be seen, the step wave response is reasonable, producing an essential correct output in about 0.8 msec after application of the step wave. The phase lag at the fundamental power frequency (i.e., 50Hz) is

about 9 degrees, which corresponds to a time delay of about 0.5 msec. which represents about 2.5% of the cycle period (i.e., which is 20 msec.). For a sampling frequency of 600 (i.e., 12 samples per a cycle), the phase lag is about which corresponds to a time delay of about 0.342msec. which represents about 20% of the sampling cycle period (i.e., which is about 1.67 msec.).

2-3 : INPUT SIGNALS SAMPLING

The sampling and hold (S/H) divices are used to sample the analog input signals (i.e., currents or voltages). Each sample is measured at instant defined by a clock. Number of samples per a cycle is determined by the sampling frequency. Figure (2-7) illustrates simply the sampling process.

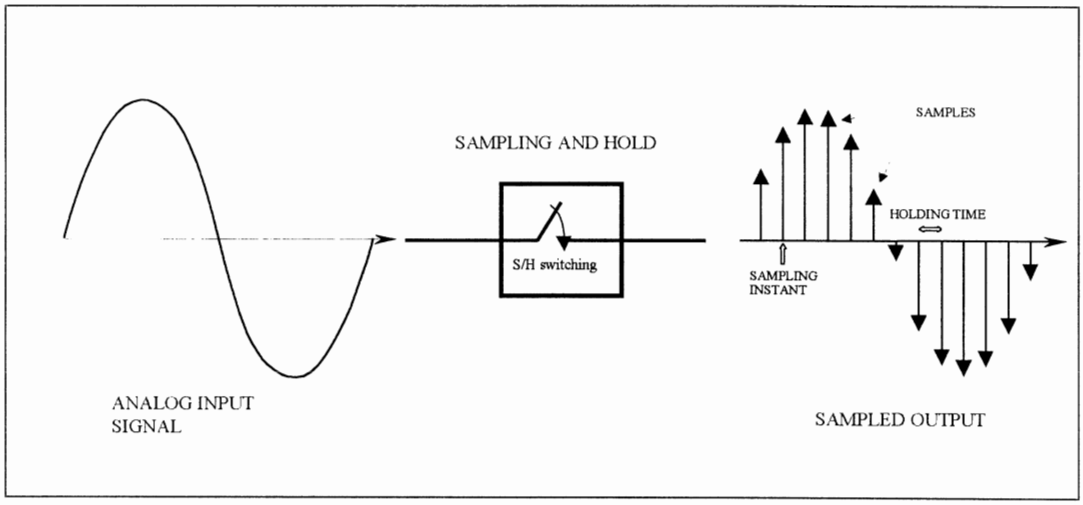

Figure 2- 7: Sampling an analog signal.

The digital relay in general requires several inputs, several conversions are performed at each sampling instant. It is desirable that all signal samples be extant at the same time. Figure(2-8) shows the alternative schemes to achieve this requirement. The first alternative employs multiplexed inputs. The high speed multiplexer, and at each instant of the sampling clock, permits one of the input signal at each multiplexing instant to be transferred to the A/D converter. It needs conversion and transmission to the processor of each sample to be very fast. In the second alternative, S/H is added to each channel. This

requires that all signals be sampled and held at the same instant for processing by a relatively slow conversion and transmission cycle for each sample. Both those alternatives are multiplexed analog input systems. The third alternative is to use individual S/H and A/D for each input channel. Although this option is technically feasible, it is not much favored because it is expensive. In general, trends in the A/D development seem to point to use high speed multiplexing without sampling and hold circuits (i.e., shown in figure (2-8) (a)), to be the preferred system.

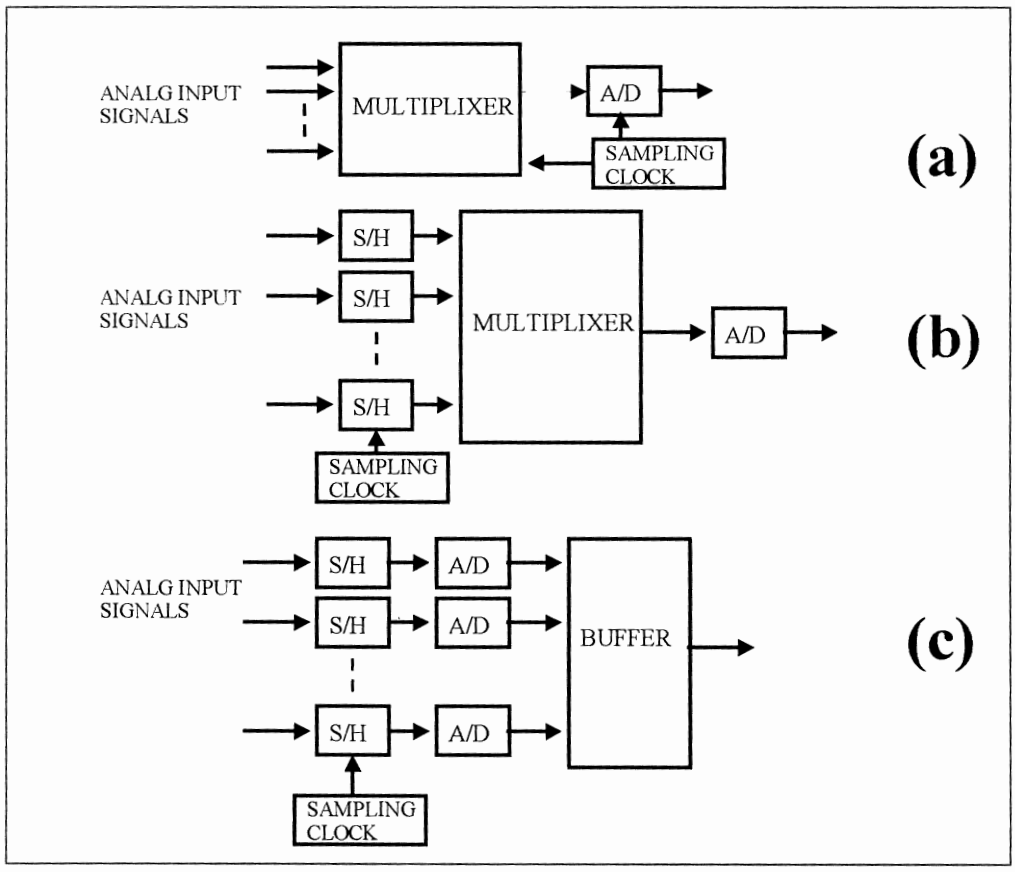

Figure 2-8: Signal sampling process and its schemes. (a) single S/H with multiplexed input. (b) S/H added to each channel. (c) Separate A/D for each channel.

Digital relay functions requires simultaneous (i.e., parallel) measurement of two or more phasor quantities. The reference for these phasors is determined by the instant at which a sample is obtained. Thus, if the phasors for signals x(t) and y(t) are computed from their

samples beginning at instants t_x and t_y, the reference for the two phasors will differ from each other by an angle θ (in radians), where;

$$\theta = (t_x - t_y)\frac{2\pi}{T} \quad \text{.....(2- 5)}$$

where 1/T is the fundamental frequency component of the signal. If the difference between (t_x) and (t_y) is known, then the phase angle between the two reference is also known, and the two phasors could always be put on a common reference by compensating θ . It would thus appear that simultaneous sampling of various input signals is not necessary, as long as the difference between them is known and compensated for.

Obviously, all computations become much simpler if θ is zero and no compensation is needed. Furthermore, samples of different signals could be combined directly. To be able to combine the samples directly, it is necessary to take the samples of the different signals simultaneously (i.e. at the same time). This fact has led to the general *simultaneous sampling* of all input signals by each digital relay.

Consider the sampling scheme shown in figure (2-8-a), in the absence of S/H circuits, the different signal samples are obtained sequentially and they are not truly simultaneous. With a 50 Hz power system frequency, one period of wave is 20 msec. This corresponds to 18 degree per msec. Thus if the entire sampling scan (i.e., by the multiplexer) can be completed in about 10 μsec, the worst error created by sequential sampling amounts to 0.18 degree, which is a negligible amount of error in any digital relaying application. In general, the frequency of conversion of the multiplexer (i.e., f_{mul}) must be much higher than the sampling frequency (f_s);

$$f_{mul} \geq K \times M \times f_s \quad \text{.....(2- 6)}$$

where, (K) is the number of input signals, and (M) is an increasing factor to assure the accuracy (i.e., M could be in the range 2 to 4). In fact, a high speed multiplexing of 10-50 μsec provides a good measure for describing any sequential data samples as being simultaneous. Of course, there are benefits to be gained by simultaneously sampling all the quantities within a station as well at all the stations within the system. This is called *sampling clock synchronization*.

Applying sampling clock synchronization in an integrated protection system means that all sampling of voltages and currents would be synchronized. This has the advantage of allowing data sharing between modules in a backup mode. Another advantage is that all the phasors computed in the integrated protection system would be on a common reference.

The obvious extension of these ideas is to synchronize sampling through the whole system. The required accuracy of synchronization can be determined by observing that with a 50 Hz power system frequency, one period of wave is 20 msec. This corresponds to 18 degree per msec. Thus, a timing error of 1μ sec. corresponds to an angular error of .018 degree. It would seem that sampling accuracy in about 1 to 10 μsec would be acceptable for almost all applications. The other important factors that determine the choice of a synchronized sampling system are the cost and uninterrupted operation of the system over a long time span. In general, satellite and radio broadcasting systems and fiber optic link based systems, are the main communication systems used to achieve the synchronize sampling through the whole power system.

2-4: ANALOG TO DIGITAL CONVERSION

The analog to digital converter (A/D) converts an analog voltage level to its digital representation. What is basically needed is a device that converts a dc signal to a binary number (i.e., a number which its word length expressed in bits), proportional to the dc level of the signal.

The word length of the A/D affects its ability to represent the analog signal with a sufficiently detailed digital representation. Suppose an A/D with 12-bit word length. The largest possible positive number that can be represented by a 12 bit A/D is 0111 1111 1111, while the smallest negative number is 1000 0000 0000, which can be represented in decimal notation as ;

$$011111111111 \equiv 2^{11} - 1 = 2047$$

$$000\,0000\,0000 \equiv -2^{11} = -2048$$

The first left bit represent the sign. The number is positive when it is 0, but it is a negative when the bit is equal to 1.

Considering that the analog input signal may be in the range of +10 to -10 volts, it is clear that each bit of the 12-bit word represents 10/2048 volts or 4.883 millivolts. That is we get a number 0 for 0 to 4.883 millivolt input voltage, a number 1 for 4.883 to 9.766 millivolt input voltage,.. etc. (i.e., notice that output digital number is corresponds to the center of the interval). Figure (2-9) illustrates the input voltages and their corresponding converted values in decimal.

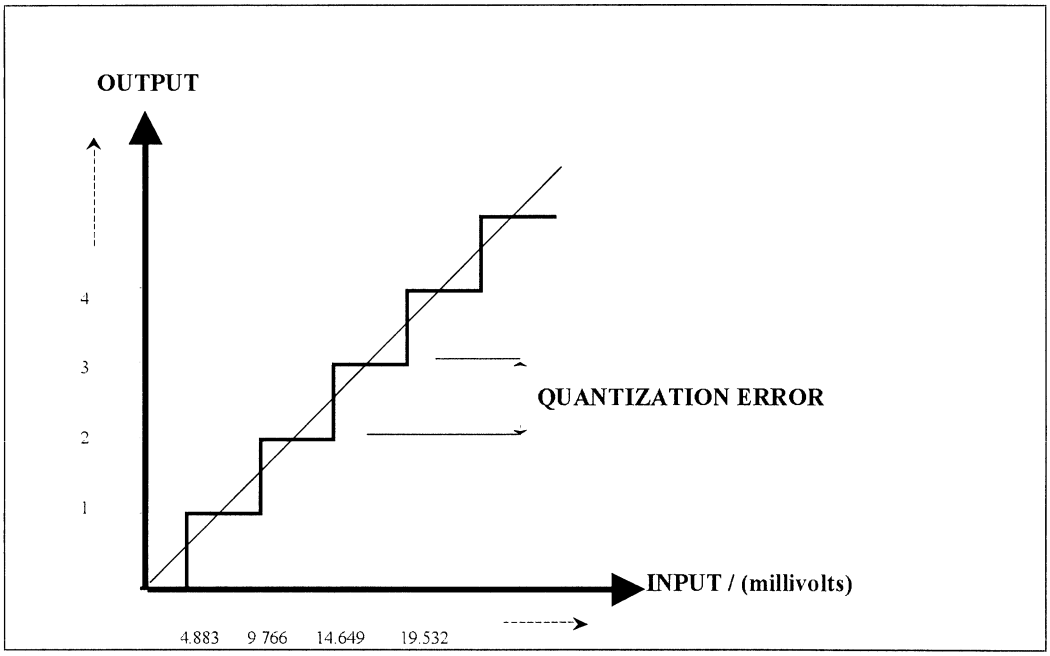

Figure 2- 9: Output of 12 bit A/D converter in decimal numbers. Input signal is of range +10 to -10 volt.

The equivalent input change for one digit change in the output (i.e., 4.883 millivolts in this case), is an important parameter of the A/D. It describes the uncertainty in the input signal for a given digital output. Thus, an output of decimal 2 represents any input voltage between 4.883 and 9.766 millivolts. This is *the quantization error* of the A/D (i.e., see figure 2-9). In general, if the word length of the A/D is N bits, and the maximum input voltage for the A/D is V volts, the quantization error (q) is given by;

$$q = \frac{V}{2 \times 2^{N-1}} = 2^{-N} V \quad \text{.....(2- 7)}$$

and normalized to the largest possible input voltage of V, the per unit quantization error is;

$$\text{per unit } q = 2^{-N} \quad \text{.....(2- 8)}$$

It is clear that the larger the number of bits in a converter word, the smaller is quantization error.

Besides the quantization error, there are other errors as well. In order to understand the source of these errors, it is well to examine the principle of operation of A/D. Detailed information about A/D types and their design can be found in the literature. One type of the A/D shown in figure (2-10) will be considered here as an example.

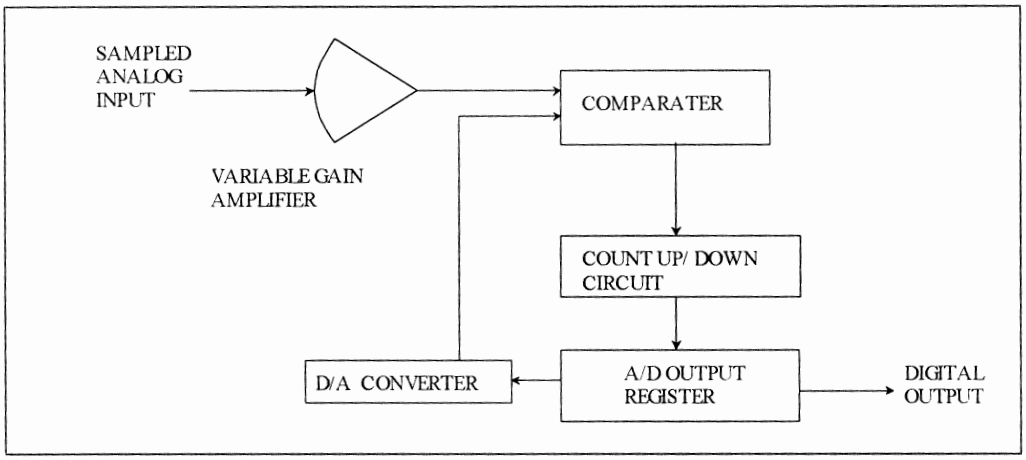

Figure 2- 10: Typical model of A/D converter.

In this considered A/D converter, the analog signal is amplified through an adjustable gain amplifier. A digital to analog converter (D/A) converts the digital number in the output register of the A/D to an analog value. This signal is compared with the input analog signal, and the difference is used to derive up the count in the A/D output

register. When the output of the A/D is within the quantization range of the analog input, the output is stable, and is the converted value of the analog signal.

The amplifier is a source of error in the A/D converter. It may have a dc *offset error* as well as a *gain error*. In addition, the gain may have a *non-linearity* as well. The combined effect of all A/D converter errors is illustrated in figure (2-11). The offset error produces a shift in the input-output characteristic, whereas the gain error produces a change in the slope.

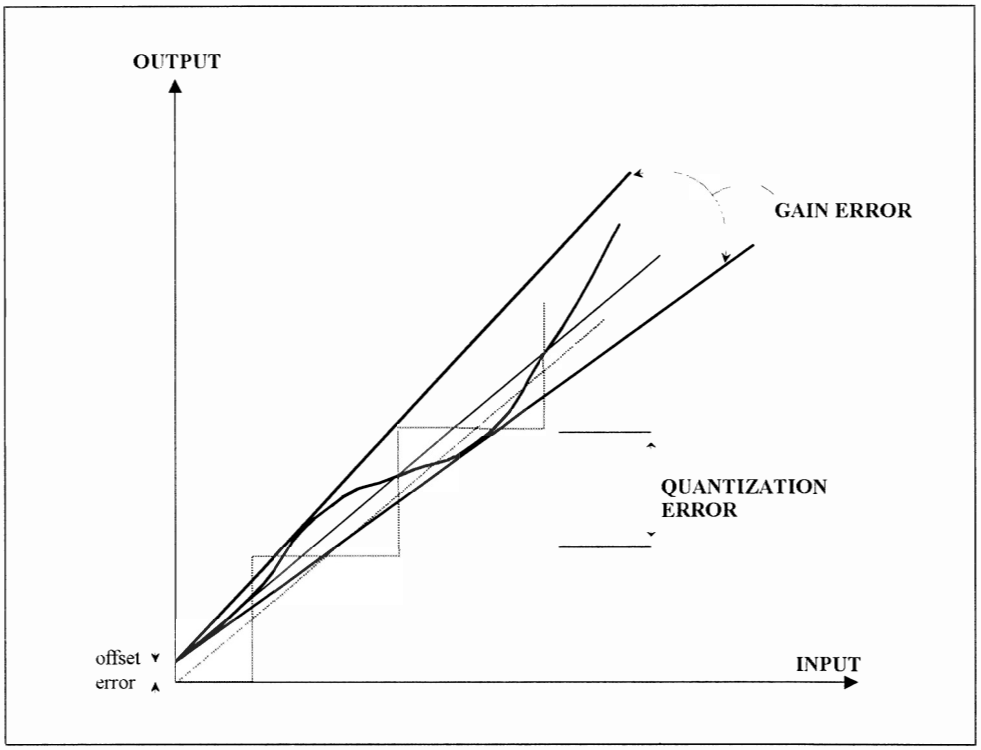

Figure 2-11: The effect of gain error, gain non-linearity, and quantization on total error of the A/D. The dashed characteristic is the optimum case.

The non-linearity produces a band of uncertainty in the input - output relationship. If the gain error and the non-linearity error are bounded by two straight lines as shown in figure (2-11), the total error in the A/D for a given voltage input V is given by ε_V;

$$\varepsilon_V = K_1 \times V_{FS} + K_2 \times V \quad \text{.....(2- 9)}$$

where, V_{FS} is the full-scale value of the input voltage, K_1 and K_2 are constants depending upon the actual uncertainties of the conversion process. It should be clear that, when the input signal is a small fraction of the full scale value, the first error term is dominate, and the error at every sample is likely to be of the same size. On the other hand, when the input signals approach the full scale, the second term may dominate, and each sample error may be proportional to its nominal value. Consequently, the error model given above is representative of the A/Ds used in relaying applications.

2-5: ORGINIZATION OF HIERARCHICAL PROTECTION SYSTEMS

It is essential for the sake of reliability of protection, that relays be able to perform their tasks independently (i.e., without any participation from other devices or relays). This is to assure that if any of these other devices fail, their failure dose not affect the relay in question. It is realized that for economic reasons as well as for functional needs of certain relays, complete independence of a relay is not possible. It would be an unfeasible and expensive task, to have independent transducers (i.e., CTs and CVTs), battery, or breaker trip coil for each relay. Similarly, functional dependence is built into some relays (e.g., a pilot relay dependence upon the relay at the other end of a transmission line for its proper operation). Thus, it is an accepted fact that to a certain extent, existing protection systems consist of a hierarchy of equipment as well as of functions. The relay engineer designs maximum reliability into this hierarchical system.

A digital relaying system offers possibilities for far greater integration within a hierarchical system. Whenever data is in digital form, possibility of communicating it to other processors and sharing it with them, exists. As in conventional relaying, the concept of functional independence among various relays must be maintained, and this can be achieved by careful hardware and software design. Organization of hierarchical system within the station as well as on the system is shown in figure (2-12). Functionally, we can identify four levels in the hierarchy.

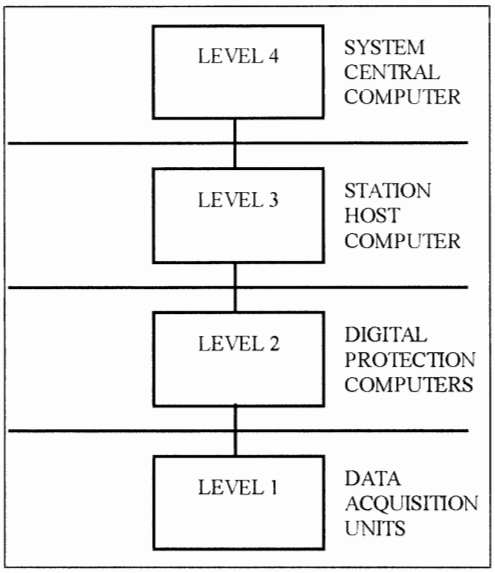

Figure 2- 12: Organization of hierarchical system

2-5-A: LEVEL 1: DATA ACQUISITION UNITS

These units obtain the sampled data from analog input signals (i.e., currents and voltages), and status information of breakers, switches and alarm points in digital form. The Data Acquisition Units (DAUs) may contain processors as subsystems, or may interface directly to level 2 computers through I/O ports. In some cases, the DAUs may be installed in the station yard, thus they must be designed to withstand greater levels of electromagnetic interference and environmental stresses. Level 1 units must transmit data to level 2 computers at very high rates. DAUs may be called upon to transmit simultaneously, many voltages and currents sampled signals, in addition to contact status inputs and communication protocol. This needs to a data transmission rate of no less than 400 kilobits per second.

Some level 1 units use fiber optics lines and multiplex data from several components in the switchyard. The data rates then become proportionally higher. Anyhow, this calls for direct access to computers at level 2 through bus interfaces or Direct Memory Access (DMA) ports.

2-2-B: LEVEL 2: DIGITAL PROTECTION COMPUTERS

These are the digital relays computers. Processing of ordered data from DAUs is done in real time. The protection digital algorithms are executed at this level. In some implementations, multiple processors are used at this level, while others use single processors. These computers, along with the appropriate DAUs, form a single protection function. They are such designed to perform independently of any other computer within the hierarchy. It may be acceptable that the independent operation modes is not optimum for a given system conditions, although it is sufficient for the available protection needs.

When fault related tasks are not active, the protection computers may perform many other functions. Measurements of currents, voltages, and active and reactive power can be carried out. Station oscillography can be performed by storing appropriate waveform data for later processing. However, the frequency responses of these recordings are limited by the sampling rate used in digital protection relays.

The communication link to level 3 computer (i.e., station host computer) is relatively low speed communication link. Through these links, the host computer can communicate control commands to the equipment supervised by the digital relays computers. The link may also be used for a user access terminal, which may be connected to the host computer (e.g., one terminal serving the needs of the entire station). Alternatively, each protection computer may be supplied with its own MMC interface. The link to the station host computer could also be used to communicate status change information of contacts, relays, switches and circuit breakers, so that a coordinated sequence of event log can be constructed in the station host.

2-2-C: LEVEL 3: STATION HOST COMPUTER

The station host computer acts as a data concentrator, and as a canal for communication between digital protection computers and the system center. It takes care of all tasks requiring coordination of information from various protection computers. It also provides an interface between the protection computers and the station operators.

Through this interface, the relay settings, calibration, target interrogation or diagnostic and maintenance functions can be performed. This may include adaptive protection tasks, and construction of partially processed sequence of events records. Communication to lower level computers is local (i.e., within the control house). Communication to system control center is likely to be over a switched telephone network or over microwave links. Fiber optics and satellite communications are used in some applications.

In some systems, the host computer may be eliminated. Some of its tasks can be absorbed by the protection computers at the lower level, and the central computer at the upper level.

The physical structure at this level can be done according to two alternatives;

ALTERNATIVE 1

A system that takes advantage of the possibilities offered in connection with today's communication technology is shown in figure (2-13). With this system design, the communication network has no master, and thereby, all protection computers on the bus have the same access rights to the bus. With the exception of a mutual bus connection, all units operate independently. This means that the functions can be distributed in such a way that each protection computer has complete functions, controlling, and monitoring.

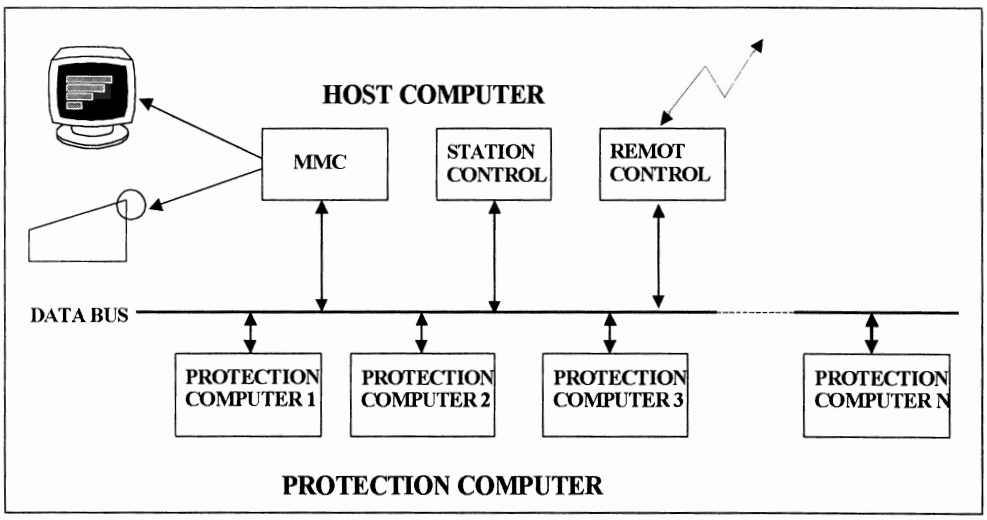

Figure 2- 13: Physical structure on station level, alternative 1.

In this solution, the station host computer is used for the controlling and monitoring of the station functions. Station functions include program functions that carry out sequential control of the equipment supervised by the digital relays computers. An advantage is that the protection computer can be controlled manually and monitored from the station MMC or from the central control computer directly.

ALTERNATIVE 2

Figure (2-14) shows a system of conventional structure, with a station host computer as the midpoint. This type of systems is often referred to as being star coupled. In this solution , station availability is to a large degree dependent on the station host computer availability. This is due to the fact that all communications between the process and the operator, locally or via remote control, is done through the station host computer. The communication between the station host computer level and any protection computer is of point-to-point type.

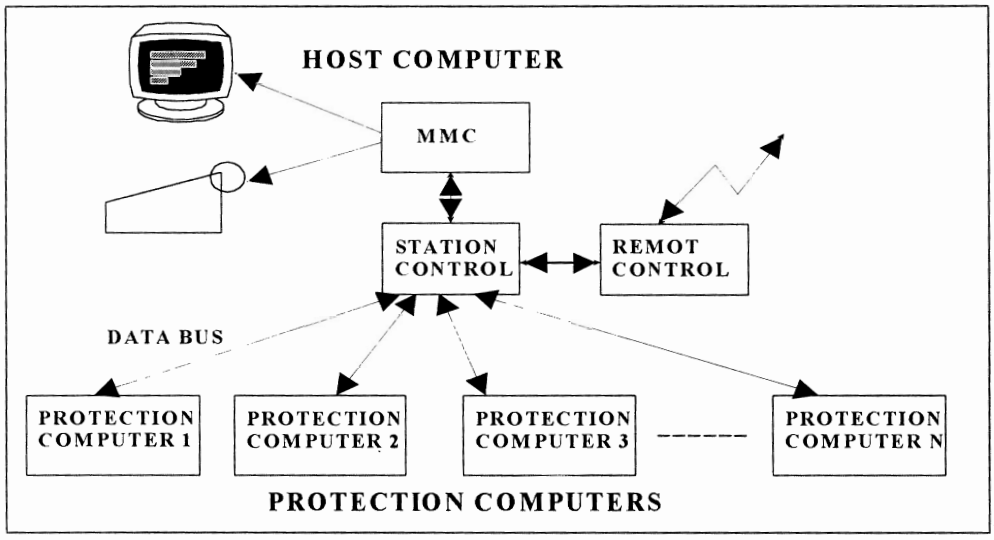

Figure 2- 14 : Physical structure on station level, alternative 2.

This alternative requires that the station computer has the capacity, to handle the information that is transmitted between the protection computers, and to evaluate the signals that are to be sent further to the station MMC or to the remote control.

2-2-D: LEVEL 4: SYSTEM CENTER COMPUTER

This computer is primarily responsible for initiating supervisory control commands to be transmitted to the various stations host computers. It also collects measurements from stations, which may be used for system wide monitoring and contingency evaluation. As maintained before, communication with stations host computers is likely to be over a switched telephone network or over microwave links. High-speed data links (i.e., Fiber optics and satellite communications) may be used in some applications. The central computer is also responsible for keeping various historical records, relating sequence of events, equipment health monitoring, maintenance schedules, system and component capability limits, ...etc. The central computer will play a more direct role if adaptive relaying becomes accepted by the protection community of a system.

REFERENCES

(2.1) A. G. PHADKE and J. S. THORP, " COMPUTER RELAYING FOR POWER SYSTEMS", BOOK, JOHN WILEY & SONS INC. 1988.

(2.2) "DIGITAL SUBSTATION CONTROL SYSTEM", ABB LECTURE No. C01-05aE, MAY 1989.

(2.3) "COMPUTER-AIDED RELAY PROTECTION COORDINATION", EPRI EL-6145, PROJECT 2444-2, FINAL REPORT, DEC. , 1988.

(2.4) "DIGITAL PROTECTION TECHNIQUES AND SUBSTATION FUNCTIONS", REPORT BY WORKING GROUP 34.01 OF STUDY COMMITTEE 34, CIGRE`, 16 MAY, 1989.

(2.5) E. A. UDREN and M. SACKIN, " RELAYING FEATURES OF AN INTEGRATED MICROPROCESSOR-BASED SUBSTATION CONTROL AND PROTECTION SYSTEM", IEE CONFERENCE PUBLICATIONS, No.185, LONDON 1980.

CHAPTER THREE

MATHEMATICAL PRINCIPLES FOR DIGITAL PROTECTION ALGORITHMS

In this chapter, a background material of mathematics needed to understand the digital protection algorithms, will be presented. The treatment of the following materials is of course simple. One may refer to literature books for more details.

3-1: FOURIER SERIES

The Fourier series provides a technique for examining the input signals and determining their frequency harmonic components. The nature of these harmonic components has an important bearing on the performance of the digital algorithms.

A signal f(t) is said to be periodic if there is a T such that;

$$f_{(t)} = f_{(t+T)} \text{ , for all t} \quad \ldots\ldots (3\text{-}1)$$

If f(t) is periodic and not a constant, then let T_o be the smallest positive value of T for which equation (3-1) is satisfied. The period T_o is called the fundamental period of f(t). The need for a concern with the smallest such T is made clear by considering a sinusoid. If f(t)= sin(ωt), then equation (3-1) is satisfied for;

$$T = \frac{2n\pi}{\omega_o}; n = 1,2,... \quad \ldots\ldots (3\text{-}2)$$

The smallest positive value is of course,

$$T_o = \frac{2\pi}{\omega_o}$$

Associated with the fundamental period, a fundamental frequency is defined by,

$$\omega_o = \frac{2\pi}{T_o} \qquad \text{... (3- 3)}$$

If $f(t)=e^{j\omega_o t}$ then equation (3-1) requires,

$$e^{j\omega_o(t+T)} = e^{j\omega_o t}$$

$$e^{j\omega_o t}\left[e^{j\omega_o t} - 1\right] = 0 \quad \text{for all t}$$

which implies that $\omega_o T_o = 2n\pi$; n=1,2,3,.. The conclusion is that the fundamental period is $T_o=2\pi/\omega_o$, and the fundamental frequency is ω_o. The real and imaginary parts are $\cos(\omega_o t)$ and $\sin(\omega_o t)$ respectively, and they have fundamental period $T_o=2\pi/\omega_o$ and fundamental frequency ω_o.

Let $f_1(t)$ and $f_2(t)$ are both periodic signals with fundamental periods T_o and T_1, respectively. Then the sum (i.e., $f_1(t)+f_2(t)$) is not necessary periodic. Consider $f(t) = [\sin(t) + \sin(\pi t)]$, the fundamental period of $\sin(t)$ is 2π while the fundamental period of $\sin(\pi t)$ is 2. It is not possible to find integers (n) and (m) such that, $2m = 2\pi n$ since (p) is not the ratio of integers, so that there is no T that satisfies equation (3-1). On the other hand if,

$$f(t)= e^{j\omega_o t} + e^{2j\omega_o t}$$

then the two fundamental periods differ only by a factor of 2 (i.e., $2\pi/\omega_o$ and π/ω_o). Thus, the fundamental period of the sum is the larger, $2\pi/\omega_o$. In fact it is easy to see that any finite sum of the form,

$$f(t) = c_o + c_1 e^{j\omega_o t} + c_2 e^{2j\omega_o t} + c_3 e^{3j\omega_o t} + \ldots + c_N e^{jN\omega_o t}$$

will be periodic with fundamental frequency ω_o. Including both positive and negative terms in the sum,

$$f(t) = \sum_{k=-N}^{k=N} c_k e^{jk\omega_o t} \qquad \text{... (3- 4)}$$

f(t) is also a periodic signal with fundamental frequency ω_o. The objective of Fourier analysis is to decompose an arbitrary periodic signal into components as in equation(3-4).

3-1-A : EXPONENTIAL FOURIER SERIES

Given a periodic signal with fundamental frequency ω_o, the exponential Fourier series is written as,

$$f(t) = \sum_{k=-\infty}^{k=\infty} c_k e^{jk\omega_o t} \quad \text{..... (3- 5)}$$

The task is to determine c_k. An important property of the exponential makes the calculation a simple process. Note that,

$$\int_0^{T_o} e^{jm\omega_o t}\, dt = \begin{cases} T_o\,; m = 0 \\ 0 \quad ; m \neq 0 \end{cases} \quad \text{..... (3- 6)}$$

The value of the integer is clear for m = 0, while for $m \neq 0$,

$$\int_0^{T_o} e^{jm\omega_o t}\, dt = \frac{1}{jm\omega_o}\left[e^{jm\omega_o t}\right]_0^{T_o} = 0$$

Since $\omega_o T_o = 2\pi$, equation (3-6) is also true for integration over any period (i.e., the integration could have been from τ to $\tau + T_o$). To compute the Fourier series coefficients it is only necessary to multiply equation(3-5) by $e^{-jn\omega_o t}$ and integrate over a period ;

$$\int_0^{T_o} f(t)\, e^{-jn\omega_o t}\, dt = \int_0^{T_o} \sum_{k=-\infty}^{k=\infty} c_k e^{j(k-n)\omega_o t}\, dt \quad \text{..... (3- 7)}$$

From equation(3-5), every term on the right hand side of equation(3-7) vanishes except the n_{th}, yielding;

$$\int_0^{T_o} f(t)\, e^{-jn\omega_o t}\, dt = T_o c_n \qquad \text{..... (3- 8)}$$

or

$$c_n = \frac{1}{T_o} \int_0^{T_o} f(t)\, e^{-jn\omega_o t}\, dt \qquad \text{..... (3- 9)}$$

Equation (3-9) can be evaluated over any convenient period.

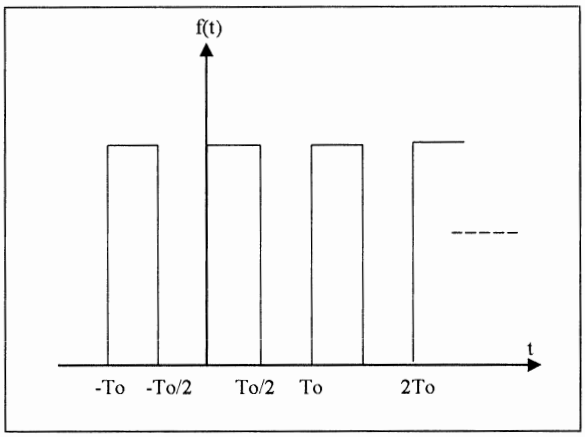

Figure (3- 1) : Periodic square wave.

Consider the square wave of figure (3-1). The n_{th} coefficient is given by;

$$c_n = \frac{1}{T_o} \int_0^{T_o/2} e^{-jn\omega_o t}\, dt = \left[\frac{e^{-jn\omega_o t}}{-jn\omega_o T_o} \right]_0^{T_o/2}$$

$$= \left[\frac{e^{-jn\omega_o T_o/2} - 1}{-jn2\pi} \right] = \left[\frac{e^{-jn\pi} - 1}{-jn2\pi} \right]$$

$$= \frac{(-1)^n - 1}{-jn2\pi} = \begin{cases} \dfrac{1}{jn\pi} & , \text{ n odd} \\ 0 & , \text{ n even , } n \neq 0 \end{cases}$$

$c_o = 1/2$

The coefficient C_o (i.e., the average value of the signal) must frequently be evaluated separately. The approximations formed by the finite sum,

$$f(t) = \sum_{k=-N}^{k=N} c_k e^{jk\omega_o t} \quad , N = 1,3,5,.....$$

3-1-B: SINE AND COSINE FOURIER SERIES

Through the use of the Euler identity;

$$e^{jk\omega_o t} = \cos(k\omega_o t) + j\sin(k\omega_o t) \quad \text{..... (3- 10)}$$

we can write equation (3-4) in sinusoidal and cosinusoidal terms as;

$$\sum_{k=-\infty}^{k=\infty} c_k e^{jk\omega_o t} = a_o + \sum_{k=1}^{\infty} a_k \cos(k\omega_o t) + \sum_{k=1}^{\infty} b_k \sin(k\omega_o t) \quad \text{.....(3- 11)}$$

where;

$a_o = c_o$

$$a_k = c_k + c_{-k} \qquad k \neq 0 \quad \text{..... (3- 12)}$$

$$b_k = j(c_k - c_{-k}) \qquad k \neq 0 \quad \text{..... (3- 13)}$$

Thus, using equation (3-9) we get,

$$a_k = \frac{1}{T_o} \int_0^{T_o} f(t) \cos(k\omega_o t) \, dt \quad \text{..... (3- 14)}$$

$$b_k = \frac{1}{T_o}\int_0^{T_o} f(t)\ \sin(k\omega_o t)\ dt \quad \text{..... (3- 15)}$$

Equations (3-12) and (3-13) result from expanding the kth and k-th terms of the exponential series using equation(3-10),

$$c_{-k}e^{-jk\omega_o t}+.....+\ c_k e^{jk\omega_o t} =$$
$$c_{-k}\cos(\omega_o t)\ + c_k\cos(\omega_o t)\ -\ c_{-k}\ j\sin(\omega_o t)\ +\ c_k\ j\sin(\omega_o t)$$

If the Fourier series is written as;

$$f(t)\ = c_o + \left(c_1\ e^{j\omega_o t} +\ c_{-1}\ e^{-j\omega_o t}\right) + \left(c_2\ e^{2j\omega_o t} +\ c_{-2}\ e^{-2j\omega_o t}\right) +$$
$$+\ .....\ +\ \left(c_k\ e^{jk\omega_o t} +\ c_{-k}\ e^{-jk\omega_o t}\right)$$

The various terms can be recognized as,

c_o	: is the dc component (average value)
$\left(c_1\ e^{j\omega_o t} +\ c_{-1}\ e^{-j\omega_o t}\right)$	: is the fundamental frequency component
$\left(c_k\ e^{jk\omega_o t} +\ c_{-k}\ e^{-jk\omega_o t}\right)$	: is the k_{th} harmonic component

Thus, Fourier series expansion can be used to resolve any periodic function into its frequency components. The coefficient c_k represents the amount of the signal at the frequency equal to $(k\omega_o)$.

For example, consider the half-wave rectified sinusoid shown in figure (3-2). The fundamental frequency is ω_o. Using equation (3-9);

$$c_n = \frac{1}{T_o}\int_0^{T_o} f(t)\ e^{-jn\omega_o t}\ dt$$

The Fourier series coefficients are,

$$c_o = \frac{A}{\pi}$$

$$c_1 = \frac{A}{4j}$$

$$c_k = -\frac{A}{\pi(1-k)^2}; \quad \text{for k is even}$$

Hence the first few terms of the Fourier expansion are;

$$f(t) = \frac{A}{2} + \frac{A}{2\pi}\sin(\omega_o t) - \frac{2A}{3\pi}\cos(2\omega_o t) - \frac{2A}{15\pi}\cos(4\omega_o t) - \ldots.$$

We can compute a fundamental frequency phasor from the fundamental term in the Fourier series. If we take a cosine waveform as the reference signal, then, the voltage,

$$v(t) = \sqrt{2}V \cos(\omega_o t)$$

is corresponding to a phasor V which has angle ϕ, and the voltage

$$v(t) = \sqrt{2}V \cos(\omega_o t + \phi)$$

is corresponding to a complex phasor, $Ve^{j\phi}$, then the fundamental frequency phasor is directly related to the first exponential Fourier series coefficient;

$$V e^{j\phi} = \frac{\sqrt{2}}{T_o}\int_0^{T_o} v(t)e^{j\omega_o} dt \quad \text{.......... (3- 16)}$$

3-1-C: WALSH FUNCTIONS

A family of complex signals are said to be orthogonal over an interval $0 \le t \le T$, if;

$$\int_0^T \varphi_n(t) \cdot \varphi_m^*(t)\ dt = 0 \quad ; m \ne n \quad \text{.......... (3- 17)}$$

Where, $\varphi^{*}_{m}(t)$ is the complex conjugate of $\varphi_{n}(t)$. Many orthogonal periodic functions have been applied in digital relaying. We shall consider the Walsh functions in brief as an example. More details can be found in mathematics literature books.

The Walsh functions are set of orthogonal signals on the interval [0,1] that only take on the values ± 1. As such, they were appealing for digital implementation since multiplication by a Walsh function involves only algebraic operations. Consider the Walsh functions shown in figure (3-2). The expansion of a function in Walsh functions in the interval [0,1] can be,

$$f(t)= \sum_{k=0}^{\infty} d_k \, w_k(t) \qquad \text{..... (3- 18)}$$

where,

$$d_k = \int_0^1 f(t)\, w_k(t)\, dt \qquad \text{..... (3- 19)}$$

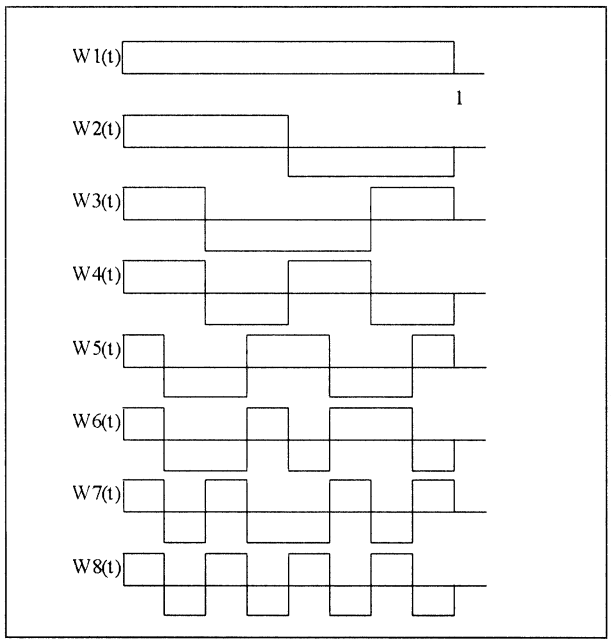

Figure (3- 2) : The first eight Walsh functions.

Let f(t) is represented by a sine and cosine Fourier series in the form,

$$f(t) = f_0 + f_1 \sin 2\pi t + f_2 \cos 2\pi t + f_3 \sin 4\pi t + f_4 \cos 4\pi t + \ldots\ldots \qquad \text{.(3- 20)}$$

The coefficients d_k in equation (3-18) and the coefficients f_k in equation (3-20), each represents f(t) and can be related through equation(3-19). In general if **f** represents the Fourier coefficients and **d** the Walsh coefficients , i.e.;

$$f = \begin{bmatrix} f0 \\ f1 \\ f2 \\ f3 \\ . \\ . \\ fn \end{bmatrix}, \quad d = \begin{bmatrix} d0 \\ d1 \\ d2 \\ d3 \\ . \\ . \\ dn \end{bmatrix} \qquad \text{..... (3- 21)}$$

then,

$$[d] = [A] \cdot [f] \qquad \text{..... (3- 22)}$$

where; **[A]** is an n by n matrix with entries,

$$a_{k,m-1} = \int_0^1 W_k(t) \sin(2m\pi t)\, dt \qquad \text{..... (3- 23)}$$

$$a_{k,m} = \int_0^1 W_k(t) \cos(2m\pi t)\, dt \qquad \text{..... (3- 24)}$$

in which (m) is even and (k) represents the number of row. Equation (3-23) represents the odd elements of the rows (i.e., a_{11}, a_{13}, a_{15}...), while equation (3-24) represents the even elements of the rows (i.e., a_{12}, a_{14}, a_{16}...). The k_{th} row of **[A]** represents the Fourier coefficients of the k_{th} Walsh function $w_k(t)$, while the m_{th} row represents the coefficients of the Walsh expansion of the m_{th} Fourier function. The first 11 rows and columns of **[A]** are shown below,

$$A = \begin{bmatrix} 1 & 0 & 0 & 0 & 0 & 0 & 0 & 0 & 0 & 0 & 0 \\ 0 & 0.9 & 0 & 0 & 0 & 0.3 & 0 & 0 & 0 & 0.18 & 0 \\ 0 & 0 & 0.9 & 0 & 0 & 0 & 0.3 & 0 & 0 & 0 & 0.18 \\ 0 & 0 & 0 & 0.9 & 0 & 0 & 0 & 0 & 0 & 0 & 0 \\ 0 & 0 & 0 & 0 & 0.9 & 0 & 0 & 0 & 0 & 0 & 0 \\ 0 & -0.373 & 0 & 0 & 0 & 0.724 & 0 & 0 & 0 & 0.435 & 0 \\ 0 & 0 & -0.373 & 0 & 0 & 0 & 0.724 & 0 & 0 & 0 & 0.435 \\ 0 & 0 & 0 & 0 & 0 & 0 & 0 & 0.9 & 0 & 0 & 0 \\ 0 & 0 & 0 & 0 & 0 & 0 & 0 & 0 & 0.9 & 0 & 0 \\ 0 & -0.074 & 0 & 0 & 0 & -0.484 & 0 & 0 & 0 & 0.65 & 0 \\ 0 & 0 & -0.074 & 0 & 0 & 0 & -0.484 & 0 & 0 & 0 & 0.65 \end{bmatrix} \quad \ldots\ldots\ldots (3\text{-}25)$$

From equations (3-21),(3-22),(3-23),(3-24), and (3-25);

$$f_o = d_o \quad \ldots\ldots\ldots (3\text{-}26)$$

$$f_1 = 0.9d_1 - 0.373d_5 - 0.74d_9 + \ldots\ldots \quad \ldots\ldots\ldots (3\text{-}27)$$

$$f_2 = 0.9d_2 + 0.373d_6 - 0.74d_{10} + \ldots\ldots \quad \ldots\ldots\ldots (3\text{-}28)$$

.

.

Because of the connection between the two sets of coefficients, it is possible to obtain an approximation to the Fourier coefficients by first finding the Walsh coefficients and then using the expressions similar to equations (3-26 , 27, and 28).

For example, Let f(t) = A sin(2πt), and using only w1(t) then;

d1=0.9A, d5=-0.373A, d9=-0.074A,
and d2=d3=d4=d6=d7=d8=d10=0

Thus,

f1= $(.9)^2A + (.373)^2A + (.074)^2A$
f2=0

Hence, f1, which should be equal to A, is 0.81A. It is increased to 0.949A if w1(t) and w5(t) are used, and is equal to 1.004A if w1(t), w5(t), and w9(t), are used.

3-2: FOURIER TRANSFORMS

The technique of representing a signal as a sum of exponential can be extended to a non-linear function using Fourier transform. The transform pair can be obtained by writing a Fourier series and taking the limit as the period becomes infinite. Consider a time signal as shown in fig (3-3-a), then, $x(t) = 0$; $t > T_1$ and $t < -T_1$. Select a period $T_o >> T_1$, and let,

$$f(t) = \sum_{-\infty}^{\infty} x(t - nT_o) \quad \text{..... (3- 29)}$$

to form a periodic function made up of shifted replicas of x (t) as shown in figure(3-3-b). It can be seen that f(t) is periodic, with fundamental period T_o and fundamental frequency $\omega_o = 2\pi/T_o$. The Fourier series coefficients are given by,

$$c_k = \frac{1}{T_o} \int_{-T_o/2}^{T_0/2} x(t) e^{-jk\omega_o t} dt \quad \text{..... (3- 30)}$$

As T_o approaches infinity, f(t) limits to x(t), and f(t) can be written as,

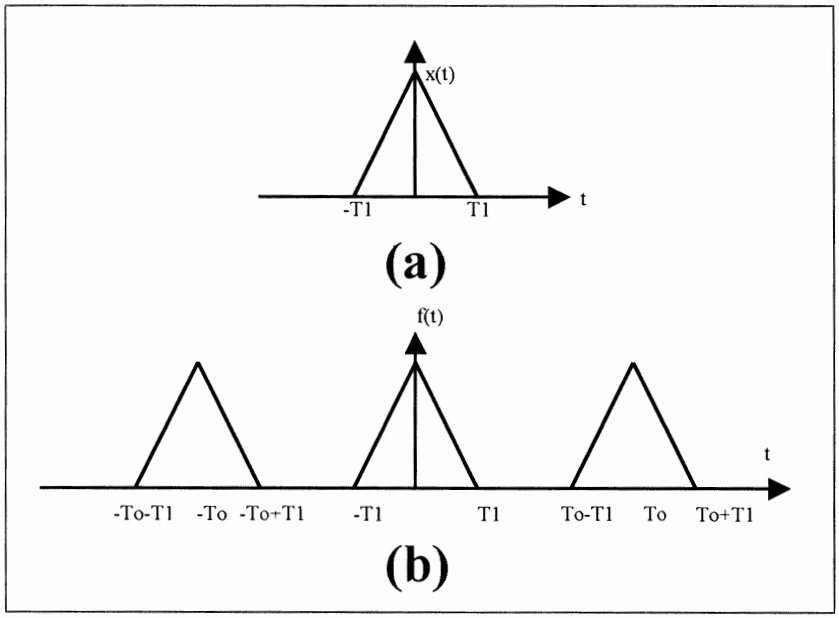

Figure (3- 3): a- A time limited function. b- Shifted replicas of x(t).

$$f(t) = \sum_{k=-\infty}^{\infty} c_o e^{jk\omega_o t} \, dt \quad \text{..... (3- 31)}$$

Substituting equation(3-30) into (3-31), we get,

$$f(t) = \sum_{k=-\infty}^{\infty} \left[\frac{1}{T_o} \int_{-T_o/2}^{T_0/2} x(t) e^{-jk\omega_o t} \, dt \right] e^{jk\omega_o t} \quad \text{..... (3- 32)}$$

as $T_o = 2\pi/\omega_o$, then the last equation becomes,

$$f(t) = \frac{1}{2\pi} \sum_{k=-\infty}^{\infty} \left[\int_{-T_o/2}^{T_0/2} x(t) e^{-jk\omega_o t} \, dt \right] \omega_o e^{jk\omega_o t}$$

If T_o approaches infinity in such away that;

$\omega_o \to d\omega$, $k\omega \to \omega$,

$\lim_{T_o \to \infty} f(t) = x(t)$,

and $\sum_{k=-\infty}^{\infty} \to \int_{-\infty}^{\infty}$

then the last equation becomes;

$$x(t) = \frac{1}{2\pi} \int_{-\infty}^{\infty} \left[\int_{-\infty}^{\infty} x(t) e^{-j\omega t} \, dt \right] e^{j\omega t} \, d\omega \quad \text{..... (3- 33)}$$

$$x(t) = \frac{1}{2\pi} \int_{-\infty}^{\infty} \hat{X}(\omega) e^{j\omega t} \, d\omega \quad \text{..... (3- 34)}$$

or;

$$\hat{X}(\omega) = \int_{-\infty}^{\infty} x(t) e^{-j\omega t} \, dt \quad \text{..... (3- 35)}$$

$$x(t) = \frac{1}{2\pi} \int_{-\infty}^{\infty} \hat{X}(\omega) e^{j\omega t} \, d\omega \quad \text{..... (3- 36)}$$

The last equations represents the Fourier transform (F) and the inverse Fourier transform (F^{-1}) respectively. The connection between the two functions x(t) and $\hat{X}(\omega)$ is shown in the following equations,

$$x(t) \xrightarrow{F} \hat{X}(\omega) \quad \text{..... (3- 37)}$$

$$\hat{X}(\omega) \xrightarrow{F^{-1}} x(t) \quad \text{..... (3- 38)}$$

3-3: PROPERTIES OF FOURIER TRANSFORMS

There are a number of properties of Fourier transforms, which are useful in understanding the resolution of a signal into its frequency spectrum [3.4].

1- Linearity:

If $x_1(t) \xrightarrow{F} \hat{X}_1(\omega)$

and $x_2(t) \xrightarrow{F} \hat{X}_2(\omega)$

then $c_1x_1(t) + c_2x_2(t) \xrightarrow{F} c_1\hat{X}_1(\omega) + c_2\hat{X}_2(\omega)$

2- Delay Rule:

If $x(t) \xrightarrow{F} \hat{X}(\omega)$

then $x(t - t_1) \xrightarrow{F} \hat{X}(\omega)\, e^{-j\omega t_1}$

3- Frequency Shift or Modulation:

If $x(t) \xrightarrow{F} \hat{X}(\omega)$

then $x(t)\, e^{j\omega_o t} \xrightarrow{F} \hat{X}(\omega - \omega_o)$

4- Differentiation in Time:

If $x(t) \xrightarrow{F} \hat{X}(\omega)$ and $x'(t)$ exists

then $x'(t) \xrightarrow{F} j\omega\, \hat{X}(\omega)$

in general $\frac{d^n}{dt^n} x(t) \xrightarrow{F} (j\omega)^n\, \hat{X}(\omega)$

5- Differentiation in Frequency:

If $x(t) \xrightarrow{F} \hat{X}(\omega)$ and $\frac{d}{d\omega}\hat{X}(\omega)$ exists

then,

$$(-jt)\, x(t) \xrightarrow{F} \frac{d}{d\omega}\hat{X}(\omega)$$

In general;

$$(-jt)^n\, x(t) \xrightarrow{F} \frac{d^n}{d\omega^n}\hat{X}(\omega)$$

6- Even and Odd Properties:

If $x(t) \xrightarrow{F} \hat{X}(\omega)$ and $x(t)$ is real;

then,

$$\mathrm{Re}\left[\hat{X}(\omega)\right] = \int_{-\infty}^{\infty} x(t)\cos(\omega t)\, dt \quad ; \text{an even function of } \omega.$$

and,

$$\mathrm{Im}\left[\hat{X}(\omega)\right] = -\int_{-\infty}^{\infty} x(t)\sin(\omega t)\, dt \quad ; \text{an odd function of } \omega.$$

Note that;

- If x(t) is real and even, (i.e., x(t)=x(-t)), then $\hat{X}(\omega)$ is real and even.

- If x(t) is real and odd, (i.e., x(-t)= -x(t)), then $\hat{X}(\omega)$ is real and odd.

7- Time Scaling:

If $x(t) \xrightarrow{F} \hat{X}(\omega)$, then;

$$x(at) \xrightarrow{F} \frac{\hat{X}(\frac{\omega}{a})}{a} \quad ; a > 0$$

8- Convolution in Time:

Given two signals with Fourier transforms,

$$x_1(t) \xrightarrow{F} \hat{X}_1(\omega) \ , \ x_2(t) \xrightarrow{F} \hat{X}_2(\omega)$$

and well defined convolution $x_1 * x_2$, then;

$$x_1(t) * x_2(t) \xrightarrow{F} \hat{X}_1(\omega) * \hat{X}_2(\omega)$$

9- Convolution in Frequency:

Given,

$$x_1(t) \xrightarrow{F} \hat{X}_1(\omega) \ , \ x_2(t) \xrightarrow{F} \hat{X}_2(\omega)$$

and $\hat{X}_1(\omega) * \hat{X}_2(\omega)$ defined, then;

$$x_1(t) * x_2(t) \xrightarrow{F} \frac{1}{2\pi} \hat{X}_1(\omega) * \hat{X}_2(\omega)$$

10 - Symmetry or duality:

if $f(t) \xrightarrow{F} g(\omega)$, then;

$g(t) \xrightarrow{F} 2\pi f(-\omega)$

11- Periodic Function:

a) $\delta(t) \xrightarrow{F} 1$

b) $1 \xrightarrow{F} 2\pi\,\delta(t)$

c) $e^{j\omega_o t} \xrightarrow{F} 2\pi\,\delta(\omega - \omega_o)$

d) $\cos(\omega_o t) = \frac{1}{2}\left[e^{j\omega_o t} + e^{-j\omega_o t}\right] \xrightarrow{F} \pi\left[\delta(\omega - \omega_o) + \delta(\omega + \omega_o)\right]$

e) $\sin(\omega_o t) = \frac{1}{2j}\left[e^{j\omega_o t} - e^{-j\omega_o t}\right] \xrightarrow{F} \frac{\pi}{j}\left[\delta(\omega - \omega_o) - \delta(\omega + \omega_o)\right]$

3-4: SAMPLING FOR DIGITAL POWER SYSTEM PROTECTION.

The immediate application of Fourier transforms in digital protection is in the description of the frequency content of signals and of the effect of filters and algorithms on those signals.

Given that x(t) is a band-limited signal; i.e.

$$x(t) \xrightarrow{F} \hat{X}(\omega) \quad \text{and} \quad \hat{X}(\omega) = 0 \text{ for } |\omega| > \omega_m$$

and let $f(t) = \sum_{k=-\infty}^{\infty} p_a(t - nT_o)$ is a periodic signal shown in figure(3-4), then the product of x(t) and f(t) produces a new signal z(t), called *the sampled signal* (i.e., z(t) = x(t) . f(t)).

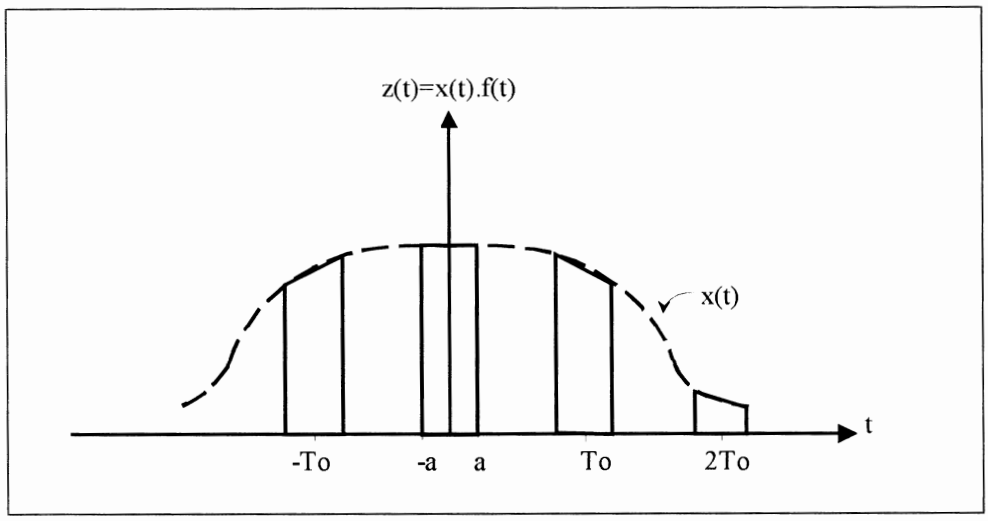

Figure (3- 4): Sampled signal.

It possible to recover the signal x(t) from the signal z(t) with a filter if the samples are close enough together. The process can be understood better in the frequency domain. The Fourier transform of z(t) using the convolution property is,

$$\hat{Z}(\omega) = \frac{\hat{X}(\omega) * \hat{R}(\omega)}{2\pi} \quad \text{..... (3- 39)}$$

Since f(t) is a periodic function then ;

$$r(t) = \sum_{k=-\infty}^{\infty} c_k e^{jk\omega_o t} \xrightarrow{F} \hat{R}(\omega) = 2\pi \sum_{k=-\infty}^{\infty} c_k \delta(\omega - \omega_o) \quad \text{..... (3- 40)}$$

and equation (3-39) can be written as,

$$\hat{Z}(\omega) = \frac{2\pi}{2\pi} \sum_{k=-\infty}^{\infty} c_k \, \hat{X}(\omega)\, \delta(\omega - k\omega_o) \quad \text{..... (3- 41)}$$

Considering that,

$$\hat{X}(\omega) * \delta(\omega - k\omega_o) = \int_{-\infty}^{\infty} \delta(\mu - k\omega_o)\, \hat{X}(\omega - \mu)\, d\mu$$

$$= \hat{X}(\omega - k\omega_o)$$

then equation(3-41) will be,

$$\hat{Z}(\omega) = \sum_{k=-\infty}^{\infty} c_k\, \hat{X}(\omega - k\omega_o) \qquad \text{... (3- 42)}$$

The last equation represents a spectrum made up of shifted replicas of $\hat{X}(\omega)$ as shown in figure (3-5).

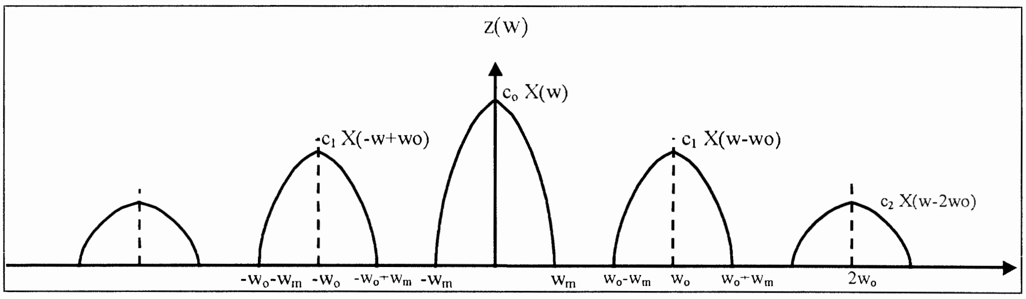

Figure (3- 5) : The spectrum of a sampled signal.

As shown in the figure, $\omega m < \omega o - \omega m$ or, $\omega o > 2\omega m$, then the spectrum of x(t) can be recovered from z(t) with an ideal low pass filter with a cut off frequency of ωm. The frequency $\omega o = 2\omega m$ (i.e., twice the highest frequency in the band-limited signal), is the Nyquist sampling frequency. It can be seen from figure (3-5), that if the sampling frequency is less than the Nyquist frequency, there will be overlap in the shifted replicas of X(w) and the output of the low-pass filter will not be the original signal x(t). This effect is called *aliasing*. If the signals to be sampled at a sampling rate corresponding to the frequency ωs then, to avoid aliasing it is necessary to filter the signal to a bandwidth of $\omega s/2$. Such a filter is referred to as an *anti-aliasing filter*.

Consider now a continuos signal f(t), if we take N samples of f(t) at intervals of T seconds to form a finite duration discrete-time signal as shown in figure (3-7) , with;

$$f[n] = f(nT) \quad 0 < n < N-1$$

$$\hat{F}(\omega) = \sum_{n=0}^{N-1} f(nT)\, e^{-j\omega T} \qquad \text{..... (3- 43)}$$

then the transform $F(\omega)$, is a continuos and periodic function of ω with a Fourier series with only a finite number of terms (N) as shown by equation(3-42) . The time function is described by N numbers (i.e., f[0], f[1], f[2],..., f[N-1]), while the function of ω is continuos.

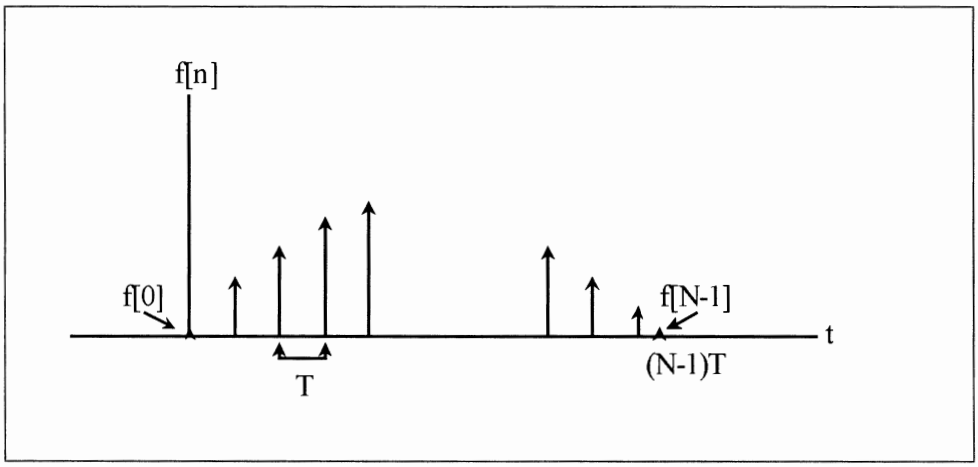

Figure (3- 6): Finite duration discrete-time signal.

It would be desirable to obtain a finite description of the transform. This description is of N numbers which completely describes the transform $\hat{F}(\Omega)$, where $\Omega_0 = 2\pi/NT$. The key is to consider the periodic extension of the time limited discrete-time signal. It can be shown that the Discrete Fourier Transform (DFT) and Inverse Transform (IDFT) are,

[DFT] $$\hat{F}(k\Omega_0) = \sum_{n=0}^{N-1} f(nT)\, e^{-jkn\Omega_0 T} \qquad \text{..... (3- 44)}$$

[IDFT] $$f(nT) = \frac{1}{N} \sum_{k=0}^{N-1} \hat{F}(k\Omega_0)\, e^{jnk\Omega_0 T} \qquad \text{..... (3- 45)}$$

which relate a sampled periodic time function ,shown in figure (3-6), and a similar sampled periodic function of ω as shown in figure(3-7).

There are N samples per period (i.e., cycle) in each domain. In the frequency domain, the samples are at an interval of T second and the period is NT seconds. On the frequency domain the samples are spaced at $2\pi/NT=\Omega_o$ radians and the period is $2\pi/T$.

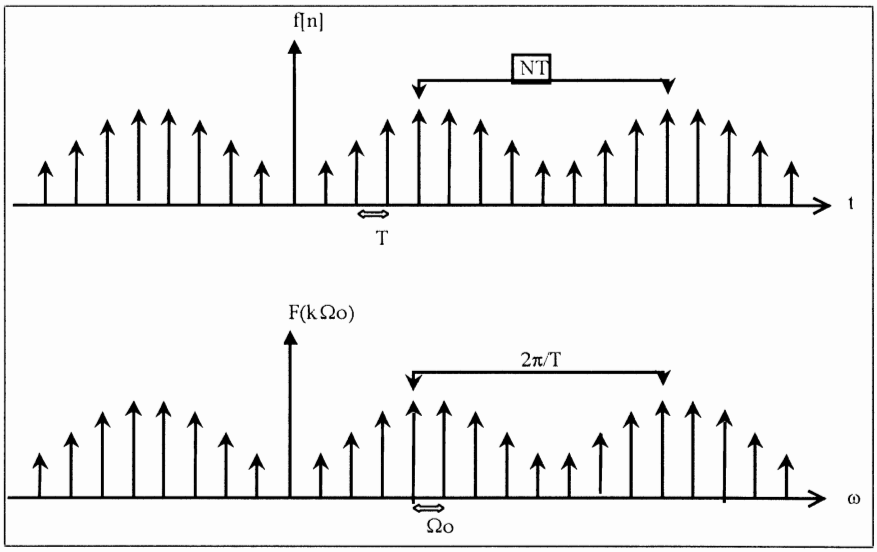

Figure (3- 7): Discrete Fourier Transform pair.

A more compact form of equations (3-43) and (3-44) can be obtained as,

$$F_k = \sum_{n=0}^{N-1} f_n \, w^{nk} \qquad \text{..... (3-46)}$$

$$f_n = \frac{1}{N} \sum_{k=0}^{N-1} F_k \, w^{-nk} \qquad \text{..... (3- 47)}$$

where,

$F_k = \hat{F}(k\Omega_o)$

$f_n = f(nT)$

$w = e^{-j\Omega_o T} = e^{-j\frac{2n}{N}}$

Equations (3-45), and (3-46) can also be expressed in matrix form as,

$$\begin{bmatrix} F_o \\ F_1 \\ \cdot \\ \cdot \\ F_o \end{bmatrix} = \begin{bmatrix} w_o & w_o & \cdot & \cdot & w_o \\ w_o & w_1 & w_2 & . & \\ w_o & w_2 & w_4 & . & \\ w_o & w_3 & w6 & . & \\ \cdot & \cdot & \cdot & \cdot & \end{bmatrix} \begin{bmatrix} f_o \\ f_1 \\ \cdot \\ \cdot \\ f_{N-1} \end{bmatrix} \quad \text{..... (3- 48)}$$

In protection applications, N (i.e., number of samples per a cycle) is small and is no more than 20 samples/ cycle for most algorithms, and only a few of frequency harmonic components (i.e., F_k), are wanted. Generally, only the fundamental frequency component (F_1) is used in impedance relaying while a few harmonics (i.e., fundamental (F_1), second (F_2), and fifth (F_5)) are used in transformer protection.

If we consider the signal, $v(t) = \sqrt{2}\ V \cos(\omega t + \varphi)$, with N samples per period ($T=2\pi/\omega$), the calculation in equation (3-44) yields,

$$F_1 = \frac{N\sqrt{2}}{2} V\, e^{j\varphi}$$

The fundamental frequency phasor associated with a signal x(t) is then given as,

$$X_1 = \frac{\sqrt{2}}{N} \sum_{n=0}^{N-1} x_n\, e^{\frac{-j2\pi n}{N}} \quad \text{..... (3-49)}$$

where, $x_n = x(\frac{2\pi n}{N\omega})$. Equation (3-49) provides the basis of a number of relaying algorithms.

REFERENCES

(3.1) "DIGITAL PROTECTION TECHNIQUES AND SUBSTATION FUNCTIONS", REPORT BY WORKING GROUP 34.01 OF STUDY COMMITTEE 34 , CIGRE`, 16 MAY 1989.

(3.2) "EVALUATION OF ULTRAHIGH-SPEED RELAY ALGORITHMS", EPRI EL-4996, PROJECT 1422-2, FINAL REPORT, MAY, 1985.

(3.3) G. S. HOPE AND V. S. UMAMAHESWARAN, "SAMPLING FOR COMPUTER PROTECTION OF TRANSMISSION LINES", IEEE TRANS. ON PAS, VOL. PAS-93, No. 5, SEPT./OCT. 1974, pp. 1522-1533.

(3.4) A. G. PHADKE AND J. S. THORP, " COMPUTER RELAYING FOR POWER SYSTEMS", BOOK, JOHN WILEY & SONS INC. 1988.

(3.5) G. B. THOMAS, " CALCULUS AND ANALYTIC GEOMETRY", BOOK, ADDISON-WELSLY PUBLISHING COMP., INC., FOURTH PRINTING 1965.

(3.6) F. AYRES, "THEORY AND PROBLEMS OF MATRICES", SCHAUM`S OUTLINE SERIES, McGRAW-HILL BOOK COMP. 1962.

CHAPTER FOUR

DIGITAL ALGORITHM FOR TRANSMISSION LINE PROTECTION BASED ON FUNDAMENTAL FREQUENCY COMPONENTS

Most digital algorithms for transmission line protection which depends the fundamental frequency components, are based on the well-known technique of distance or impedance relaying, whereby the impedance seen by a relay is proportional to the distance between the fault and the relaying station. Thus, any estimated impedance lower than impedance of the whole line corresponds to a fault inside the protected zone. The fundamental impedance of the circuit is given by,

$$Z = V / I \quad \text{..... (4-1)}$$

Where, Z is complex and V and I, are phasors. To determine Z, one must estimate the magnitudes and the phase angles of the fundamental frequency components of the steady state voltage and current signals. When both of the input signals are pure sinusoids, the digital estimation is fairly accurate and easy to obtain. The accurate estimation of such parameters becomes more difficult, however, in the presence of transients.

4-1: FOURIER ALGORITHMS

The most common way to estimate the phasors from sampled signals is by correlating the signals with sine and cosine functions of the fundamental frequency. This can be done with a data window equal to one cycle of the fundamental frequency (i.e., execution time of the algorithm is equal to one cycle period). However, if shorter data windows are used to reduce the time operation of the relay, then the results accuracy is affected seriously by other components, specially the dc components of the signals. DC components are large in short circuits currents, and introduce large errors, because in case of sub-cycle data windows these components are not orthogonal to the

cosinusoidal correlating function. Thus, modified algorithms are needed.

4-1-A: FOURIER ALGORITHM WITH ONE-CYCLE DATA WINDOW

The incoming ac data samples for one cycle are correlated with the stored samples of reference fundamental sine and cosine wave to extract the complex value of the fundamental components in rectangular forms [4.7]. The general expressions of the sine and cosine components of voltage and current signals at a sample point k are;

$$V_s = \frac{2}{N}\sum_{r=1}^{N-1} v_{(k-N+r)} \sin(\frac{2\pi}{N} r) \quad \text{..... (4-2)}$$

$$V_c = \frac{2}{N}\sum_{r=1}^{N-1} v_{(k-N+r)} \cos(\frac{2\pi}{N} r) \quad \text{..... (4-3)}$$

Similarly for current signal;

$$I_s = \frac{2}{N}\sum_{r=1}^{N-1} i_{(k-N+r)} \sin(\frac{2\pi}{N} r) \quad \text{..... (4-4)}$$

$$I_c = \frac{2}{N}\sum_{r=1}^{N-1} i_{(k-N+r)} \cos(\frac{2\pi}{N} r) \quad \text{..... (4-5)}$$

where, the v_k and i_k are the voltage and current samples respectively, and N is number of samples taken for fundamental cycle. From equation (4-1) and using the complex forms of V and I, Z can then be measured as;

$$Z = \frac{V}{I} = \frac{V_c + jV_s}{I_c + jI_s} = \frac{V_s \cdot I_s + V_c \cdot I_c}{I_s^2 + I_c^2} + j\frac{V_c \cdot I_s - V_s \cdot I_c}{I_s^2 + I_c^2} = R + jX \quad (4\text{-}6)$$

where,

$$R = \frac{V_s \cdot I_s + V_c \cdot I_c}{I_s^2 + I_c^2} \quad \text{..... (4-7)}$$

$$X = \frac{V_c \cdot I_s - V_s \cdot I_c}{I_s^2 + I_c^2} \quad \text{..... (4-8)}$$

then the magnitude of Z is;

$$|Z| = \sqrt{R^2 + X^2} \quad \text{..... (4-9)}$$

and the phase angle is;

$$\angle Z = \theta = -\arctan\left(\frac{R}{X}\right) \quad \text{..... (4-10)}$$

The frequency response of a Fourier algorithm with one-cycle data window is shown in figure (4-1). The sampling rate (N) is 12 samples/cycle. It can be seen that this algorithm rejects dc component.

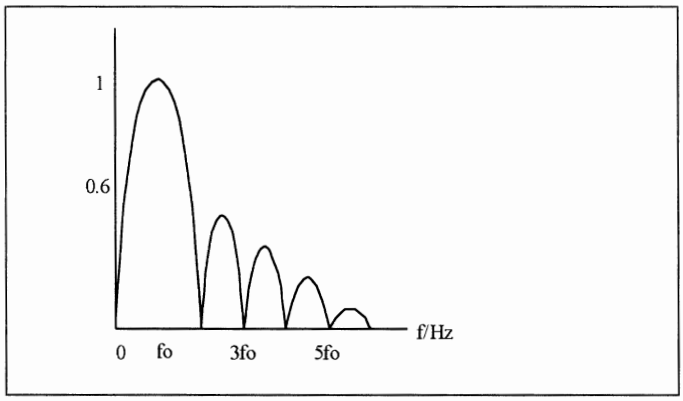

Figure(4-1) : Frequency response of a Fourier algorithm with one-cycle data window of 12 samples/cycle.

4-1-B : FOURIER ALGORITHM WITH SUB-CYCLE DATA WINDOW

If the extraction of the fundamental components which are contained in the currents and voltages is done by means of correlating the signals with sine/cosine functions of the fundamental frequency,

and the data window is shorter than one period, the presence of a aperiodic components in the signals gives rise to large errors. Thus, it has been suggested that to reduce the errors, the signals ought to be correlated with sine/cosine functions, which have periods equal to the data window length [4.5,4.6].

Real and imaginary parts of the spectrum $I(\omega)$ may be expressed respectively in the following way,

$$M_i(\omega) = 0.5\,[I(\omega) + I(-\omega)] \quad \text{..... (4-11)}$$

$$N_i(\omega) = 0.5\,[I(\omega) - I(-\omega)] \quad \text{..... (4-12)}$$

where, $M_i(\omega)$ and $N_i(\omega)$ are equal to the results of correlation of the signal i(t) with sine/cosine functions,

$$M_i = \int_{-T_\omega/2}^{T_\omega/2} i(t)\cos(\omega t)\,dt \quad \text{..... (4-13)}$$

$$N_i = \int_{-T_\omega/2}^{T_\omega/2} i(t)\sin(\omega t)\,dt \quad \text{..... (4-14)}$$

T_ω is the time span corresponding to data window. The real and imaginary parts of Z are respectively,

$$R = \frac{K^2 M_i M_v + P^2 N_i N_v}{K^2 M_i^2 + P^2 N_i^2} \quad \text{..... (4-15)}$$

$$X = \frac{-K\,P\,N_i M_v + K\,P\,M_i N_v}{K^2 M_i^2 + P^2 N_i^2} \quad \text{..... (4-16)}$$

where, (M_i, N_i) and (M_v, N_V) are the factors M and N calculated for the current and voltage respectively. The coefficients K and P depend on the data window,

$$K = \frac{\pi(1-r^2)}{r\sin(\pi r)} \quad \text{..... (4-17)}$$

$$P = \frac{-\pi(1-r^2)}{\sin(\pi r)} \qquad \text{..... (4-18)}$$

where, $r = \omega_1 / \omega_2$, and ω_1 is the fundamental frequency and ω_2 is the frequency corresponding to the data window. The amplitude and phase angle of the complex impedance can be calculated using equations (4-9) and (4-10). The frequency response of this algorithm for a half-cycle data window, is shown in figure (4-2).

Compared with the standard practice of extracting the fundamental components by means of correlating the signals with a sine/cosine functions of the fundamental frequency, the above method minimize errors due to the presence of aperiodic components in the signal, but increases errors which result from oscillatory components. However, in most practical cases amplitudes of oscillatory components in the currents are very small, while in voltages they are not very large either.

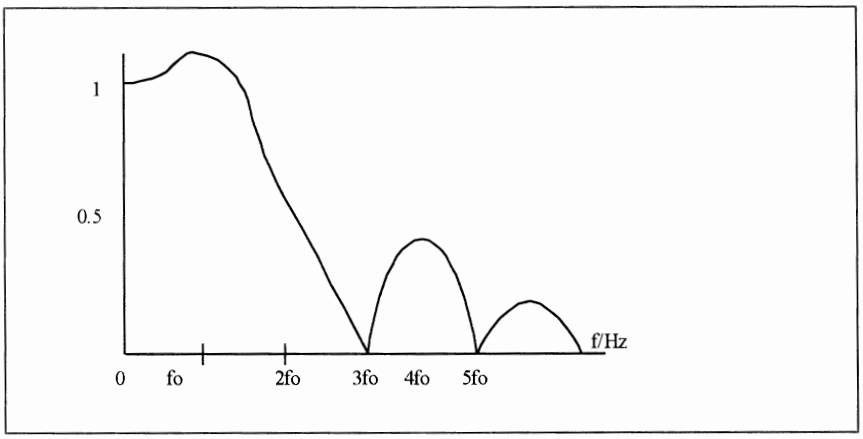

Figure(4-2) : Frequency response of a half cycle Fourier algorithm , 12 samples/cycle.

4-1-C : FOURIER ALGORITHMS BASED ON SPLITTING THE SIGNALS INTO TWO PHASE -SHIFTED COMPONENTS

To overcome the weakness of the previous two methods, another algorithm has been developed. It is based on splitting the signal into two phase-shifted components, and to correlating both of them with a

sinusoidal function only [4 4]. To develop the formulas, the input signal is assumed to be in the simplest form;

$$i_{(t)} = I_1 \cos(\omega_1 t - \alpha_1) \quad \text{..... (4-19)}$$

The signal may be split into two mutually phase-shifted components in a number of ways. The easiest is the following;

$$i_a(t) = i(t)$$
$$i_b(t) = i(t - T_s)$$

where, $T_s = 2\beta / \omega_1$, is the time difference between i_a and i_b. Both $i_{a(t)}$ and $b_{a(t)}$ are connected with the sinusoidal function, giving $F_{a(t)}$ and $F_{b(t)}$ respectively,

$$F_a(t) = \int_{t-T}^{t} i_a(\tau) \sin\left[\omega_1\left(\tau - t + \frac{T}{2}\right)\right] d\tau \quad \text{..... (4-20)}$$

$$F_{b(t)} = \int_{t-T_s-T}^{t-T_s} i_b(\tau) \sin\left[\omega_1\left(\tau - t + T_s + \frac{T}{2}\right)\right] d\tau \quad \text{..... (4-21)}$$

where, T is the duration of the data window.

Knowing the integrals $F_{a(t)}$ and $F_{b(t)}$ the amplitude I_1 and the phase angle α_1 may be expressed by means of the following formulas;

$$I_1 = \frac{\omega_1}{\omega_1 T - \sin(\omega_1 T)} \sqrt{\left[\left(\frac{F_a + F_b}{\cos\beta}\right)^2 + \left(\frac{F_a - F_b}{\sin\beta}\right)^2\right]} \quad \text{..... (4-22)}$$

$$\alpha_{1r} = \arctan\left[\left(\frac{F_b + F_a}{F_b - F_a}\right)\tan\beta\right] \quad \text{..... (4-23)}$$

where, α_{1r} is the phase angle related to the middle of the data window;

$$\alpha_{1r} = \omega_1(t - T/2) - (\alpha_1 - \beta)$$

Equations (4-22) and (4-23) become simpler if the phase angle between i_a and i_b becomes $\pi/2$ ($\beta=\pi/4$). Then,

$$I_1 = \frac{2\omega_1}{\omega_1 T - \sin(\omega_1 T)} \sqrt{F_a^{\,2} + F_b^{\,2}} \qquad \text{..... (4-24)}$$

$$\alpha_{1r} = \arctan\left(\frac{-F_a}{F_b}\right) - \frac{\pi}{4} \qquad \text{..... (4-25)}$$

If the above method of splitting is applied, one may notice that,

$$F_b(t) = F_a(t\text{-}Ts)$$

which greatly simplifies computations, because to obtain $F_b(t)$ one does not need to perform multiplications and intigrations, but simply to recall from the computer memory $F_a(t\text{-}Ts)$. However, this method of splitting increases the time of measurements by Ts.

Figure (4-3) shows the frequency response of the algorithm. In general the frequency characteristic show s better rejection of non-fundamental frequency components. The algorithm computational burden depends on the method of the splitting, but it is more or less the same. Correlating with Walsh function instead of sinusoid can reduce the computational burden.

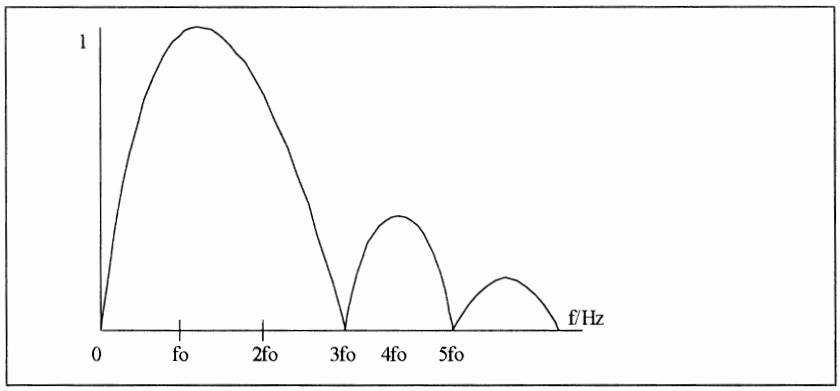

Figure(4-3): Frequency response of the splitting algorithm for a half-cycle data window.

4-1-D : WALSH FUNCTIONS ALGORITHMS

The Walsh functions have the advantage that all the multiplictions required in the evaluation of Fourier transforms are ±1 [4.1]. If we take $N = 2^n$ then,

$$F_n = \frac{1}{2^n}\sum_{k=1}^{2^n} f_k \cdot w_n(k\theta) \qquad \text{..... (4-26)}$$

More details are in section (3-1-c). For example the first 4 Walsh functions are shown in figure (4-4) along with the sample values $w_n(k\theta)$. An expansion in terms of the first four Walsh functions would involve the calculations,

$$F_1 = \tfrac{1}{4}(f_1 + f_2 + f_3 + f_4)$$
$$F_2 = \tfrac{1}{4}(f_1 + f_2 - f_3 - f_4)$$
$$F_3 = \tfrac{1}{4}(f_1 - f_2 - f_3 + f_4)$$
$$F_4 = \tfrac{1}{4}(f_1 - f_2 + f_3 - f_4)$$

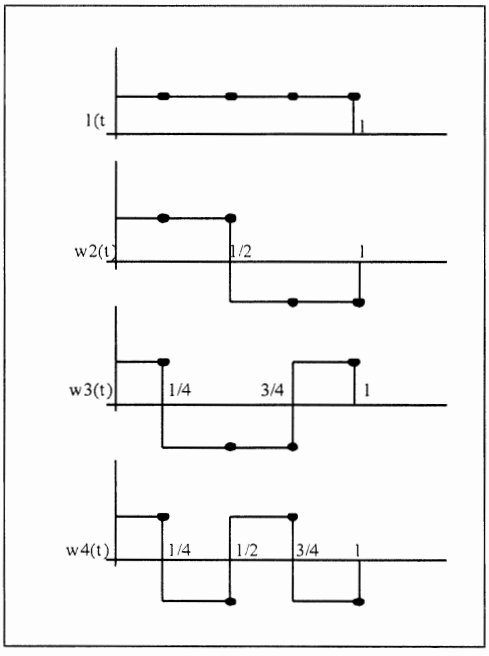

Figure(4- 4) : The first four Walsh functions and their sample values.

The only problem with the Walsh expansion is that a large number of Walsh terms must be included in order to obtain an accurate estimate of the components. The need for a large number of terms and the need to convert from Walsh to Fourier counterbalance the advantage of simplicity of equation (4-26). The frequency response of the Walsh algorithm is much alike the full cycle Fourier algorithm if a sufficient number of Walsh coefficients are used.

4-2 : DIFFERENTIAL EQUATIONS SOLUTION ALGORITHMS

The differential equation algorithms are based on a model of the system rather than on a description of the waveforms. Consider the single-phase model of a short faulted line shown in figure(4-5),

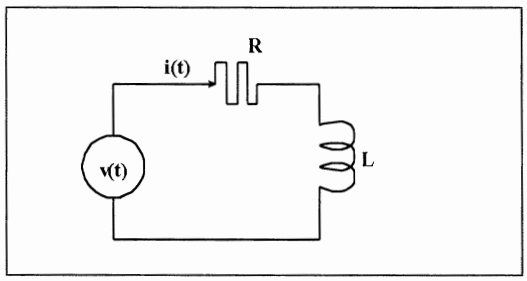

Figure(4- 5): Series R-L model of a transmission line.

which can be described by,

$$v(t) = R \cdot i(t) + L\frac{di}{dt} \qquad \text{(4-27)}$$

All the methods using this equation attempt to find values of R and L such that the equation is satisfied by the input signals of voltage and currents. It is clear from the solution of equation (4-27) that the dc offset is intrinsically considered in such algorithms.

4-2-A: SOLVING THE DIFFERENTIAL EQUATIONS BY DIGITAL DIFFERENTIATION

Solution for R and L parameters is accomplished by numerical differentiation over two successive time periods and solution of the resulting simultaneous liner equations [4.8].

If one takes samples of line voltage and current waveforms at uniform time increments T=Δt and replaces the derivatives in equation(4-27), by its finite difference (i.e., central) for each of two successive set of sampling, one gets,

$$\left.\frac{di}{dt}\right]_{t_k} \cong \frac{i_k - i_{k-1}}{2\Delta t} = \frac{i_k - i_{k-1}}{2T}$$

then equation (4-27) can be obtained as,

$$\begin{bmatrix} i_k & \frac{i_{k+1}-i_{k-1}}{2T} \\ i_{k+1} & \frac{i_{k+2}-i_k}{2T} \end{bmatrix} \cdot \begin{bmatrix} R \\ L \end{bmatrix} = \begin{bmatrix} v_k \\ v_{k+1} \end{bmatrix} \quad \text{..... (4-28)}$$

Equation (2-28) can be solved for R and L;

$$R = \frac{v_k}{i_k} - \left(\frac{i_{k+1} - i_{k-1}}{i_k}\right)\left[\frac{(v_{k+1}i_k) - (v_k i_{k+1})}{i_k(i_{k+2} - i_k) - i_{k+1}(i_{k+1} - i_k)}\right] \quad \text{..... (4-29)}$$

$$L = 2T\left[\frac{(v_{k+1}i_k) - (v_k i_{k+1})}{i_k(i_{k+2} - i_k) - i_{k+1}(i_{k+1} - i_k)}\right] \quad \text{..... (4-30)}$$

4-2-B: SOLVING THE DIFFERENTIAL EQUATIONS BY DIGITAL INTEGRATION

Since derivatives of measured quantities are difficult to produce, a more tractable form of equation (4-27) can be obtained by integrating equation (4-27) over two consecutive intervals [4.10];

$$\int_{t_0}^{t_1} v(t)\,dt = R\int_{t_0}^{t_1} i(t)\,dt + L\frac{[i(t_1) - i(t_0)]}{T} \quad \text{..... (4-31)}$$

$$\int_{t_1}^{t_2} v(t)\,dt = R\int_{t_1}^{t_2} i(t)\,dt + L\frac{[i(t_2)-i(t_1)]}{T} \quad \text{..... (4-32)}$$

If the samples are equally spaced at an intervals $T=\Delta t$, and using the Trapezoidal method of integration, then,

$$\int_{t_0}^{t_1} v(t)\,dt \cong \frac{[v_k + v_{k+1}]}{2}$$

where v_k is the sample value at t_0 and V_{k+1} is the sample value at t_1, ... etc. Thus, equations (4-31) and (4-32) can be written for samples at k, k+1, and k+2 as,

$$\begin{bmatrix} \frac{T}{2}(i_{k+1}+i_k) & (i_{k+1}-i_k) \\ \frac{T}{2}(i_{k+2}+i_{k+1}) & (i_{k+2}-i_{k+1}) \end{bmatrix}\begin{bmatrix} R \\ L \end{bmatrix} = \begin{bmatrix} \frac{T}{2}(v_{k+1}+v_k) \\ \frac{T}{2}(v_{k+2}+v_{k+1}) \end{bmatrix} \quad \text{..... (4-33)}$$

The three samples of current and voltage are sufficient to estimate of R and L as,

$$R = \left[\frac{(v_{k+1}+v_k)(i_{k+2}-i_{k+1}) - (v_{k+2}+v_{k+1})(i_{k+1}-i_k)}{(i_{k+1}+i_k)(i_{k+2}-i_{k+1}) - (i_{k+2}+i_{k+1})(i_{k+1}-i_k)}\right] \quad \text{..... (4-34)}$$

$$L = \frac{T}{2}\left[\frac{(i_{k+1}+i_k)(v_{k+2}+v_{k+1}) - (i_{k+2}+i_{k+1})(v_{k+1}+v_k)}{(i_{k+1}+i_k)(i_{k+2}-i_{k+1}) - (i_{k+2}+i_{k+1})(i_{k+1}-i_k)}\right] \quad \text{..... (4-35)}$$

This algorithm of a short data window and thus it is not as selective as longer data window algorithms. The extension of the differential equation approach to a longer window takes a number of forms. One approach for example is to make the intervals of the integration in equations (4-31) and (4-32) longer.

4-2-C: MODIFYING THE DIFFERENTIAL EQUATION ALGORITHMS

The major strength of the differential equation algorithms, is that the estimations of R and L are correct as long as v(t) and i(t) satisfy the differential equation. It is well known that the voltage signal seen by the relay just after fault inception has non-fundamental frequency components caused by the power system itself. If the faulted line can accurately be modeled as a series R-L line then the current will respond to these non-fundamental frequency components in the voltage and no error in estimating R and L will result. A somewhat more realistic model of the faulted line can be used to investigate the impact of these power system signals on such algorithms [4.9].

The circuit shown in figure (4-6) includes the shunt capacitance of the transmission line at the relay terminal.

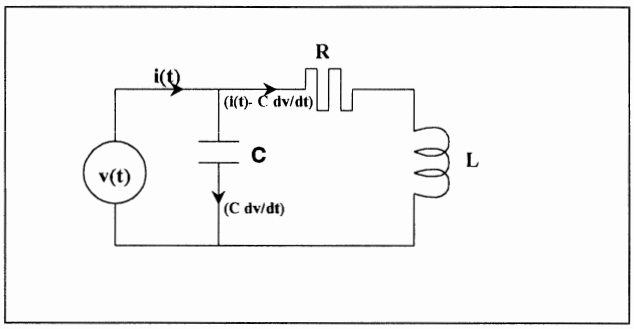

Figure(4- 6) : A single-phase line model with shunt capacitance.

The voltage source v(t) represents the voltages made up of fundamental plus non-fundamental components whose frequency and phase are unpredictable. The current i(t) is the current measured by the relay. the actual relationship between the measured voltage and current is given by,

$$v(t) = R \cdot i(t) + L\frac{di(t)}{dt} - R \cdot C\frac{dv(t)}{dt} - L \cdot C\frac{d^2v(t)}{d^2t} \qquad \text{..... (4-36)}$$

Compare the last equation with equation (4-27), the last two terms in equation (4-36) must be regards as error terms. The magnitude of these

terms is a function of fault location and the frequency of the signal in v(t). The dependence on fault location is quadratic, reaching a maximum for a fault at the end of the line.

If one takes samples of line voltage and current waveforms at uniform time increments $T=\Delta t$ and replaces the derivatives in equation(4-36), by its finite difference (i.e., central) for each of two successive set of sampling, one gets,

$$\left.\frac{di}{dt}\right]_{t_k} \cong \frac{i_k - i_{k-1}}{\Delta t} = \frac{i_k - i_{k-1}}{T}$$

then a more elaborate version of equation (4-33) can be obtained by considering 4 consecutive intervals,

$$\begin{bmatrix} \frac{T}{2}(i_{k+1}+i_k) & (i_{k+1}-i_k) & -(v_{k+1}-v_k) & -\frac{1}{T}(v_{k+1}-2v_k+v_{k-1}) \\ \frac{T}{2}(i_{k+2}+i_{k+1}) & (i_{k+2}-i_{k+1}) & -(v_{k+2}-v_{k+1}) & -\frac{1}{T}(v_{k+2}-2v_{k+1}+v_k) \\ \frac{T}{2}(i_{k+3}+i_{k+2}) & (i_{k+3}-i_{k+2}) & -(v_{k+3}-v_{k+2}) & -\frac{1}{T}(v_{k+3}-2v_{k+2}+v_{k+1}) \\ \frac{T}{2}(i_{k+4}+i_{k+3}) & (i_{k+4}-i_{k+3}) & -(v_{k+4}-v_{k+3}) & -\frac{1}{T}(v_{k+4}-2v_{k+3}+v_{k+2}) \end{bmatrix} \cdot \begin{bmatrix} R \\ L \\ RC \\ LC \end{bmatrix} =$$

$$\begin{bmatrix} \frac{T}{2}(v_{k+1}+v_k) \\ \frac{T}{2}(v_{k+2}+v_{k+1}) \\ \frac{T}{2}(v_{k+3}+v_{k+2}) \\ \frac{T}{2}(v_{k+4}+v_{k+3}) \end{bmatrix} \quad \text{..... (4-37)}$$

If equation (4.37) is thought of as partitioned matrix in the form,

$$\begin{bmatrix} M11 & M12 \\ M21 & M22 \end{bmatrix} \cdot \begin{bmatrix} P \\ CP \end{bmatrix} = \begin{bmatrix} E1 \\ E2 \end{bmatrix} \quad \text{..... (4-38)}$$

where,

$$M11 = \begin{bmatrix} \frac{T}{2}(i_{k+1}+i_k) & (i_{k+1}-i_k) \\ \frac{T}{2}(i_{k+2}+i_{k+1}) & (i_{k+2}-i_{k+1}) \end{bmatrix}$$

$$M12 = \begin{bmatrix} (i_{k+2}-i_{k+1}) & -\frac{1}{T}(v_{k+1}-2v_k+v_{k-1}) \\ -(v_{k+2}-v_{k+1}) & -\frac{1}{T}(v_{k+2}-2v_{k+1}+v_k) \end{bmatrix}$$

$$M21 = \begin{bmatrix} \frac{T}{2}(i_{k+3} + i_{k+2}) & \frac{T}{2}(i_{k+3} - i_{k+2}) \\ \frac{T}{2}(i_{k+4} + i_{k+3}) & (i_{k+4} - i_{k+3}) \end{bmatrix}$$

$$M22 = \begin{bmatrix} -(v_{k+3} - v_{k+2}) & -\frac{1}{T}(v_{k+3} - 2v_{k+2} + v_{k+1}) \\ -(v_{k+4} - v_{k+3}) & -\frac{1}{T}(v_{k+4} - 2v_{k+3} + v_{k+2}) \end{bmatrix}$$

$$P = \begin{bmatrix} R \\ L \end{bmatrix}$$

$$CP = \begin{bmatrix} RC \\ LC \end{bmatrix}$$

$$E1 = \begin{bmatrix} \frac{T}{2}(v_{k+1} + v_k) \\ \frac{T}{2}(v_{k+2} + v_{k+1}) \end{bmatrix}$$

$$E2 = \begin{bmatrix} \frac{T}{2}(v_{k+3} + v_{k+2}) \\ \frac{T}{2}(v_{k+4} + v_{k+3}) \end{bmatrix}$$

then, the estimation can be formed by solving the second set of equations and substituting into the first set to get,

$$\begin{bmatrix} R \\ L \end{bmatrix} = \left(M_{11} - M_{12} \cdot M_{22}^{-1} \cdot M_{21}\right)^{-1} \cdot (E_1 - M_{12} \cdot M_{22}^{-1} \cdot E_2) \quad \text{..... (4-39)}$$

4-3: FAULT CLASSIFICATION

All the previous presented algorithms are essentially single-phase algorithms. The Fourier algorithms are for a single current and voltage and the differential-equation algorithms are of a single-phase R-L model [4.1]. A line relay using one of those algorithms would protect one terminal of a three-phase transmission line. If the phases are labeled as a, b, and c then there are a total of ten possible faults that can be seen by the relay as illustrated in table (4-1). Since the fault type is not known, the algorithm must process samples of all the voltages and currents in order to determine the fault type.

The simplest distance relaying algorithm would process six single-phase distance equations corresponding to three phase to ground faults and three phase to phase faults. Generally, there are three procedures to process the six equations,

Type of Faults	Descriptions
Three single phase to ground faults	a-ground, b-ground, c-ground
Six double phase to ground faults	a-b, b-c, c-a, a-b-ground, b-c-ground, c-a-ground
One three phase fault	a-b-c

Table(4-1) : Transmission line faults clasification.

4-3-A: SIMPLE RELAY PROGRAM

It is by processing all six-distance equations between successive samples. Although it may be hard to fulfill this procedure, but the next generations of high-speed microprocessors will make such a procedure practical. The flow chart of this procedure is shown in Figure (4-7). In this program, all the six distances are computed and checked against the relay characteristic to determine the appropriate relay response.

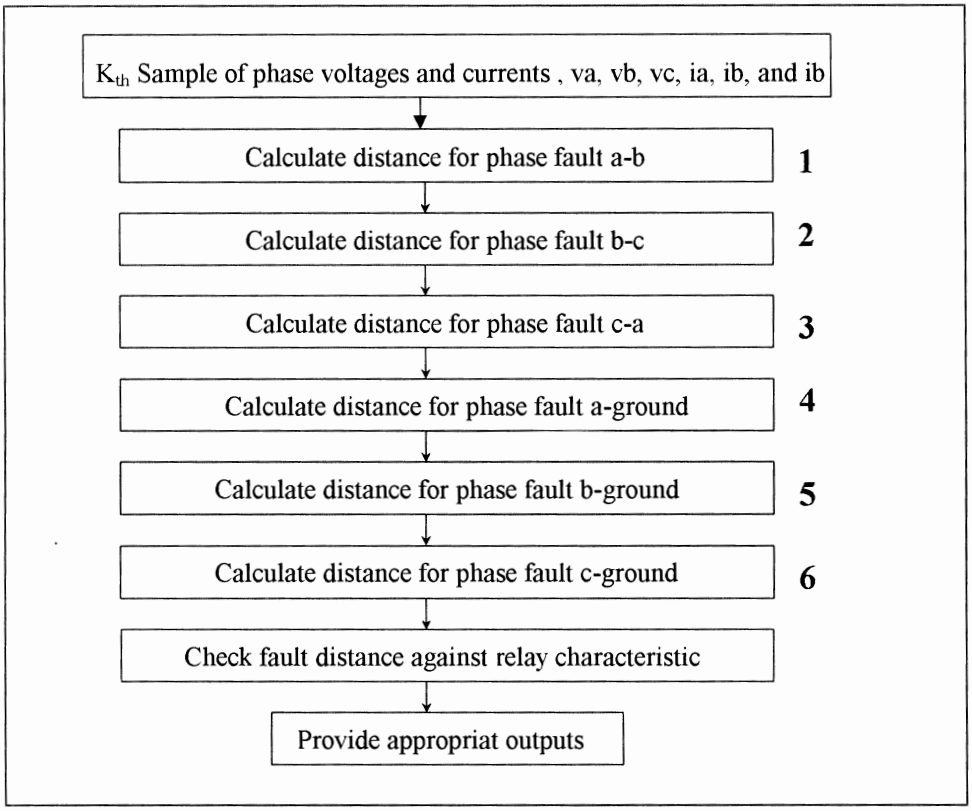

Figure(4- 7) : A simple relay program.

For a given fault, only some of the distance calculations will produce correct fault distances. For example, for a phase a-b fault, only block 1 will produce the correct fault distance, while for a three phase fault will produce correct distance in all six blocks.

4-3-B: CLASSIFICATION RELAY PROGRAM

In this procedure, only one of the six equations would be processed for any fault, and considerable computational efficiency would be achieved. The program flowchart is shown in figure (4-8). Such program has been based on the voltage deviation criterion to classify a fault. The voltage sample of any phase compared with its value one cycle ago. If the voltage difference reaches or exceeds a threshold while other phases remain undisturbed, then a single phase to ground fault at that phase is declared. This is mentioned for each phase, and if two phases reach the threshold simultaneously, a phase to phase fault is declared. Voltage classifier could be supplemented with a similarly designed current classifier.

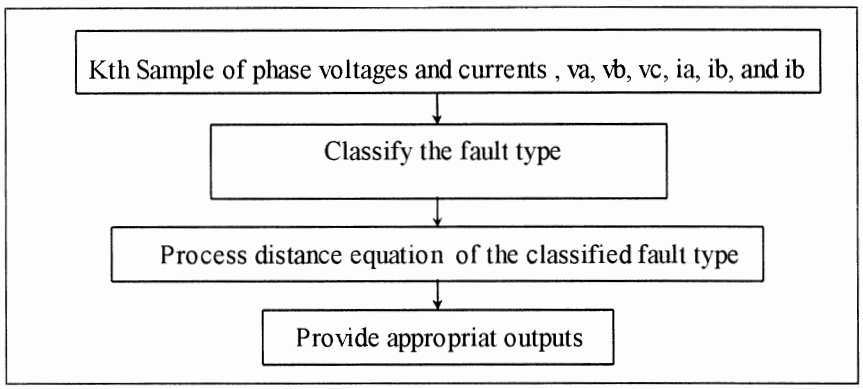

Figure(4- 8): Classification relay program.

Fault classification schemes based upon voltage and/or currents are used in several practical relaying programs. They produce correct fault classification under most reasonable conditions. Anyhow, it fails to classify in some cases. The voltage based classifiers fail to classify when short lines are supplied from a weak system or when a long line is fed from a strong system. In the former case all voltages deviate considerably from nominal , while in the latter case faults near a zone boundary produce hardly any voltage deviation in the faulted phase at

the relay location. The current classifier are also confused when load currents are significant compared to the fault current. Whenever the classification is uncertain , it must be recognized as such, and all six equations must be processed at each sample time (i.e., using the first program).

Another limitation of the classification programs is that, no fault processing can start until the classification is finished and a valuable time is lost. This makes for slower relay response time.

4-4: SYMMETRICAL COMPONENT ALGORITHMS

This algorithm makes use of the symmetrical component theory. The most significant feature of this algorithm is the single performance equation, which is used to determine the distance to a fault from a transmission line terminal regardless of the type of the fault. Thus, it overcomes the uncertainty of the fault classifiers and their attendant delay of response in a neat manner [4.11].

If we are familiar with the definition of the symmetrical component theory, the symmetrical component of the three phase voltages and currents are,

$$\begin{bmatrix} E_o \\ E_1 \\ E_2 \end{bmatrix} = \begin{bmatrix} 1 & 1 & 1 \\ 1 & \alpha & \alpha^2 \\ 1 & \alpha^2 & \alpha \end{bmatrix} \cdot \begin{bmatrix} E_a \\ E_b \\ E_c \end{bmatrix} \quad \text{..... (4-40)}$$

$$\begin{bmatrix} I_o \\ I_1 \\ I_2 \end{bmatrix} = \begin{bmatrix} 1 & 1 & 1 \\ 1 & \alpha & \alpha^2 \\ 1 & \alpha^2 & \alpha \end{bmatrix} \cdot \begin{bmatrix} I_a \\ I_b \\ I_c \end{bmatrix} \quad \text{..... (4-41)}$$

where for voltages,

E_a, E_b, and E_c : are the phase to ground voltages.

E_o, E_1, and E_2 : are the zero, positive, and negative sequence quantities of the voltage respectively.

I_a, I_b, and I_c : are the phase currents.

I_o, I_1, and I_2 : are the zero, positive, and negative sequence quantities of the current respectively.

$\alpha = e^{\frac{j2\pi}{3}}$

Equations (4-40) and (4-41) normally assume a steady state, and the fundamental frequency is implied by the phasor representations used. Using equation (3-49), the fundamental frequency phasor associated with a signal x(t) is given as,

$$X_1 = \frac{\sqrt{2}}{N} \sum_{n=0}^{N-1} x_n \, e^{-j2\pi n / N}$$

where,
N : is number of samples per a cycle.
$x_n = x(\frac{2\pi n}{N\omega})$

Consider a fault takes place at a fraction (k) of the line length away from the relay as shown in figure (4-9), then with a pre-fault load currents of $\bar{I}_0, \bar{I}_1$, and $\bar{I}_2$, we can define the changes in the component currents as,

$$\begin{aligned} \Delta I_o &= I_o - \bar{I}_o \\ \Delta I_1 &= I_1 - \bar{I}_1 \\ \Delta I_2 &= I_2 - \bar{I}_2 \end{aligned} \quad \text{..... (4-42)}$$

The voltage drops in the line can be defined as,

$$\begin{aligned} \Delta E_o &= \Delta I_o \cdot Z_o \\ \Delta E_1 &= \Delta I_1 \cdot Z_1 \\ \Delta E_2 &= \Delta I_2 \cdot Z_2 \end{aligned} \quad \text{..... (4-43)}$$

where, Z_o, Z_1, and Z_2 are the sequence impedance of the entire line.

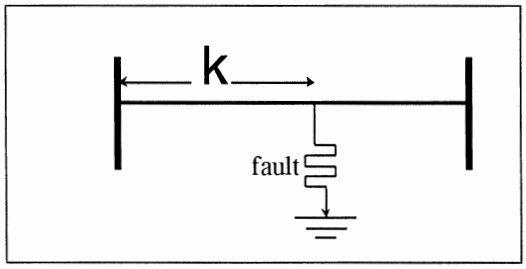

Figure (4- 9): A fault of a fraction k of the line length.

The following ratios are defined [4.11] which play an important role in determining fault location for all faults,

$$k_o = \frac{E_o}{\Delta E_o}$$

$$k_1 = \frac{E_1}{\Delta E_1}$$

$$k_2 = \frac{E_2}{\Delta E_2} \qquad \text{..... (4-44)}$$

$$k_1 = \frac{Z_1 \cdot \bar{I}_1}{\Delta E_1}$$

Consider a three-phase fault with a fault resistance R_f, would involve only the positive sequence network. The voltage equation is then;

$$\Delta E_1[k_1 - k(1+k_1)] - R_f I_1 = 0 \qquad \text{..... (4-45)}$$

or;

$$k = \frac{k_1}{1+k_1} + \varepsilon_r$$

where, $\varepsilon_r = \dfrac{-R_f I_1}{\Delta E_1(1+k_1)}$. Considering all possible fault types, a general expression for the fractional distance to the fault can be obtained [4.11] in the form,

$$k = \frac{k_1 + k_2 k_2' + k_o k_o'}{1 + k_o' + k_2' + k_1} \qquad \text{..... (4-46)}$$

where,

$$k_o' = \left| \frac{\Delta E_o}{\Delta E_1} \right|$$

and

$$k_2' = \begin{cases} 1 & \text{if } |\Delta E_2| \cong |\Delta E_1| \\ 0 & \text{otherwise} \end{cases}$$

REFERENCES

(4.1) A. G. PHADKE AND J. S. THORP, " COMPUTER RELAYING FOR POWER SYSTEMS", BOOK, JOHN WILEY & SONS INC. 1988.

(4.2) "EVALUATION OF ULTRAHIGH SPEED RELAY ALGORITHMS", EPRI EL-3996, PROJECT 1422-2, FINAL REPORT, MAY 1985.

(4.3) W. J. SMOLINSKI AND B. JEYASURYA, "IDENTIFICATION OF A BEST ALGORITHM FOR DIGITAL DISTANCE PROTECTION OF TRANSMISSION LINES", IEEE TRANSACTIONS ON POWER APPARATUS AND SYSTEMS, VOL. PAS-102, No. 10, OCTOBER 1983, PP. 3358-3369.

(4.4) A. WISZNIEWSKI, " NEW ALGORITHM OF CALCULATING CURRENT AND VOLTAGE PHASORS FOR FAST PROTECTION", IEE PROCEEDINGS, VOL.134, PT.C, No. 1, JAN. 1987, PP. 81-82.

(4.5) A. WISZNIEWSKI, "HOW TO REDUCE ERRORS OF DISTANCE FAULT LOCATING ALGORITHMS", IEEE TRANSACTIONS ON POWER APPARATUS AND SYSTEMS, VOL. PAS-100, No. 12, DEC. 1981, PP. 4815-4820.

(4.6) A. WISZNIEWSKI, "SIGNAL RECOGNITION IN PROTECTIVE RELAYING", DEVELOPMENTS IN POWER SYSTEM PROTECTION, IEE CONFERENCE PUBLICATION No. 185, LONDON, JUNE, 1980, PP. 132-136.

(4.7) G. R. SLEMON, S. D. T. ROBERTSON, M. RAMAMOORTY, " HIGH SPEED PROTECTION OF POWER SYSTEMS BASED ON IMPROVED POWER SYSTEM MODELS", CIGRE, PARIS, JUNE 1968, PAPER 31-09.

(4.8) W. J. SMOLINSKI, "AN ALGORITHM FOR DIGITAL IMPEDANCE CALCULATING USING A SINGLE PI SECTION TRANSMISSION LINE MODEL", IEEE TRANSACTIONS ON POWER APPARATUS AND SYSTEMS, VOL. PAS-98, No.5, SEPT./OCT. 1979, PP. 1546-1551.

(4.9) W. J. SMOLINSKI, "AN ALGORITHM FOR DIGITAL IMPEDANCE CALCULATING USING A SINGLE PI SECTION TRANSMISSION LINE MODEL", IEEE TRANSACTIONS ON POWER APPARATUS AND SYSTEMS, VOL. PAS-99, No.6, NOV./DEC. 1980, PP. 2251-2252.

(4.10) A. D. MCINNES , I. F. MORRISON, "REAL TIME CALCULATIONS OF RESISTANCE AND REACTANCE FOR TRANSMISSION LINE PROTECTION BY DIGITAL COMPUTER", ELECTRICAL ENGINEERING TRANSACTIONS IE, AUSTRALIA, VOL. EE7, No. 1, 1970, PP. 16-23.

(4.11) A. G. PHADKE, M. IBRAHIM, & T. HALIBKA, "FUNDAMENTAL BASIS FOR DISTANCE RELAYING WITH SYMMETRICAL COMPONENTS", IEEE TRANSACTIONS ON POWER APPARATUS AND SYSTEMS, VOL. PAS-96, NO.2, MARCH/APRIL 1977, PP. 635-646.

CHAPTER FIVE

TRANSIENT ULTRA HIGH SPEED ALGORITHMS FOR TRANSMISSION LINE PROTECTION

5-1: INTRODUCTION

The fault energies of power transmission and super-grid systems are steadily rising as a consequence of closer meshing and increasing power generation. Power system plants are thus subjected to higher elector-dynamic and thermal stresses than before. It is the task of the transmission line protection to detect, and eliminate faults reliable, selectively, and in the shortest possible time. Its decisions have to be based mainly on the voltages and currents signals available locally.

The distance relays based fundamental frequency components to calculate the line impedance, achieve operating times of order of a period of the power system frequency. Taking the time for fault detection and circuit breakers into account, protection principles of this kind result in overall fault clearing times of three to five periods. If the frequently voiced demand for shorter fault clearing times is to be satisfied, then faster but more expensive circuit breakers and/or new protection operating principles have to be applied.

In addition to speed of operation it is often desirable to achieve the greatest possible degree of protection redundancy, particularly at the highest system voltage level. Thus a combination of an ultra high-speed (UHS) directional comparison scheme and a distance scheme appears to be an ideal solution, because the performance of the two principles complement each other perfectly in operation.

In general, the transient UHS algorithms can be divided into two groups. The first bases the evaluation of deviation signals, and the second acts on travelling wave principles.

5-2: TRANSIENT ALGORITHMS BASED ON DEVIATION SIGNALS

The operation of such a protective schemes depends on the exchange of the directional or command information rather than the exchange of quantitative information between both ends of the line. Working with local information in this way makes for faster operation. Such an approach is necessary for sensing devices for fault current limiters.

A common feature of these algorithms is that they act on the transient produced, superimposed signals, also called deviation signals, rather than on the signals themselves. The basis for using such quantities in transient protection algorithms is best explained by reference to the simple single-phase line connecting two sources as shown in figure (5-1)

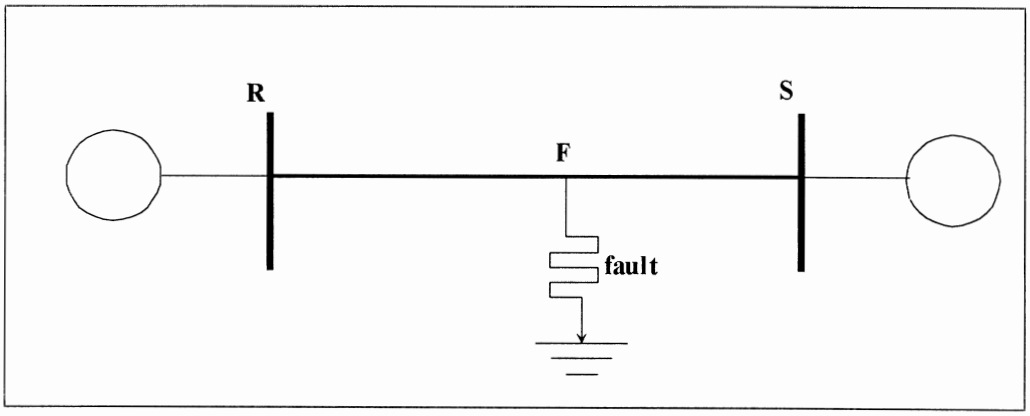

Figure (5- 1): A single-phase system showing a fault on the transmission line.

Consider a fault occurring at time t= 0, at a point F on the line located at a distance d from the relaying station at R. Prior to the occurrence of the fault the voltage at F is given by the sinusoidal steady state voltage which can be written as,

$$V_F(t) = V_F \sin(\omega t + \phi)$$

Where, V_F is the magnitude of the steady state voltage at F and ϕ is the fault angle. At t=0, upon the inception of the fault and under the assumption of zero fault impedance, the voltage at F is zero. It is as if

an imaginary sinusoidal voltage had been applied at F forcing the voltage at F to zero. This superimposed voltage has the same magnitude as the prefault voltage but is of opposite sign. Assuming linearity, the principle of superposition may be applied to yield the total solution. According to this principle, the total solution is the sum of two independent solutions, namely, the *steady state solution* due to the original sources, and the *incremental solution* due to the imaginary source, as shown in Figure (5-2).

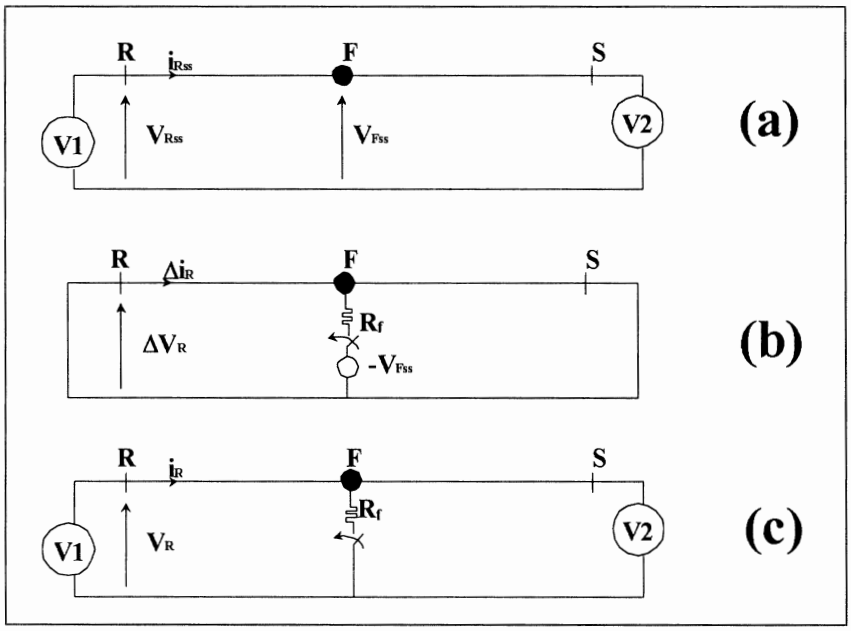

Figure (5- 2): The principle of superposition applied to the fault in figure (5-1). a- steady-state solution. b- incremental solution. c- total sum.

The circuit (a) in figure (5-2) represents the steady-state solution; circuit (b) represents the incremental solution, while (c) represents the transient solution, which is the sum of the previous solution. The deviation signals in (b) (i.e., ΔV_R and Δi_R), contains all the transient information. For that reason, the transient algorithms presented in this section effectively utilize the deviation signals of voltage and current at the relaying station R. From figure (5-2),

Transient solution = Pre-fault steady state solution + Incremental solution

or,

$$\Delta v = v_R - v_{RSS}$$
$$\Delta i = i_R - i_{RSS} \quad \text{..... (5-1)}$$

It can be noted from equation (5-1) that the steady-state signals (i.e., v_{Rss} and i_{Rss}) are subtracted from the transient measured signals (i.e., v_R and i_R), to give the deviation signals (i.e., Δv_R and Δi_R). Sinusoidal functions representing the steady-state signals can be estimated from previous measurements. These should be updated periodically to accord with changing load conditions on the system. It should be clear that under normal unfaulted steady-state conditions, the deviation quantities are zero except for the presence of noise or system generated harmonics.

Many algorithms have been proposed for transmission line protection based on deviation signals. Two algorithms will be taken as an example since the door is still opened for many ideas in this field. The first represent the first algorithm suggested by M. Vitins [5-3], which was considered as the base for the deviation, signals algorithms. This algorithm is then modified; designed and produced by ABB company [5-4].

5-2-A: THE VITINS ALGORITHM

The algorithm represents a geometrical approach to the detection of fault directional comparison protective schemes[5-3]. Figure (5-3) represents a lumped parameter model of transmission line connecting two sources. The source and line impedances are assumed to be of pure inductances. Assume that at time t=0 a fault occurred at point F, then figure (5-4) shows the superimposed fault model of the system as described earlier. If the fault resistance is zero and the prefault voltage at F is given by,

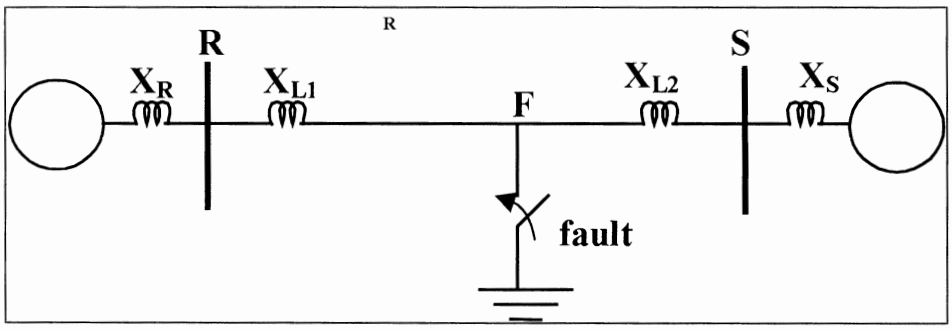

Figure (5- 3): Lumped parameter representation of a single system with a faulted line.

$$V_F = E \sin(\omega t+\gamma) \quad \text{..... (5-3)}$$

where γ, is the fault angle, then the deviation signals Δv and Δi measured at the relaying side R, are given as,

$$\Delta v(t) = \frac{X_S}{X_S+X_L} \cdot E \cos(\omega t + \gamma) \quad \text{..... (5-4)}$$

$$\Delta i(t) = \frac{1}{X_S+X_L} \cdot E \left[\sin(\omega t + \gamma) - \sin(\gamma)\right] \quad \text{..... (5-5)}$$

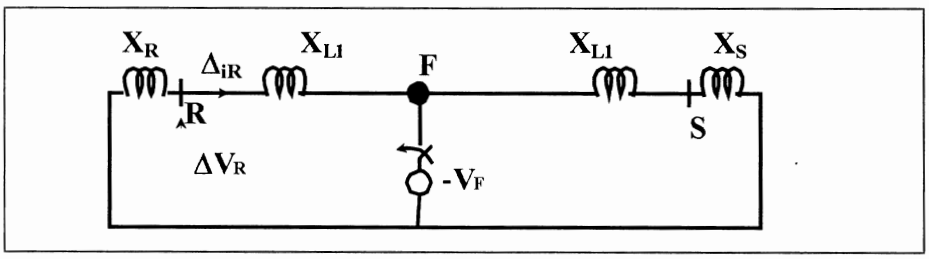

Figure (5- 4): Superimposed fault model of the circuit in figure (5-3).

where, $X_L=X_{L1}+X_{L2}$. Note that the current deviation contains dc offset the magnitude of which depends on the fault inception angle. Inclusion of resistance in the fault loop will cause this offset to decay exponentially. Furthermore, the magnitudes of the deviation signals of voltage and current will be reduced and the phase shift between the fundamental components of the deviation signals will be less than 90°.

To study the influence of system parameters and fault inception angle on the deviation signals, Vitins proposed to plot the instantaneous values of the deviation signals on a plane described by two coordinates,

Δv and $R\Delta i$, where R is an arbitrary scaling factor. Upon the occurrence of a fault, a trajectory is generated in the deviation plane as illustrated in figure (5-5).

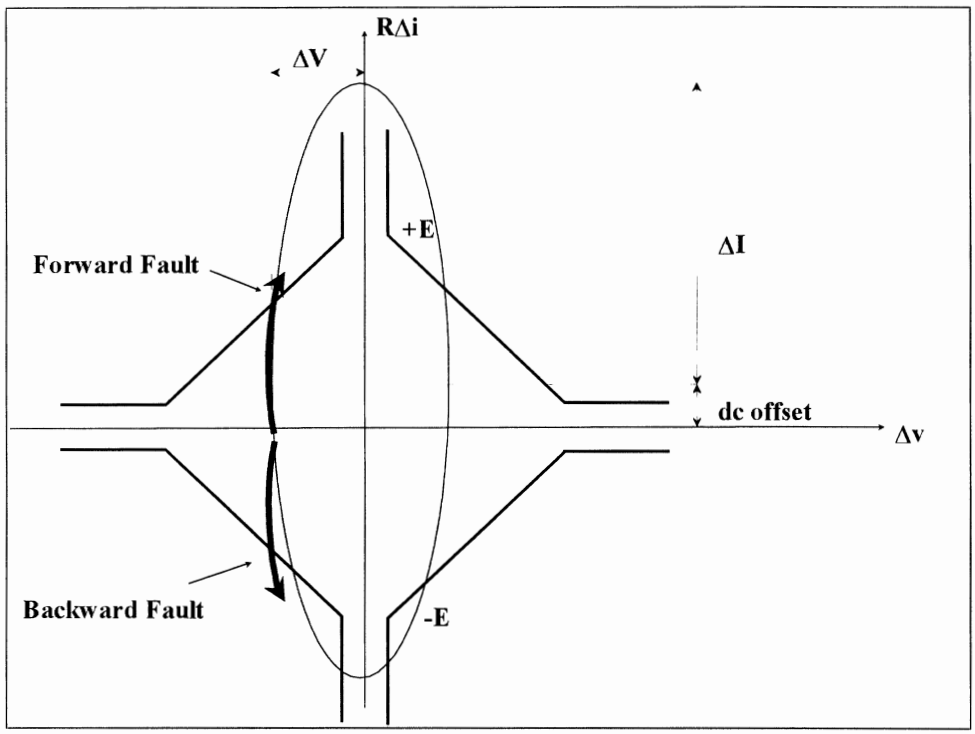

Figure (5-5): Illustrating the Trajectory and Operating Principle of the Vitins Algorithm.

Since the transmission line is being represented by an inductance, sudden changes in current are impossible. The fault trajectory initially jumps from the origin to some point on the Δv axis. The magnitude of the initial jump is greatest for faults occurring at the instant of voltage peak, and is zero for faults occurring at voltage zero crossing. In this simple case, the deviation signals contain only the fundamental frequency. As a sequence, the phase shift between the signals is 90° and the fault trajectory has an elliptical shape with its axis coincident with the $R\Delta i$ axis. The center of the trajectory is displaced along this axis by an amount proportional to the current offset. This will be a maximum for fault inception at voltage zero and zero for fault inceptions at peak voltage.

In general, the imaginary source, and therefore the fault, will be said to be in the forward direction if it lies in the direction of positive current flow, while the voltage is measured as shown figure(5-3).

Faults in the opposit direction will be said to lie in the backward or reverse direction. The sign of the phase shift between the deviation signals determines the sense of rotation of the elliptical trajectory of figure (5-5). A forward fault, such as the one modeled in figure (5-4), will produce a clockwise sense of rotation when measured at terminal R, while a reverse fault measured at the same location will produce a trajectory with anti-clockwise sense of rotation. This means that, depending upon the inception angle, the trajectory of a forward fault will depart the Δv axis for quadrants II and IV, while the trajectory of a backward fault will leave the Δv axis for quadrants I and III. Thus, according to Vitins algorithm, the sense of rotation of the fault trajectory and the point or the quadrant at which the trajectory first crosses the threshold boundary in the deviation plane can be used as an indication of fault direction.

The boundary in figure (5-5), is defined for forward faults at the point at which the linear combination $(\Delta v - R\Delta i)$ reaches the value +E or -E, where E is the rated voltage of the line. For backward faults the boundary is defined at the point at which the linear combination of $(\Delta v + R\Delta i)$ reaches the value +E or -E.

The principle of this algorithm having been demonstrated in terms of lumped parameter model, anyhow, similar results are achieved with distributed parameters lines[5-3]. Low-pass filtering of the input signals is recommended to eliminate the effects of very high frequency transients produced by close-in faults and by lighting.

The primary advantage of this algorithm is its directionality, that is the way that it indicates the direction of the fault from the point of measurements. Setting appropriate boundaries define the reach of the algorithm, but this may be in some doubt at its limits. The extended boundaries along the axis emphasize the fact that for some fault trajectories, such as those measured at very high-energy centers, there may be a problem. In such cases, the trajectory may be so close to the $R\Delta i$ axis that practical detection of even the sense of direction may be impossible.

It has been found that the energization of long transmission lines or the clearing of faults and therefore capable of passing across the threshold boundary and maloperation takes place. Thus, it is proposed in this algorithm that no switching elements are located inside the protected zone.

It takes a whole period of the power system frequency to complete one revolution along the elliptical path. However, the trajectory will in general reach the threshold boundary in a small fraction of this time so that very high speed response times, ranging from, 0 to 6 msec, can be achieved.

In general, it has been found that the essential advantages of processing the deviation signals are;

-ultra high-speed operation (no more than 6 msec.).
-determination of fault direction.
-insensitive to power swings.
-insensitive to CT saturation.
-reduce performance requirements of CTs and VTs or CVTs.

5-2-B: THE MODIFIED VITINS ALGORITHM

The Vitins algorithm has been developed and a new UHS algorithm has been designed and produced[5-4]. The algorithm uses simultaneously, two different measuring algorithms to assure reliable operation also with respect to correct detection of fault phases.

This algorithm is based on the evaluation of the deviations of power line voltages and currents from their steady state value at the instant of a fault as shown in figure (5-6). The deviation signals are considered to be consist of three major components, a system frequency component, an exponential component arising from the time constants of the system (i.e., dc offset of the current), and high frequency components. Travelling waves, which propagate through the power system from the fault location, causes these high frequency components.

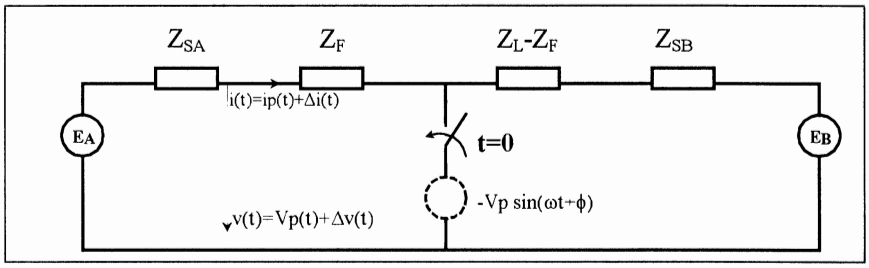

Figure (5- 6): Single-phase fault inception model.

Their frequency components are dependent on the speed of propagation c and on the distance between the fault location and the point of reflection (i.e., f = c/). The travelling wave principles will be considered in some details in coming sections. A new pair of equations is thus arrived at by correspondingly expanding equation (5-1),

$$v(t) = v_p(t) + \left[\Delta v_{ss}(t) + \Delta v_{exp}(t) + \Delta v_{tr}(t)\right]$$
$$i(t) = i_p(t) + \left[\Delta i_{ss}(t) + \Delta i_{exp}(t) + \Delta i_{tr}(t)\right] \quad \text{..... (5-6)}$$

The suffix signify the following,

ss : quasi steady-state (i.e., component at power system frequency).
exp: exponential (i.e., power system time constant).
tr : transient (i.e., travelling wave component)
p : prefault.

Considering for moment only the steady-state components (i.e., $\Delta v_{ss}(t)$ and $\Delta i_{ss}(t)$), when the instantaneous values of $\Delta v(t)$ and $\Delta i(t)$ are transferred into the Δ-plane, elliptical trajectories are obtained which are represented in section (5-2-A)[5-3]. The actual shape and size of the elliptical trajectories depends on a number of factors. It has been shown that the quotient $\Delta v/\Delta i$ corresponds to the source impedance Z_s. The shape of the trajectories for different Z_s and constant fault impedance Z_F is shown in figure (5-6).

Although the reach of the measuring systems plays a minor role in the case of the directional comparison protection, two things must be observed when deciding upon the operating characteristics to be adopted: -

1. The measurements must overreach for all kinds of faults within the protected zone and system impedance ratios.
2. The reach may not be so great that a risk exists of the healthy phase units picking up due to residual currents during an earth fault.

These consideration support the choice of an special shaped operating characteristic for dealing with such a family of trajectories shown in figure (5-7).

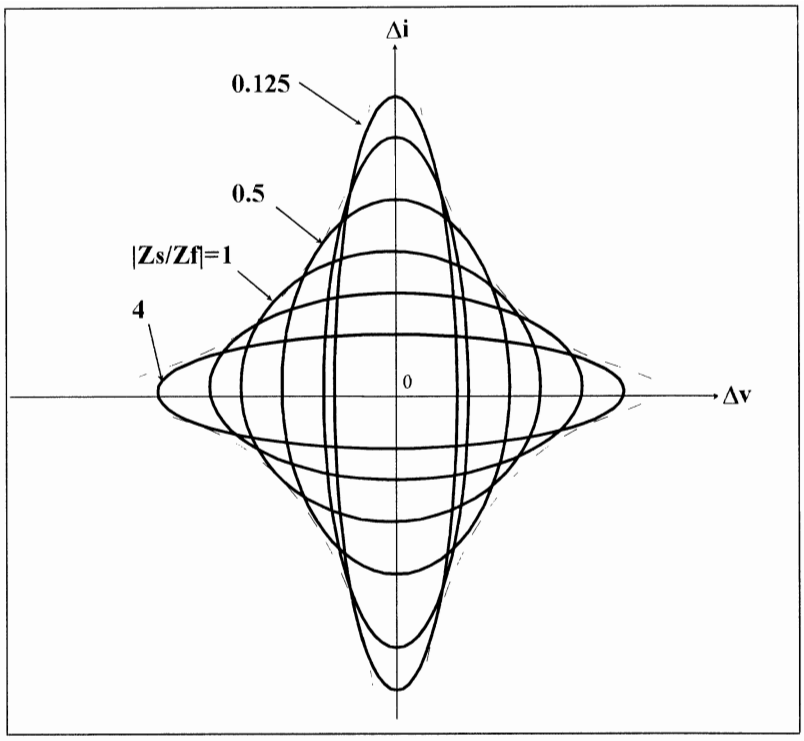

Figure(5- 7): Fault trajectories in the Δ-plane caused by forward faults. The faults accruing at a voltage maximum ($\angle Z_S=\angle Z_F=90°$).

The trajectories shown in figure (5-7) correspond to faults occurring at a voltage maximum ($\phi=90°$). At other angles of fault incidence the elliptical trajectories are shifted along the Δi-axis by an amount $\hat{I}\cos(\phi)$ as shown in figure (5-8), and it is no longer permissible to neglect the exponential term Δi_{exp}. It is therefore not possible to define an operating characteristic having a constant reach in the deviation plane (i.e., Δv, Δi-plane).

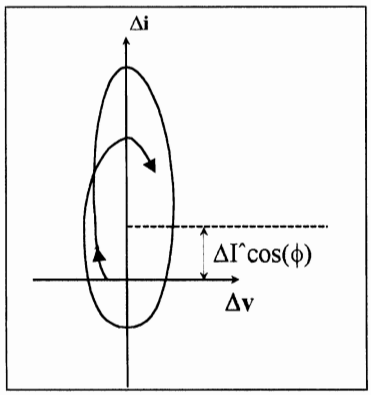

Figure(5- 8): Displacement of the trajectory along the Δi- axis caused by fault inception angles different from 90°.

5-2-B-1 : MODIFICATION OF DEVIATION PLANE

Differentiation of Δi signal eliminates the exponential term Δi_{exp} and linearises the elliptical trajectories, since:

$$\frac{\Delta v(s)}{\Delta i(s)} = -Z_S(s) \qquad \text{..... (5-7)}$$

where, s is Laplace operator, and when Z_S is inductive, then,

$$\Delta v(t) = -L_S \frac{d\Delta i(t)}{dt} \qquad \text{..... (5-8)}$$

If the differentiation is performed with the aid of a replica impedance $Z_R = j\omega L_R$, then,

$$\Delta v(t) = -L_S \frac{d\Delta i(t)}{dt} = -\frac{L_S}{L_R} \cdot \Delta v_R(t)$$

or,

$$\frac{\Delta v_R(t)}{\Delta v(t)} = -\frac{L_R}{L_S} \qquad \text{..... (5-9)}$$

The fraction $\Delta v_R(t)/\Delta v(t)$ is constant and therefore the trajectories move along straight lines passing through the origin and having a slope $-Z_R/Z_S$. In the case of constant fault impedance Z_F, the vertices of all the trajectories lies on a straight line as shown in figure (5-9). This straight line which characterizes certain fault impedance, thus forms an operating characteristic of constant reach. The misbehavior of a trajectory across this line is given by the equation,

$$\Delta v_R(t) - \frac{|Z_R|}{|Z_F|} \cdot \Delta v(t) \; > \; E \cdot \frac{|Z_R|}{|Z_F|} \qquad \text{..... (5-10)}$$

where, E is the magnitude of phase to ground voltage.

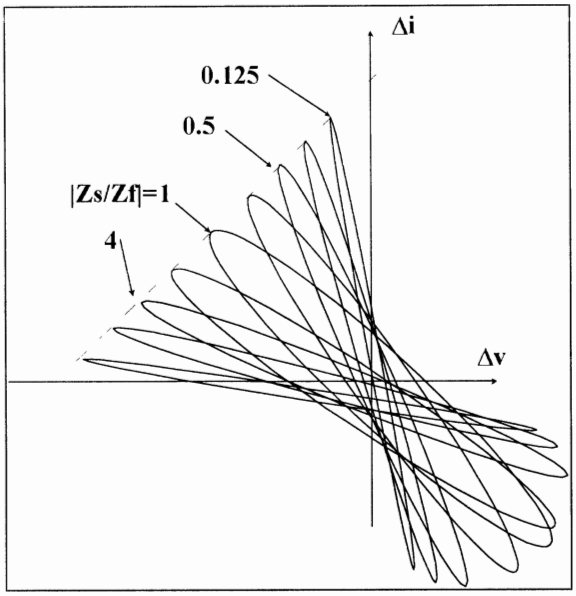

Figure(5- 9): Fault trajectories in the Δv, Δv_R-plane caused by forward faults, $\angle Zs=90°$, $\angle ZR=70°$,, Z_F is constant.

Since the exponential term Δv_{exp} can generally be neglected because of the inductive character of the fault impedance Z_F, equations (5-6) can be rewritten as;

$$v(t) = v_p(t) + \left[\Delta v_{ss}(t) + \Delta v_{tr}(t)\right]$$
$$i(t) = i_p(t) + \frac{1}{Z_R}\left[\Delta v_{ss}(t) + \Delta v_{tr}(t)\right] \qquad \text{..... (5-11)}$$

The parallel replica impedance Z_R is formed through the connection of a resistor R_R across the replica inductance L_R mentioned before and it is defined as;

$$Z_R = \frac{j\omega L_R \cdot R_R}{R_R + j\omega L_R} \qquad \text{..... (5-12)}$$

Respectively the magnitude and the characteristic angle of the replica impedance is given as,

$$|Z_R| = \frac{R_R}{\sqrt{1+\left(\frac{R_R}{\omega L_R}\right)^2}} \qquad \text{..... (5-13)}$$

$$\phi_R = \frac{\pi}{2} - \arctan\left(\frac{\omega L_R}{R_R}\right) = \arctan\left(\frac{R_R}{\omega L_R}\right)$$

It has to be noted that using equations (5-11) tends to amplify the amplitudes of the higher frequency harmonic components other than the fundamental. The maximum amplification (A_{max}) of the harmonic in relation to the fundamental system frequency (f_N) due to the use of the replica impedance and its is,

$$A_{max} = \frac{|Z_R|_{f=\infty}}{|Z_R|_{f=f_N}} = \sqrt{1+\left(\frac{R_R}{2\pi \cdot f_N \cdot L_R}\right)^2} \qquad \text{..... (5-14)}$$

For replica impedance angles (ϕ_R) greater the 70°, the trajectories becomes sufficiently linear to obtain a reasonable constant reach. Respectively, and using equation (5-14), the maximum amplification (Amax) for ϕ_R =70°, is 2.9. Using low-pass filters can further reduce this amplification.

5-2-B-2: OPERATING CHARACTERISTIC IN THE MODIFIED DEVIATION PLANE

The basic operating characteristic of the algorithm is shown in figure(5-10). Strips are taken out along the Δv and Δv_R-axes (i.e., parameters a and b), because the directional decision is not assured for passing of the trajectories close to the axes. This weakness is a consequence of the higher frequency components Δv_{tr} and Δv_{Rtr} and the harmonics in the voltage and current signals. Further errors originate from inaccuracies in processing the analog signals into digital forms. The strip parallel to the Δv-axis (i.e., parameters c and d), also effectively prevents the directional measurement from being affected during VTs fuse failure.

The parameters e and f achieve good distance discriminating properties of the operating characteristics selected and enable close

faults at appreciable current levels to be cleared independently of the signal from the opposite station. This will enable the faults to be cleared in the shortest possible time (i.e., 1 to 2 msec plus circuit breaker time).

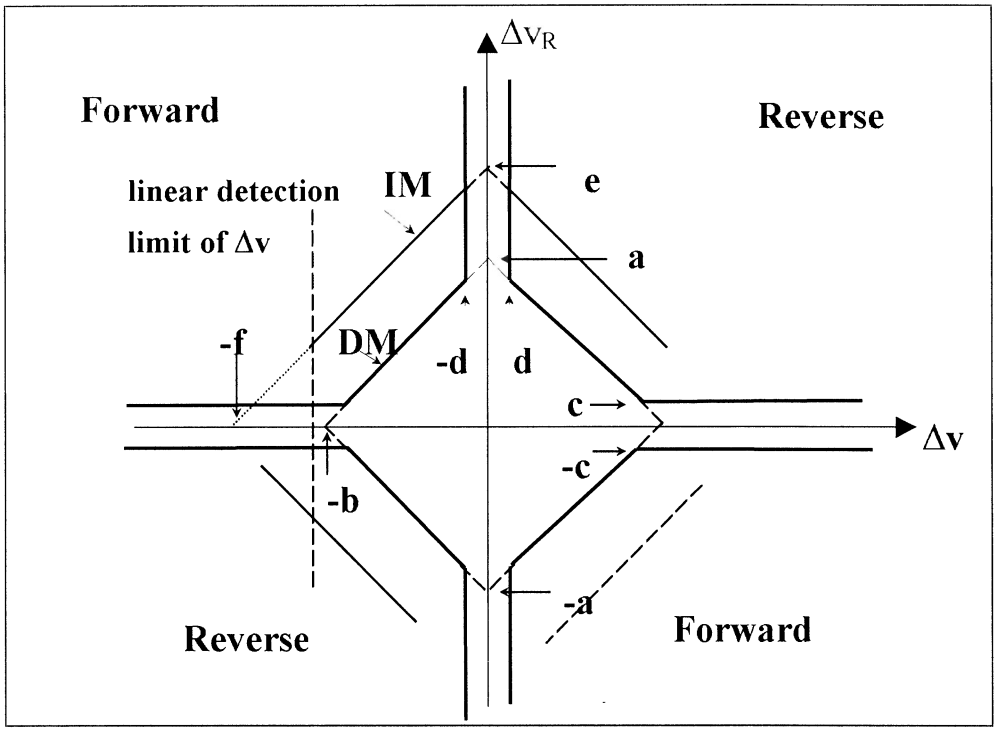

Figure(5- 10): The different operating characteristics. DM : Directional comparison mode. Im: Independent mode.

5-2-B-3: CROSS-CORRELATION FUNCTION

The evaluation of the trajectories always produces a correct directional decision. However, the travelling wave components of higher frequencies may cause a brief deviation of the trajectories into quadrants, which do not correspond to the actual direction of the fault and thus a danger of incorrect phase selection may exist.

By introducing a function, which allocates weighting to the period spent by the trajectories in each quadrant, it is possible to eliminate any influence of brief deviations into the correct quadrants on the directional decision. The function in equation (5-15) achieve this weighting due to its integrating behavior. $F(\tau)$ is continuos and always lies in the negative half of the plane for faults in the forward direction

and in the positive half for faults in the reverse direction as shown in figure(5-11).

$$F(\tau) = \int_0^{\tau} \Delta v(t) \cdot \Delta v_R(t)\, dt \quad \text{..... (5-15)}$$

It follows that the direction of a fault can be determined by a simple threshold comparison of $F(\tau)$ (i.e., parameters i and k).

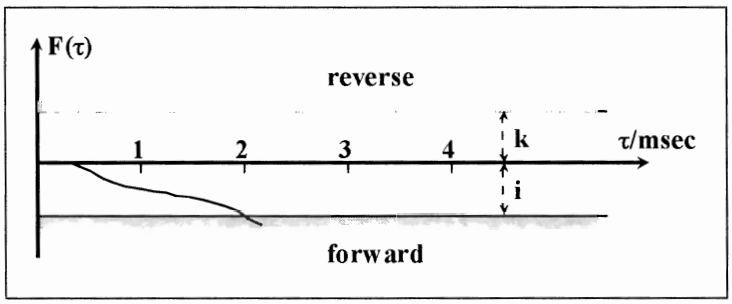

Figure(5- 11) : Cross-correlation function $F(\tau)$.

The operating time of $F(\tau)$ at particular threshold setting depends on the amplitude of the Δ-signals. The rise of $F(\tau)$ is a fast for close faults at high currents, but in certain circumstances can be slower for faults at the end of a line. By corresponding selecting the parameters i and k, it is possible to vary the significance of $F(\tau)$ for the directional decision and thus also the evaluation time.

The tripping takes place only and only if both the trajectories and cross-correlation function gives a trip decision. This increases the reliability of the algorithm without effecting the UHS of the operation response. The operating sampling rate of the input signals is about 9000 samples per a cycle. This can be made possible with high-speed but expensive A/D converters.

5-3 : TRANSIENT ALGORITHMS BASED ON TRAVELLING WAVES

The new development in transmission lines digital protection algorithms, is that they rely on the calculation of the waves travelling along the transmission lines. Those algorithms are still a matter of relaying discussion. Anyhow, it is a matter of time to find in the next future whether these concepts become proper relaying practice or

remain pure ideas. The high speed communication and data processing is an essential elements of travelling wave relaying, thus the developments of travelling wave relaying will wait the full implementation of fiber optic communication systems and electronic transducers.

It is possible to design relays which utilize the propagation phenomena of travelling waves on transmission lines to detect the presence of a fault, and to determine the fault location. Since the travelling waves constitute the earliest possible evidence available to a relay that a fault has occurred, these relays have the potential of becoming the fastest responding relays.

Anyhow the travelling wave phenomena tend to contain high frequency signals, and thus the data acquisition systems must have a correspondingly high bandwidth. This needs microcomputer systems of high capabilities to process those algorithms. Nevertheless, the travelling wave relays represent a new and interesting development in the field of relaying, and we will consider their operating principles in the next sections.

5-3-A: TRAVELLING WAVES ON TRANSMISSION LINES

Any electrical disturbance propagates as a travelling wave on a transmission line. In single-phase transmission lines, the travelling waves have a single propagation velocity and characteristic impedance, whereas in a three-phase transmission line there are at least two distinct model velocities and characteristic impedances.

5-3-A-1: TRAVELLING WAVES ON SINGLE-PHASE LINES

Figure (5-12-a) shows the pre-fault conditions on a single-phase transmission line. A fault occurs at F, where, the pre-fault voltage is (e_F). The occurrence of a fault can be simulated by superimposing on the pre-fault network voltages and currents produced by a fault network consisting of a single source of magnitude ($- e_F$) at the fault point, as shown in figure (5-12-b). The relay located at R is designed to sense the *deviations* in currents and voltages from their pre-fault values (i.e., the idea is discussed in more detail in section 5-2).

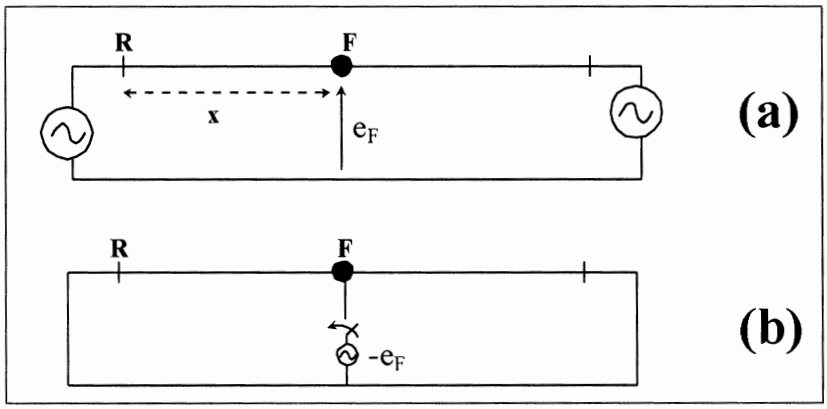

Figure(5- 12): Single-phase transmission line. a- Initial conditions. b- Fault representation.

If a fault takes place at distance x from the relay location along the transmission line, then the partial differentiation equations of voltage and current at x are,

$$\frac{\partial e}{\partial x} = -C\frac{\partial i}{\partial t}$$
$$\frac{\partial i}{\partial x} = -L\frac{\partial e}{\partial t} \qquad \text{..... (5-16)}$$

where, L and C are the inductance and capacitance of the line per unit length. The resistance of the line is assumed negligible. Solution of equations (5-17) gives[5.9] ;

$$e(x,t) = e_f(x - vt) + e_r(x + vt)$$
$$i(x,t) = \frac{1}{Z}\left[e_f(x - vt) + e_r(x + vt)\right] \qquad \text{..... (5-17)}$$

where, $Z = \sqrt{L/C}$ is the characteristic impedance of the line, and $v = \sqrt{1/(LC)}$ is the velocity of propagation.

Equations (5-18) represents two travelling waves, e_f travelling in the positive x direction (i.e., forward wave), and e_r travelling in the negative x direction (i.e., reverse wave), which can be calculated as;

$$e_f = \Delta v + Z\Delta i$$
$$e_r = \Delta v - Z\Delta i \qquad \text{..... (5-18)}$$

where, Δv and Δi are the deviation signals given in equations(5-1), and Z is the characteristic impedance of the line. The voltage and currents at any point on the line are made up of both forward and reverse components;

$$e = e_f + e_r$$
$$i = i_f - i_r \qquad \text{..... (5-19)}$$

The forward and reverse current components are related to corresponding voltage components by the characteristic impedance Z. Figure (5-13) some arbitrary shapes of the travelling waves of voltage and current.

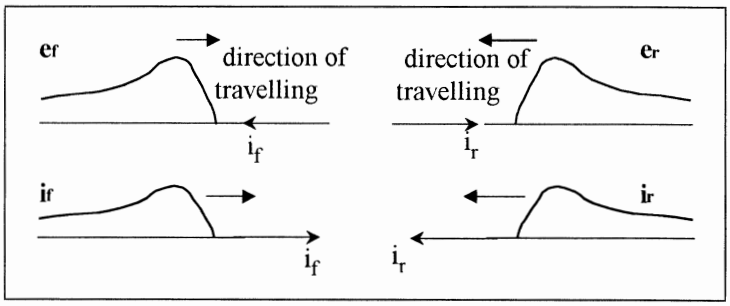

Figure (5- 13): Travelling waves of voltages and currents.

When a fault takes place as in figure (5-12-b), the fault voltage ($-e_F$) is approximately constant and it initiates two waves, both are approximately rectangular in shape and having a magnitude of ($-e_F$), moving away from the point of fault. This is illustrated in figure (5-14). These waves are reflected at any discontinuity (i.e., including at the terminals where the relay is located).

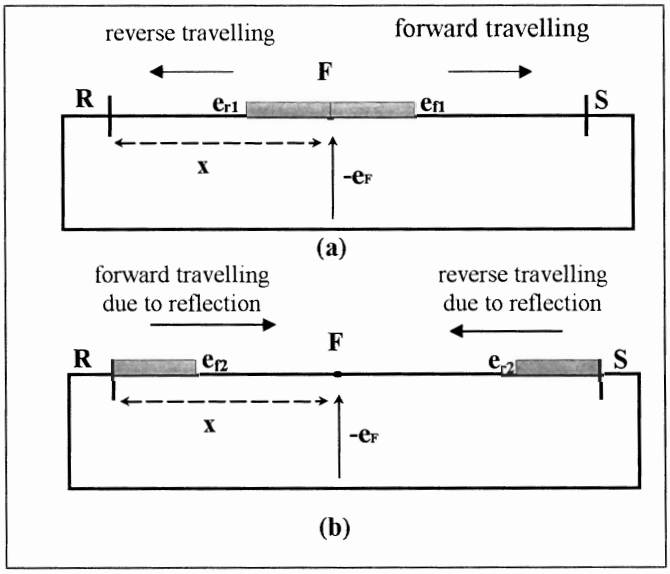

Figure (5- 14): Travelling waves created by a fault. a- the travelling of waves at time of fault occurrence. b- the travelling of the reflected waves at line terminals.

Let k_a is the reflection coefficient applicable at terminal (a), then the incoming wave e_{r1} causes a reflected wave e_{f2} moving in the forward direction, with its corresponding current[5.1] ;

$$e_{f2} = k_a e_{r1}$$
$$i_{f2} = k_a i_{r1} = \frac{e_{f2}}{Z} \quad \text{..... (5-20)}$$

The voltages and current at the termination are (e_t) and (i_t) respectively;

$$e_t = e_{r1} + e_{f2} = (1 + k_a) \cdot e_{r1}$$
$$i_t = -i_{r1} + i_{f2} = -(1 - k_a) \cdot i_{r1} \quad \text{..... (5-21)}$$

The value of the reflection coefficient k_a depends upon the termination;

1. If the termination is into another identical transmission line, there are no reflections, and k_a is zero.
2. If the termination is an open circuit, the reflection coefficient k_a is +1.
3. If the termination is a short circuit, the reflection coefficient k_a is -1.

4. For termination into inductive or capacitive circuits, the reflection coefficient k_a is an operator (i.e., it is a function of Laplace variable (s)).
5. If the termination is another transmission lines, the voltage et and the current it are established as waves on these lines, to be reflected further at their own termination.
6. The absolute value of the reflection coefficient never exceeds unity.

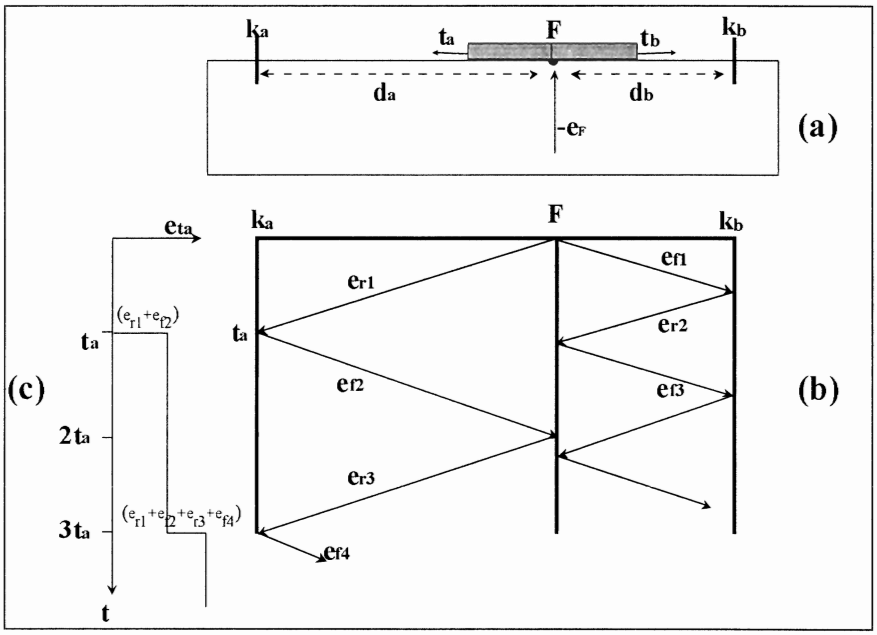

Figure(5- 15): Travelling waves due to a fault in a two-terminal line. a- Fault representation. b- The Lattice diagram. c- The voltages at terminal a.

The entire wave train, first initiated by the fault, thus travels up and down the network, fragmented by the reflections, until it is dissipated through losses and the new steady-state is established. Consider the circuit shown in figure(5-15-a). The fault is at a distance d_a from terminal (a) and at a distance d_b from terminal (b). The propagation delays for two segments are t_a (i.e., $ta = d_a/v$) and t_b (i.e., $t_a = d_b/v$) respectively. Assuming the fault is a zero impedance fault, and the reflection coefficient is real and equal -1, then;

$$e_{f1} = e_{r1}$$

$$e_{f2} = k_a \cdot e_{r1},\ e_{r2} = k_b \cdot e_{f1} \qquad \text{..... (5-22)}$$

$$e_{r3} = -e_{f2}\ ,\ e_{f3} = -e_{r2}$$

The lattice diagram in figure (5-15-b) illustrates these successive reflections.

If the power system behind the relay location (i.e., for example terminal (a)), consists of other transmission lines with their own termination, then they in turn will have similar lattice diagrams representing reflections at their terminals. Reflections that return toward terminal (a) will again disturb on it, and produce waves propagating on the faulted line. The lattice diagram of such a case is illustrated in figure (5-16).

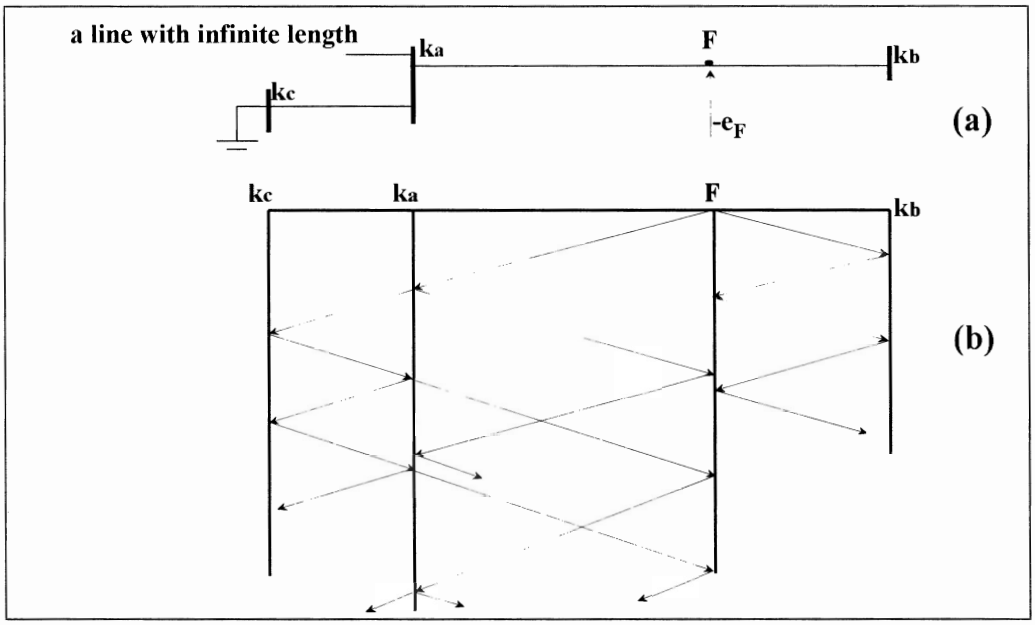

Figure (5-16): Lattice diagram of multiple reflections of waves. The line a-c is determined of finite length, while the other parallel line is assumed to be of infinite length for simplicity.

5-3-A-2: TRAVELLING WAVES ON THREE-PHASE LINES

Modern transmission lines are usually not transposed. Their inductance matrix [L] and their capacitive matrix [C] are therefore not symmetric. Mostly all of protection algorithms based travelling waves ignore this asymmetry, and [L] and [C] are given then as,

$$[L]=\begin{bmatrix} L_s & L_m & L_m \\ L_m & L_s & L_m \\ L_m & L_m & L_s \end{bmatrix}$$

$$[C]=\begin{bmatrix} C_s & C_m & C_m \\ C_m & C_s & C_m \\ C_m & C_m & C_s \end{bmatrix} \qquad \text{..... (5-23)}$$

where, L_s and L_m are the self-inductance of each phase and mutual inductance between each two phases in H/m, respectively. C_s and C_m are the capacitance between each phase and ground and the capacitance between each two phases in F/m, respectively. Those parameters are usually calculated in terms of their positive and zero values,

$$\begin{aligned} L_s &= \tfrac{1}{3}(L_0 + 2L_1) \\ L_m &= \tfrac{1}{3}(L_0 - L_1) \\ C_s &= \tfrac{1}{3}(C_0 + 2C_1) \\ C_m &= \tfrac{1}{3}(C_1 - C_0) \end{aligned} \qquad \text{..... (5-24)}$$

The three-phase transmission line consists of three phases a, b, and c. For grounded systems, addition grounding wire exists. Travelling waves moving along the three phases can be described by a voltage matrix [e] whose components are the individual voltages to ground of each phase, and by a current matrix [i] whose components are the individual phase currents;

$$[e]=\begin{vmatrix} e_a \\ e_b \\ e_c \end{vmatrix} \quad , \quad [i]=\begin{vmatrix} i_a \\ i_b \\ i_c \end{vmatrix} \qquad \text{..... (5-25)}$$

As in case of single-phase lines, the voltages at a distance x from the line terminal are related by the partial differential equations;

$$\frac{\partial[e]}{\partial x} = -[L]\frac{\partial[i]}{\partial t}$$
$$\frac{\partial[i]}{\partial x} = -[C]\frac{\partial[e]}{\partial t} \qquad \text{..... (5-26)}$$

from equations (5-23) and (5-25), equation (5-26) becomes;

$$\frac{\partial}{\partial x}\begin{bmatrix} e_a \\ e_b \\ e_c \end{bmatrix} = -\begin{bmatrix} L_s & L_m & L_m \\ L_m & L_s & L_m \\ L_m & L_m & L_s \end{bmatrix} \cdot \frac{\partial}{\partial t}\begin{bmatrix} i_a \\ i_b \\ i_c \end{bmatrix}$$
$$\frac{\partial}{\partial x}\begin{bmatrix} i_a \\ i_b \\ i_c \end{bmatrix} = -\begin{bmatrix} C_s & C_m & C_m \\ C_m & C_s & C_m \\ C_m & C_m & C_s \end{bmatrix} \cdot \frac{\partial}{\partial t}\begin{bmatrix} e_a \\ e_b \\ e_c \end{bmatrix} \qquad \text{..... (5-27)}$$

To solve equations (5-27), Clarke components[5-5] offer a possible approach. The Clarke components with phase (a) as a reference are obtained by multiplying the phase quantities by the matrix;

$$\frac{1}{3}\begin{vmatrix} 1 & 1 & 1 \\ 2 & -1 & -1 \\ 0 & \sqrt{3} & -\sqrt{3} \end{vmatrix} \qquad \text{..... (5-28)}$$

The Clarke components 0, α, and β of the phase voltages are given by;

$$\begin{vmatrix} e_0 \\ e_\alpha \\ e_\beta \end{vmatrix} = \frac{1}{3}\begin{vmatrix} 1 & 1 & 1 \\ 2 & -1 & -1 \\ 0 & \sqrt{3} & -\sqrt{3} \end{vmatrix}\begin{vmatrix} e_a \\ e_b \\ e_c \end{vmatrix} \qquad \text{..... (5-29)}$$

and of the currents are given by;

$$\begin{vmatrix} i_0 \\ i_\alpha \\ i_\beta \end{vmatrix} = \frac{1}{3}\begin{vmatrix} 1 & 1 & 1 \\ 2 & -1 & -1 \\ 0 & \sqrt{3} & -\sqrt{3} \end{vmatrix}\begin{vmatrix} i_a \\ i_b \\ i_c \end{vmatrix} \qquad \text{..... (5-30)}$$

In the this case, the solution of equations (5-27) for voltages and currents at any point (x) on the three-phase line, making use of equations (5-29) and (5-30) , is given by[5.1];

$$\begin{aligned} e_0 &= e_{f0}(x - v_0 t) + e_{r0}(x + v_0 t) \\ e_\alpha &= e_{f\alpha}(x - v_1 t) + e_{r\alpha}(x + v_1 t) \\ e_\beta &= e_{f\beta}(x - v_2 t) + e_{r\beta}(x + v_2 t) \end{aligned} \quad \text{..... (5-31)}$$

and

$$\begin{aligned} i_0 &= i_{f0} - i_{r0} \\ i_\alpha &= i_{f\alpha} - i_{r\alpha} \\ i_\beta &= i_{f\beta} - i_{r\beta} \end{aligned} \quad \text{..... (5-32)}$$

where;

$$\begin{aligned} \frac{e_{f0}}{i_{f0}} &= \frac{e_{r0}}{i_{r0}} = Z_0 = \sqrt{\frac{L_0}{C_0}} \\ \frac{e_{f\alpha}}{i_{f\alpha}} &= \frac{e_{r\alpha}}{i_{r\alpha}} = Z_1 = \sqrt{\frac{L_1}{C_1}} \\ \frac{e_{f\beta}}{i_{f\beta}} &= \frac{e_{r\beta}}{i_{r\beta}} = Z_1 \end{aligned} \quad \text{..... (5-33)}$$

and;

$$\begin{aligned} v_0 &= \frac{1}{\sqrt{L_0 C_0}} \\ v_1 &= \frac{1}{\sqrt{L_1 C_1}} \end{aligned} \quad \text{..... (5-34)}$$

Equations (5-31) and (5-32) represents the phase voltages and currents as being made up of 0, α, β components. Each of these

components represents a mode of the propagation equation. For a fully transposed line, equations (5-33) and (5-34) shows that, modes α and β have the same surge impedance and velocity (v_1) which is slightly less than the speed of light. The velocity of the zero mode has a higher impedance and lower velocity than those of α and β modes. In general, the definitions of the three modes as for Clarke components are not unique, but other possibilities exist. The most common alternative definition being the Karrenbauer transformation[5.6].

It has to be noted that when the line is untransposed every mode has its own velocity and impedance. As in the case of the transposed lines, the ground mode has the lower velocity and higher impedance.

When a fault occurs in a three-phase line, the fault is represented by voltages $-e_{aF}$, $-e_{bF}$, and $-e_{cF}$ for phases a, b, and c respectively. The corresponding pre-fault voltages are e_{aF}, e_{bF}, and e_{cF} respectively. For a three-phase fault, the boundary condition is;

$$e_a + e_b + e_c = 0$$

then from equations(5-30), the 0, α, and β components of these voltages are;

$$\begin{aligned} e_{0F} &= \tfrac{1}{3}(-e_{aF} - e_{bF} - e_{cF}) = 0 \\ e_{\alpha F} &= \tfrac{1}{3}(-2e_{aF} + e_{bF} + e_{cF}) = -e_{aF} \\ e_{\beta F} &= \tfrac{1}{3}(-e_{bF} + e_{cF}) \end{aligned} \quad \text{..... (5-35)}$$

The α and β components of the voltages travel as a forward and reverse waves of magnitude $e_{\alpha f}$, $e_{\alpha r}$, and $e_{\beta f}$, $e_{\beta r}$ respectively;

$$\begin{aligned} e_\alpha &= e_{\alpha f} + e_{\alpha r} \\ e_\beta &= e_{\beta f} + e_{\beta r} \end{aligned} \quad \text{..... (5-36)}$$

Their accompanying current waves are given as,

$$i_{\alpha f} = \frac{e_{\alpha f}}{Z_1} \quad , \quad i_{\alpha r} = \frac{e_{\alpha r}}{Z_1}$$
$$i_{\beta f} = \frac{e_{\beta f}}{Z_1} \quad , \quad i_{\beta r} = \frac{e_{\beta r}}{Z_1} \qquad \text{..... (5-37)}$$

When a phase to phase fault takes place (i.e., say a phase (a) to phase (b) fault), the fault boundary conditions are;

$$e_a = 0$$
$$e_b = -\frac{1}{2} e_{bcF} \qquad \text{..... (5-38)}$$
$$e_b = \frac{1}{2} e_{bcF}$$

The 0, α, and β components of these voltages are;

$$e_0 = 0$$
$$e_\alpha = 0 \qquad \text{..... (5-39)}$$
$$e_\beta = \frac{1}{\sqrt{3}} e_{bcF}$$

where, e_{bcF} is the pre-fault voltage between phases b and c. Similarly , the modal travelling waves initiated by various types of faults can be calculated.

In general, the detection of waves in three-phase lines is better performed in the modal domain. Any fault in a three-phase transmission line initiates a set of modal travelling waves (i.e., 0, α , and β) at the point of a fault inception. The waves propagate towards terminals, and are reflected with a proper reflection coefficient. Anyhow, the reflections in this case, at the fault point and at the line terminals are more complex than those in single-phase lines. The picture becomes more complex with unbalanced faults. Many algorithms have been proposed for transmission lines, which act on detecting the travelling waves. We shall consider the main proposals divided into three groups according to their aspects of protection.

5-3-B : DIRECTIONAL PROTECTION ALGORITHMS BASED ON TRAVELLING WAVES

The operating principles of this algorithm [5.6,5.7,5.8] can be explained by considering the relay station R protecting the interconnection R-S in figure (5-17). When a fault occurs in the backward direction somewhere in the system R (i.e., point (a)), the first disturbance sensed at R corresponds to a refracted wave entering the line R-S in the forward direction. No wave moving in the backward (i.e., reverse) direction will be detected at R until a time equal to twice the travel time on the line has past. This is the time required for the refracted wave to travel to S, be reflected, and then return to R. The direction of travelling waves are calculated using equations (5-18) as explained in the previous section which is rewritten again for remembering;

$$\begin{aligned} e_f &= \Delta v + Z\Delta i \\ e_r &= \Delta v - Z\Delta i \end{aligned} \qquad \text{..... (5-40)}$$

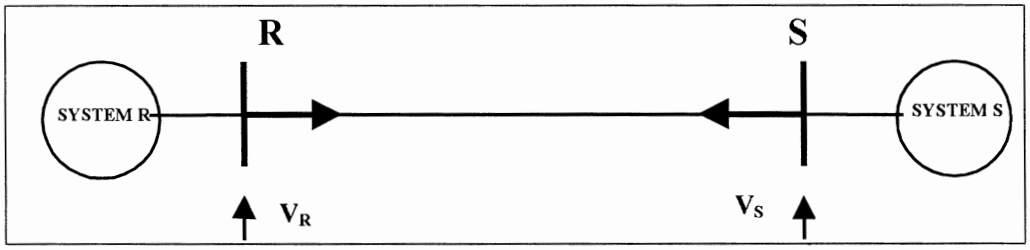

Figure (5-17): A single-phase line interconnecting two systems.

It should be remembered that e_f is a voltage signal moving in the forward direction, and e_r is a voltage signal moving in the forward direction. Thus, for a fault in the backward direction (i.e., point a),

$$\begin{aligned} e_f &= 0 \\ e_r &= 0 \qquad \text{for } t < 2\tau \end{aligned} \qquad \text{..... (5-41)}$$

where, τ is the travel time of the line.

When a fault occurs in the forward direction (i.e., point b), the first disturbance sensed at relay R (i.e., e_R), is the composite of two waves moving in opposite direction (i.e., equations 5-21);

$$e_R = e_r + K_R\, e_r = (1 + K_R)\, e_r \qquad \text{..... (5-42)}$$

The first is the incident wave produced by the fault itself (e_r) which is traveling in the reverse direction. The second is the reflected wave produced by the reflection of the incident wave at the line termination R (i.e., equal to $K_R e_r$, where K_R is the reflection coefficient at R); this will be moving in the forward direction.

The direction of the fault is determined by a travelling wave discriminant whose value is zero for backward faults and an assigned constant for faults in the forward direction[5.6]. This discriminant is computed as follows;

$$D(t) = (\Delta v - Z\Delta i)^2 + \left(\frac{1}{\omega}\right)^2 \left(\frac{d}{dt}\Delta v - Z\frac{d}{dt}\Delta i\right)^2 \qquad \text{..... (5-43)}$$

where, Δv and Δi are the deviations of the line voltage and current, Z is the line characteristic impedance and ω is the angular frequency. The value of the discriminant is independent of the fault inception angle although it is well known that travelling waves produced by a fault depends on this angle. This may pose a problem when detecting faults occurring close to a voltage zero crossing. From equations (5-40), the discriminant can also be written as a function of the reverse travelling wave deviation function as;

$$D(t) = (e_r)^2 + \left(\frac{1}{\omega}\right)^2 \left(\frac{d}{dt} e_r\right)^2 \qquad \text{..... (5-44)}$$

Referring again to figure (5-17), we can note that for a fault in the backward direction with respect to relay R (i.e., at point (a)), the travelling wave discriminant, evaluated at R (i.e., e_R) is 0, and thus D = 0, for the time when the first reflection at S return to R (i.e., equations 5-41). This interval is twice the interval time of the line (τ).

For $t \geq 2\tau$, the travelling wave discriminant evaluated at R using equation (5-44), coincides with its theoretical value D_{th}. This situation remain from the time at which the first wave is sensed at R to the time at which its reflected wave arrives back at R after being reflected either at the fault location for an internal fault, or at the opposite end for external fault. The theoretical value of the discriminant is given[5.6] by;

$$D_{th} = 8V_{rms}^2 \qquad \text{..... (5-45)}$$

where; V_{rms} is the prefault rms voltage of the line.

Consider the situation depicted in figure (5-18) which shows an internal fault, F, located at a distance l_1 from R and l_2 from S. The total length of the line is l. The prefault voltage at the fault location is given by;

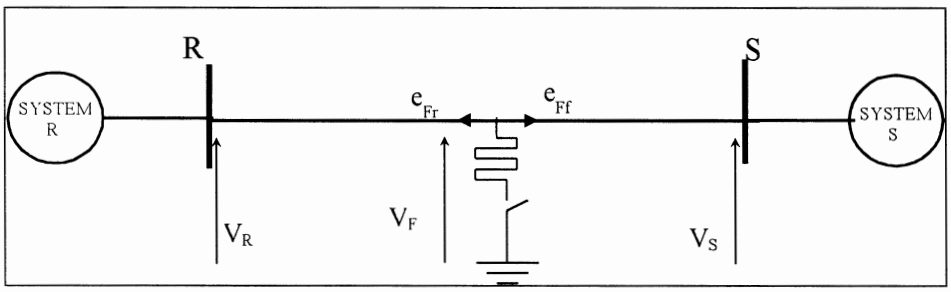

Figure(5- 18): Internal fault on a single-phase line.

$$V_F = \sqrt{2}V_{rms}\sin(\omega t_o + \phi) \qquad \text{..... (5-46)}$$

and the voltage and current deviations at the fault location are given by;

$$\Delta V_F = -\sqrt{2}V_{rms}\sin(\omega t_o + \phi)$$

$$\Delta I_F = \frac{\Delta V_F}{Z} \qquad \text{..... (5-47)}$$

for $t_o \leq t \leq t_o + 2\tau_1$, where Z is the characteristic impedance of the line, and τ_1 is the travel time from the fault location to the relay station R (i.e., $\tau_1 = l_1/v$, and v is the propagation velocity). The magnitude of the deviation travelling wave function at the fault location (F) is ;

$$e_r(t)\big|_{at\ F} = -2\sqrt{2}V_{rms}\sin(\omega t_o + \phi) \quad \text{for } t_o \le t \le t_o + 2\tau_1 \quad \text{..... (5-48)}$$

As the voltage waves travel undistorted on a lossless line[5.2], then the wave generated at F moving in the negative direction during the time interval $t_o \le t \le t_o+2\tau_1$ can be observed at terminal R during the time interval $t_o+\tau_1 \le t \le t_o+3\tau_1$. As the travelling waves and the function travelling waves are proportional to each other then;

$$e_r(t)\big|_{at\ R} = e_r(t-\tau_1)\big|_{at\ F} \quad \text{for } t_o + \tau_1 \le t \le t_o + 3\tau_1 \quad \text{..... (5-49)}$$

Combining equations (5-49) and (5-47);

$$e_r(t)\big|_{at\ R} = -2\sqrt{2}V_{rms}\sin(\omega(t-\tau_1)+\phi) \quad \text{for } t_o + \tau_1 \le t \le t_o + 3\tau_1 \quad \text{..... (5-50)}$$

using the results in equation (5-44) ;

$$D(t) = 8V_{rms}^2\sin^2[\omega(t-\tau_1)+\phi] + 8V_{rms}^2\cos^2[\omega(t-\tau_1)+\phi]$$

which yields;

$$D(t) = 8V_{rms}^2 = D_{th} \quad \text{for } t_o + \tau_1 \le t \le t_o + 3\tau_1 \quad \text{..... (5-51)}$$

The rms voltage at the fault location is unknown in a lossy line, the voltage at the relay is therefore substituted instead. This is a reasonable approximation specially for close-in faults. In general, the computed value of the discriminant will depend on the fault location because of two reasons;

1. The prefault location determines the initial voltage deviation.
2. The distance separating the fault and the relaying station determines the attenuation suffered by the wave as it travels.

Thus, a difference between the calculated discriminant given in equation (5-44), and its theoretical value given in equation (5-51), is expected. It is therefore necessary to select a suitable threshold value, other than the theoretical discriminant, with which to compare the

calculated discriminant for detection of forward faults. Finding such a threshold, two aspects have to be considered;

1. The selected threshold level should be low enough for the relay at one end of the protected line to over reach the other end under all situations.
2. The selected threshold level should be high enough to assure that the relay is not triggered by noise.

On the other hand, during external fault, the originated waves travel to the far end of the line and reflect from that far end arrive to the close terminal of the line. This may produce a discriminant exceeding the threshold level. Anyhow, the travel of the wave takes no less than twice the travel time of the protected line (τ)(i.e.; equation 5-41). To avoid this problem, the relay must be inhibited whenever a disturbance occurs whose discriminant does not exceed the threshold value within a time interval, which is shorter than twice the travel time of the protected line. The relay should be inhibited until the disturbance completely disappears.

As in section (5-3-A-2), It is possible to fined theoretical values for the modal discriminants for different kinds of faults in three-phase lines. The theoretical modal discriminants using Clarke components are given[5.6] by,

$$D_{0th} = \frac{8}{3}\left[\frac{Z_0}{Z_0 + 2Z_1}\right]^2 V^2$$

$$D_{\alpha th} = \frac{8}{3}\left[\frac{Z_1}{Z_0 + 2Z_1}\right]^2 V^2 \qquad \text{..... (5-52)}$$

$$D_{\beta th} = \frac{8}{3}\left[\frac{Z_1}{Z_0 + 2Z_1}\right]^2 V^2$$

where, Z0 and Z1 are the ground and line mode impedances respectively (i.e., as in section 5-3-A-2), and V is the rms line to ground voltage. Note that the calculated modal discriminants using Clarke components are given by,

$$D_0(t) = e_{r0}^2 + \left(\frac{1}{\omega}\frac{d}{dt}e_{r0}\right)^2$$

$$D_\alpha(t) = e_{r\alpha}^2 + \left(\frac{1}{\omega}\frac{d}{dt}e_{r\alpha}\right)^2 \quad \text{..... (5-53)}$$

$$D_\beta(t) = e_{r\beta}^2 + \left(\frac{1}{\omega}\frac{d}{dt}e_{r\beta}\right)^2$$

where, e_{r0}, $e_{r\alpha}$, and $e_{r\beta}$, are calculated using equations (5-30) and (5-40).

It has been shown that for external faults in the backward direction, a certain amount of delay is introduced in detecting the first disturbance and in setting the timer which measures in the interval between detection of the disturbance and the first wave moving in the reverse direction. Depending on the setting of the relay and on the length of the protected line, this may be a problem. This problem may be overcome by introducing a new travelling wave discriminant, similar to that of equation (5-44), but based on the forward travelling wave deviation function and its time derivative[5.2]. This discriminant provides an immediate indication of any forward moving wave arriving at the relay station. The new discriminant is calculated as;

$$D_f(t) = e_f^2 + \left(\frac{1}{\omega}\frac{d}{dt}e_f\right)^2 \quad \text{..... (5-54)}$$

and it is referred to as the forward discriminant. The reverse discriminant given by equation (5-44) can then be rewritten as;

$$D_r(t) = e_r^2 + \left(\frac{1}{\omega}\frac{d}{dt}e_r\right)^2 \quad \text{..... (5-55)}$$

The indexes f and r have been added to both disciminants to distinguish them from one another and to indicate the kind of travelling wave deviation function used in their commutation. Using equations (5-33), the 0, α, and β modal of both forward and reverse disciminants can be calculated as in equations (5-56) and (5-57) respectively,

$$D_{f0}(t) = e_{f0}^2 + \left(\frac{1}{\omega}\frac{d}{dt}e_{f0}\right)^2$$
$$D_{f\alpha}(t) = e_{f\alpha}^2 + \left(\frac{1}{\omega}\frac{d}{dt}e_{f\alpha}\right)^2 \quad \text{..... (5-56)}$$
$$D_{f\beta}(t) = e_{f\beta}^2 + \left(\frac{1}{\omega}\frac{d}{dt}e_{f\beta}\right)^2$$

$$D_{r0}(t) = e_{r0}^2 + \left(\frac{1}{\omega}\frac{d}{dt}e_{r0}\right)^2$$
$$D_{r\alpha}(t) = e_{r\alpha}^2 + \left(\frac{1}{\omega}\frac{d}{dt}e_{r\alpha}\right)^2 \quad \text{..... (5-57)}$$
$$D_{r\beta}(t) = e_{r\beta}^2 + \left(\frac{1}{\omega}\frac{d}{dt}e_{r\beta}\right)^2$$

Another problem is when faults takes place very close to line termination. In this case the value of discriminant rapidly increases to a value higher than the theoretical discriminant. The reason for this is the short travel time for waves between a close-in fault and the relay station. The relay sees the contribution of multiple reflections, which reinforce each other. Two alternative methods have been suggested to solve this problem. The first, is to use informations from both sides of the line and to operate when both relays at both terminations indicate an internal fault. The second is to use the local available information[2].In this case the following condition could be included;

$$|\Delta V(t)| > |V_{ss}(t)| \quad \text{..... (5-58)}$$

The output of the relay is blocked whenever this condition is satisfied. Anyhow, an additional method has to be used to find out whether the fault is permanent, which is a limitation.

In general, the directional digital relays based on travelling waves, appears to perform satisfactorily if more suitable threshold levels are selected for modal disciminants. The actual values will depend on the noise present in the input data, the sampling rate and the characteristics of the low-pass filters and differentiators used.

5-3-C: DISTANCE PROTECTION ALGORITHMS BASED ON TRAVELLING WAVES

Typical algorithm of such kind[5.9] , has usually two models., the first detects the direction of a disturbance sensed at the relay station, and the second determines the distance from the relay station to the fault when a fault is in the forward direction. The directional module is as described in the previous section.

Consider the situation of figure(5-18) which shows an internal fault on a transmission line. Let us suppose that this fault occurred at t_o, that the line is lossless, and that the fault resistance is zero. The relay station at R will become aware of the fault at a time $(t_o+\tau_1)$ by the arrival of a reverse wave from the fault. The forward wave leaving station R at that instant will return with its sign reversed at a time $2\tau_1$ later, having been reflected at the fault. Thus;

$$e_r(t)\big|_{at\ R} = -e_f(t-2\tau_1)\big|_{at\ S} \qquad \text{for } t_o + 3\tau_1 \le t \le t_o + 5\tau_1 \qquad \text{..... (5-59)}$$

where; all the quantities have the same significance as maintained before. The arrival of the reflected wave can be easily measured. This can be translated into distance to the fault;

$$l = v\,\tau_t \qquad \text{..... (5-60)}$$

where, τ_t is the total travel time $2\tau_1$. The relay is tripped if this distance is less than the length of the line.

Anyhow, in practical situation the line will be lossy, it will be located above ground and the fault resistance may not be zero. In these circumstances all travelling waves on the line will be attenuated and distorted. Moreover, waves arriving at R from the forward direction are not only those reflected from the fault but also waves coming from the other end of the line. This complicates the measurement of fault distance by the method just described.

A distance module algorithm[5.9] has been proposed, which is based on discrete cross-correlation of samples of the forward travelling wave (x) function with samples of the delayed signal (y) as a function of the

delay τ. The discrete cross-correlation function $\Phi_{xy}(\tau)$ measures how similar the two are as a function of delay τ;

$$\Phi_{xy}(\tau) = \sum_{k=1}^{N}\left[x_{(k\Delta t+\tau)} \times y_{(k\Delta t)}\right] \quad \text{..... (5-61)}$$

where, Δt is the sampling time. The implementation of this method requires that a section of the forward travelling wave function be stored. This section should contain the complete wave shape of the initial disturbance, and include some samples recorded before the disturbance and some samples recorded after the direction of the disturbance has been detected. The length of the time spent by the recorded section is inversely proportional to the wave velocity of the line. The cross- correlation function has a maximum when the negative of the reversed travelling wave coincides the initial section of the forward travelling wave. The difference of time between the arrival of the fist disturbance and the peak of the cross-correlation function is then a measure of the total travel time.

Let S_1 and S_2 be the relaying signals, which represent a section of the forward travelling wave e_f and reverse travelling wave e_r respectively. Meaningful correlation can only be achieved between e_f and e_r, when they have the same mean levels. The correlation is therefore performed between sections of e_f and e_r from which their corresponding means have been removed. The elements of these new sections are defined as follows;

$$S_1(k\Delta t) = e_f(k\Delta t) - \frac{1}{N}\sum_{j=1}^{N} e_f(j\Delta t) \quad \text{..... (5-62)}$$

for k= 1,2, ... , N.

$$S_2(k\Delta t + m\Delta t) = e_r(k\Delta t + m\Delta t) - \frac{1}{N}\sum_{j=1}^{N} e_r(j\Delta t + m\Delta t) \quad \text{..... (5-63)}$$

for k= 1,2, ... , N , and m = 0, 1, ...,∞.

Thus, equation (5-61) becomes as;

$$\Phi(m\Delta t) = \frac{1}{N}\sum_{k=1}^{N}\left[S_1(k\Delta t) \times S_1(k\Delta t + \tau)\right] \quad \text{..... (5-64)}$$

where, $m\Delta t$ is the delay between the sections, N is the number of samples in every section and k is the sequence of every particular sample in its corresponding section. Let $m_{max.}$ be the value of m for which $\Phi(m\Delta t)$ is maximum, then the total arrival time is given as;

$$\tau_t = m_{max.} \cdot \Delta t \quad \text{..... (5-65)}$$

Figure (5-19) illustrates the technique required for the cross-correlation between sections of the signals e_f and e_r with different mean levels.

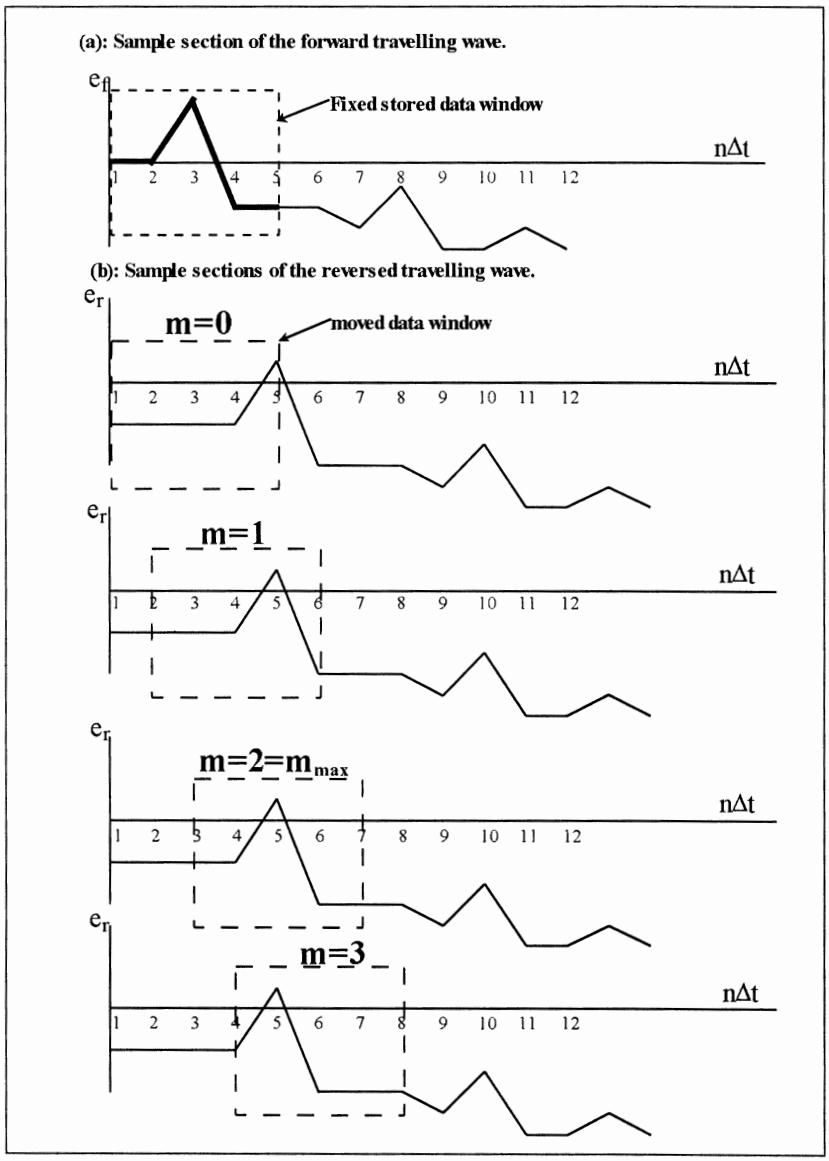

Figure(5- 19): Operation technique of the cross-correlation locator.

The manner, in which this technique is done, is as follows. The sample section of the forward travelling wave (i.e., remains fixed as a stored data window as shown in figure (5-19-a). The sample section of the negative of the reverse travelling wave is constantly being refreshed with a latest moving data window. Cross- correlation is performed repeatedly as each new version of moving data windows replaces the existing one. As the example in figure (5-19), $\Phi(m\Delta t)$ becomes maximum as the both waves coincide at m=2, the total time then is $2\Delta t$.

In general, such algorithms of distance protection based on travelling waves are full of difficulties. For three-phase lines , the Clarke modal transformations explained before may be employed. Ground mode waves are subjected to severe attenuation and distortion of waveshapes as the waves propagate along the transmission lines. Unbalanced faults and faults through impedance further complicate matters by coupling different modes at the fault point. When fault inception angles are such that travelling waves are small in magnitude (i.e., corresponding to a zero crossing), the maximum of the cross-correlation function is often lost in the measurement noise. On the other hand, close-in faults might create problems for this algorithm because of the many signals produced by repeated reflections of the wave. All these considerations make a travelling wave distance relay somewhat difficult to set now. A time is needed for more studies in this field.

5-3-D : TRAVELLING WAVE CURRENT DIFFERENTIAL ALGORITHMS

It is well known that in any current differential relay scheme, the currents entering and leaving the protected element are compared. During normal operation or on the occurrence of an external fault the currents are equal, but are unequal when an internal fault occurs. Such relays are set to trip when the differential current exceeds a pre-set pickup value. Relays of this type have good selectivity and have been used widely for the protection of generators, buses and transformer. Currents entering and leaving the terminals of medium or long transmission lines are not exactly equal under either normal or fault conditions mainly because of charging current. These difficulties have been surmounted using differential technique based on travelling

waves[5.10, 5.11, 5.12, 5.13]. This algorithm is referred to as a travelling wave current differential (TWCD) algorithm.

The operating time of TWCD relays is greater than other UHS relays based on travelling wave which are discussed before. This is because of the travelling time between the ends of the transmission line. Anyhow, it was pointed out in the previous sections that travelling wave relays described in the last sections were unable to detect forward faults in the presence of waves from other disturbances because they are designed to react to the first deviation from steady state. Thus, the TWCD algorithm is important because it is capable of detecting any internal fault at any time, independent of the system prefault condition, making it more reliable and convenient to apply than other travelling wave algorithms.

To derive the operating principles of the TWCD algorithm, consider the simple line diagram of figure (5-20). The voltage at terminals R and S can be calculated constantly using equations (5-18). For lossless line, the following equations are valid in the absence of any internal fault;

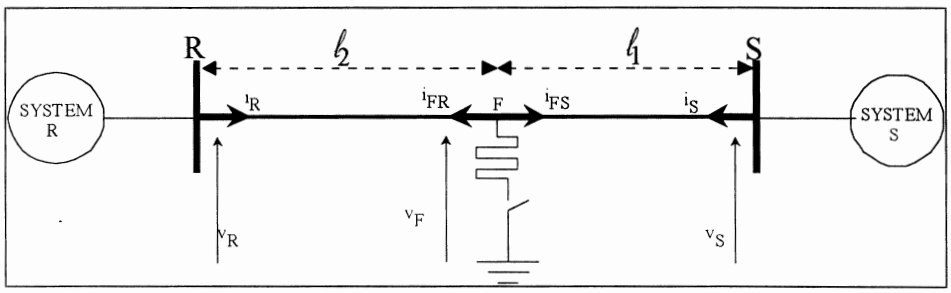

Figure (5- 20): Internal fault in a single-phase transmission line.

$$e_r(t)\big|_{at\ R} = e_f(t-\tau)\big|_{at\ S} \qquad \text{..... (5-66)}$$

$$e_r(t)\big|_{at\ S} = e_f(t-\tau)\big|_{at\ R} \qquad \text{..... (5-67)}$$

where, τ is the travelling time of the line, and the proprieties for directionality are the same as discussed in section (5-3-B).

When an internal fault occurs, neither equation (5-66) applies at R after the arrival of the first disturbance, nor does equation (5-67) apply

at S[5.2]. In the TWCD algorithm two functions are derived[5.10, 5.11, 5.12, 5.13], their computation needs the exchange of information on the line to ground voltage and the line current between the two ends of the line. These functions are defined as follows;

$$\varepsilon(t) = \frac{1}{Z}\left[e_r(t)\big|_{\text{at R}} - e_f(t-\tau)\big|_{\text{at S}}\right] \quad \text{..... (5-68)}$$

$$\xi(t) = \frac{1}{Z}\left[e_r(t)\big|_{\text{at S}} - e_f(t-\tau)\big|_{\text{at R}}\right] \quad \text{..... (5-69)}$$

so that, $\varepsilon(t)$ is evaluated at R and $\xi(t)$ is evaluated at S. These function are called the *fault current functions*. Combining equations (5-18) into equations (5-68) and (5-69) we get;

$$\varepsilon(t) = \frac{1}{Z}\left[\Delta v_R(t) - \Delta v_S(t-\tau)\right] - \left[\Delta i_R(t) + \Delta i_S(t-\tau)\right] \quad \text{..... (5-70)}$$

$$\xi(t) = \frac{1}{Z}\left[\Delta v_S(t) - \Delta v_R(t-\tau)\right] - \left[\Delta i_S(t) + \Delta i_R(t-\tau)\right] \quad \text{..... (5-71)}$$

Assume that the fault at F in figure(5-20) takes place at t=0. We can define $e_f(t)|_{FR}$ and $e_r(t)|_{FR}$ as the forward and backward travelling wave functions moving between F and R as observed at F. Thus;

$$e_f(t)\big|_{FR} = \Delta v_F(t) + Z\,\Delta i_{FR}(t) \quad \text{..... (5-72)}$$

$$e_r(t)\big|_{FR} = \Delta v_F(t) - Z\,\Delta i_{FR}(t) \quad \text{..... (5-73)}$$

where, v_F is the voltage at the fault location F , and i_{FR} is the current flowing from F to R as shown in figure(5-20). The fault current i_F is given by,

$$i_F = -(i_{FR} + i_{FS}) \quad \text{..... (5-74)}$$

With no fault, i_F is zero and i_{FR}=-i_{FS} . Similar functions can be defined for the forward and backward travelling wave functions moving between F and S as observed at F;

$$e_f(t)\big|_{FS} = \Delta v_F(t) + Z\,\Delta i_{FS}(t) \quad \text{..... (5-75)}$$

$$e_r(t)\big|_{FS} = \Delta v_F(t) - Z\,\Delta i_{FS}(t) \quad \text{..... (5-76)}$$

Using the properties of travelling waves when moving on a lossless line, the following relationships can be stated for the wave proceeding from R to F;

$$e_r(t)\big|_R = e_f(t-\tau_2)\big|_{FR} \quad \text{..... (5-77)}$$

$$e_f(t-\tau)\big|_S = e_r(t-\tau_2)\big|_{FS} \quad \text{..... (5-78)}$$

where, τ , τ_1, τ_2, are the traveling time for ℓ , ℓ_1, and ℓ_2 respectively. Equations (5-77) and (5-78) means that the travelling wave at R in the reverse direction with respect to R (i.e., $e_r(t)|_R$) at time t, is similar to the wave traveled from F to R at time t-τ_2 in the forward direction with respect to F (i.e., $e_f(t-\tau_2)|_{FR}$). This wave will reflect at R , traveled in the forward direction with respect to S at time t-τ (i.e., $e_f(t-\tau)|_S$), which is similar to the wave traveled from F to S at time t-τ_2 in the reverse direction with respect to F (i.e., $e_r(t-\tau_2)|_{FS}$). Substituting equations (5-77), and (5-78) into (5-70) ;

$$\varepsilon(t) = \frac{1}{Z}\left[-e_r(t-\tau_2)\big|_{FS} - e_f(t-\tau_2)\big|_{FR}\right] \quad \text{..... (5-79)}$$

Then substituting equations (5-18) and (5-74) into (5-79) gives;

$$\varepsilon(t) = i_F(t-\tau_2) \quad \text{..... (5-80)}$$

Similarly,

$$e_r(t)\big|_S = e_f(t-\tau_1)\big|_{FS} \quad \text{..... (5-81)}$$

$$e_f(t-\tau)\big|_R = e_r(t-\tau_1)\big|_{FR} \quad \text{..... (5-82)}$$

Equations (5-81) and (5-82) means that the travelling wave at S in the reverse direction with respect to S (i.e., $e_r(t)|_S$) at time t , is similar to the wave traveled from F to S at time $t-\tau_1$ in the forward direction with respect to F (i.e., $e_f(t-\tau_1)|_{FS}$). This wave will reflect at S , traveled in the forward direction with respect to R at time $t-\tau$ (i.e., $e_f(t-\tau)|_R$), which is similar to the wave traveled from F to S at time $t-\tau_1$ in the reverse direction with respect to F (i.e., $e_r(t-\tau_2)|_{FR}$). Substituting equations (5-77), and (5-78) into (5-70);

$$\xi(t) = \frac{1}{Z}\left[-e_r(t-\tau_1)|_{FR} - e_f(t-\tau_1)|_{FS}\right] \quad \text{..... (5-83)}$$

Then substituting equations (5-18) and (5-74) into (5-83) gives;

$$\xi(t) = i_F(t-\tau_1) \quad \text{..... (5-84)}$$

Equations (5-80) and (5-84) confirm that $\varepsilon(t)$ and $\xi(t)$ correspond to the delayed value of the fault current as seen at the fault location for any internal fault. Both equations (5-80) and (5-84), or in other means equations (5-70) and (5-71) have the following properties[5.10];

$$\begin{aligned} \varepsilon(t) = 0 \quad & \text{implies no internal fault.} \\ \varepsilon(t) \neq 0 \quad & \text{implies internal fault.} \end{aligned} \quad \text{..... (5-85)}$$

and;

$$\begin{aligned} \xi(t) = 0 \quad & \text{implies no internal fault.} \\ \xi(t) \neq 0 \quad & \text{implies internal fault.} \end{aligned} \quad \text{..... (5-86)}$$

Then we can detect any internal fault by $\varepsilon(t)$ and $\xi(t)$. It is noted that functions $\varepsilon(t)$ and $\xi(t)$ are independent of each other.

It is well known as described earlier that a three phase line can be decomposed into three single phase lines using a modal transform (i.e., Clarke, Karrenbauer,.. etc.). Using Clarke transform, the voltage and

currents modes are calculated as in equations (5-29) and (5-30) which is stated here for remembering;

$$\begin{vmatrix} e_0 \\ e_\alpha \\ e_\beta \end{vmatrix} = \frac{1}{3}\begin{vmatrix} 1 & 1 & 1 \\ 2 & -1 & -1 \\ 0 & \sqrt{3} & -\sqrt{3} \end{vmatrix}\begin{vmatrix} e_a \\ e_b \\ e_c \end{vmatrix} \quad \text{and} \quad \begin{vmatrix} i_0 \\ i_\alpha \\ i_\beta \end{vmatrix} = \frac{1}{3}\begin{vmatrix} 1 & 1 & 1 \\ 2 & -1 & -1 \\ 0 & \sqrt{3} & -\sqrt{3} \end{vmatrix}\begin{vmatrix} i_a \\ i_b \\ i_c \end{vmatrix}$$

The discussion in single-phase line is applicable to each modal line. Thus, the time functions for fault detection in a three-phase line are given as[5.10];

$$\varepsilon_k(t) = \frac{1}{Z_k}\left[\Delta v_{Rk}(t) - \Delta v_{Sk}(t-\tau_k)\right] - \left[\Delta i_{Rk}(t) + \Delta i_{Sk}(t-\tau_k)\right] \quad \text{... (5-87)}$$

$$\xi_k(t) = \frac{1}{Z_k}\left[\Delta v_{Sk}(t) - \Delta v_{Rk}(t-\tau_k)\right] - \left[\Delta i_{Sk}(t) + \Delta i_{Rk}(t-\tau_k)\right] \quad \text{... (5-88)}$$

where,

$\varepsilon_k(t)$ and $\xi_k(t)$: are the k-mode of the functions $\varepsilon(t)$ and $\xi(t)$ respectively.

$\Delta v_{Rk}(t)$ and $\Delta v_{Sk}(t)$: are the k-mode of the voltages $\Delta v_R(t)$ and $\Delta v_S(t)$ respectively.

$\Delta i_{Rk}(t)$ and $\Delta i_{Sk}(t)$: are the k-mode of the currents $\Delta i_R(t)$ and $\Delta i_S(t)$ respectively.

Z_k : is the k-mode of the characteristic impedance of the line.

τ_k : is the k-mode of the travelling time of the line.

k : is any of the Clarke modes 0, α, and β.

The fault detection can be done in the three phase lines using the following logic,

$\varepsilon_0(t)$ AND $\varepsilon_\alpha(t)$ AND $\varepsilon_\beta(t) = 0$ implies no internal fault.

$\varepsilon_0(t)$ OR $\varepsilon_\alpha(t)$ OR $\varepsilon_\beta(t) \neq 0$ implies internal fault. ....(5-89)

and;

$\xi_0(t)$ AND $\xi_\alpha(t)$ AND $\xi_\beta(t) = 0$ implies no internal fault.

$\xi_0(t)$ OR $\xi_\alpha(t)$ OR $\xi_\beta(t) \neq 0$ implies internal fault. ... (5-90)

This algorithm can be easily modified for the protection of multi-terminal lines [5.10, 5.11, 5.12].

It has been found that a separated phase implementation of this algorithm is also possible [5.13]. In this computation, it is assumed that every phase conductor is independent of the others and inter-phase coupling is neglected. Equations (5-70) and (5-71) are used to calculate the phase fault currents $\varepsilon_{ph}(t)$ and $\xi_{ph}(t)$ at their corresponding terminals for each phase. The values of voltage and current used are the line to ground voltage and the line current of the phase whose fault current function is being evaluated. The Line impedance Z and travel time τ are calculated from the positive sequence parameters of the line at power frequency. It has been found that this simplified version of the TWCD relay performs satisfactorily in most applications. However, one problem was identified[5.2]. The fault current functions $\varepsilon_{ph}(t)$ and $\xi_{ph}(t)$ may assume non-zero values for external faults or for healthy phases during the occurrence of an internal fault, and may lead to maloperation. This happens when the values of Z and t depart too far from their true values because they are in actual frequency dependent. The application of low-pass filter to the input signals can help to correct the situation by eliminating the undesired transient frequency components and preventing the undesired output of the relay.

As mentioned before, the main advantage of the TWCD relay is its immunity to transients already existing at the time of the occurrence of an internal fault. Another advantage is its insensitivity to the presence of a fault resistance. Both these facts improve the reliability of the TWCD algorithm. Its major disadvantages are its relatively long operating time and its communication requirements. Anyhow, it is possible to reduce communication requirements (i.e., and hence improved the operating speed) by as much as a half if the travelling wave functions $e_r(t)|_R$ and $e_r(t)|_S$ at R and S are calculated locally for every mode or phase, depending on the implementation used[5.2] . In this way three quantities, rather than six, are exchanged between R and S. The delayed values of these travelling wave function can be used directly in equations (5-68) and (5-69) for the calculation of the fault functions, rather than using equations (5-70) and (5-71).

REFERENCES

(5.1) A. G. PHADKE AND J. S. THORP, " COMPUTER RELAYING FOR POWER SYSTEMS", BOOK, JOHN WILEY & SONS INC. 1988.

(5.2) "EVALUATION OF ULTRAHIGH SPEED RELAY ALGORITHMS", EPRI EL-3996, PROJECT 1422-2, FINAL REPORT, MAY 1985.

(5.3) M. VITINS, "A FUNDAMENTAL CONCEPT FOR HIGH SPEED RELAYING", IEEE TRANSACTIONS ON POWER APPARATUS AND SYSTEMS, VOL. PAS-100, 1981, PP. 163-173.

(5.4) F. ENGLER, O. E. LANZE, M. HANGGLI, AND G. BACCHINI, "TRANSIENT SIGNALS AND THEIR PRECESSING IN AN ULTRA HIGH-SPEED DIRECTIONAL RELAY FOR EHV/UHV TRANSMISSION LINE PROTECTION", IEEE TRANSACTIONS ON POWER APPARATUS AND SYSTEMS, VOL. PAS-104, NO. 6, JUNE 1985, PP. 1463-1473.

(5.5) EDITH CLARKE, "CIRCUIT ANALYSIS OF A-C POWER SYSTEMS", VOL. ONE, JOHN WILEY & SONS. NEW YORK, 1943.

(5.6) H. W. DOMMEL AND J. M. MICHELS, " HIGH SPEED RELAYING USING TRAVELLING WAVE TRANSIENT ANALAYSIS", IEEE PES WINTER MEETING, NEW YORK CITY, 1978, PAPER NO. A78 214-9.

(5.7) A. T. JHONS AND R. K. AGGARWAL, " NEW HIGH SPEED DIRECTIONAL BLOCKING SCHEME FOR TRANSMISSION LINE PROTECTION", IEE CONF. PUB. NO. 185, SECOND INT. CONF. ON DEVELOPEMENTS IN POWER SYSTEM PROTECTION, LONDON, 1980, PP. 93-96.

(5.8) A. T. JHONS, " A NEW ULTRE HIGH SPEED DIRECTIONAL COMPARISON TECHNIQUE FOR THE PROTECTION OF EHV TRANSMISSION LINES", IEE PROC. VOL. 127, Pt C, 1980, PP. 228-239, AND DISCUSSION ibid. VOL. 128, 1981, PP. 169-172.

(5.9) P. A. CROSSLEY AND P. G. MCLAREN, "DISTANCE PROTECTION BASED ON TRAVELLING WAVES", IEEE TRANSACTIONS ON POWER APPARATUS AND SYSTEMS, VOL. PAS-102, NO. 9, SEPTEMBER 1983, PP. 2971-2983.

(5.10) T. TAKAGI, J. BABA, K. UEMURE, AND T. SAKAGUCHI, "FAULT PROTECTION BASED ON TRAVELLING WAVE THEORY", IEEE, PES SUMMER MEETING, 1977, PAPER NO. A77 750-3.

(5.11) T. TAKAGI, et al. "FAULT PROTECTION BASED ON TRAVELLING WAVE THEORY- PART II: SENSITIVITY ANALUSIS AND LABORARORY TESTS", IEEE, PES WINTER MEETING, 1978, PAPER NO. A78 220-6.

(5.12) T. TAKAGI, et al., "FEASIBILITY STUDY FOR CURRENT DIFFERENTIAL CARRIER RELAY BASED ON TRAVELLING WAVE THEORY", IEEE, PES WINTER MEETING, 1978, PAPER NO. A78 132-3.

(5.13) T. TAKAGI, et al., "DIGITAL DIFFERENTIAL RELAYING SYSTEM FOR TRANSMISSION LINE PRIMARY- ITS THEORY AND FIELD EXPERIENCE", IEEE, PES WINTER MEETING, 1978, PAPER NO. A79 096-9.

above. For the differential algorithm to be restrained from tripping, it becomes necessary to characterize the relay as shown in figure (6-2).

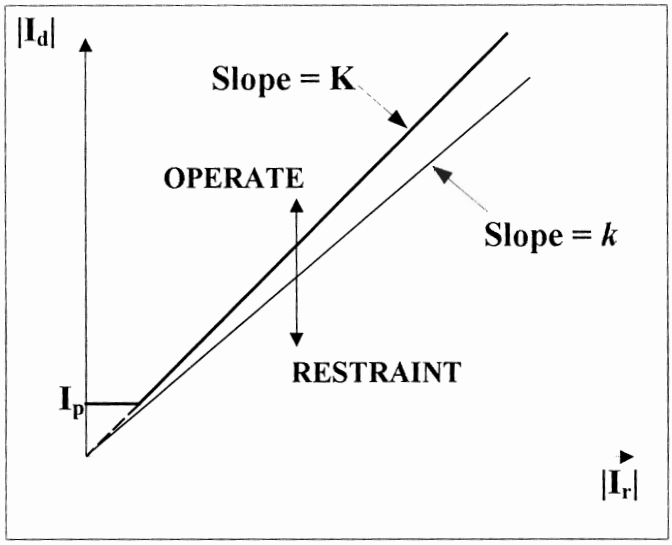

Figure (6- 2): Percentage differential protection characteristics.

In figure (6-2), the slop K is made greater than the *k* of equation (6-4) for more safety margin. The current I_p is the minimum pickup current which cause the relay to start operation. I_p is adjustable with a range of 20-50 % of the transformer rated current. Tripping takes place if the following condition is true,

$$|I_d| \geq K \cdot |I_r| \cdot \quad \text{..... (6-5)}$$

It is obvious that the smaller the setting K of the relay, the more sensitive is the relay in detecting small fault current. The slop K is adjustable in the range of 10-50 % .

The previous characteristics have been developed to be of two slopes as shown in figure (6-3) [6.1,6.4,6.15,6.22]. The current I_c in figure (6-3) represents the maximum expected differential current that may appear due to the current transformers error. The slope K_1 is related to the fixed minimum threshold current (I_p) and it is adjustable in the range of 10-50 %. Reducing K_1 and increasing I_c will increase the sensitivity to the lower fault currents. The second slope K_2 is so designed to be higher than K_1 to make the relay to restraint for high external through currents.

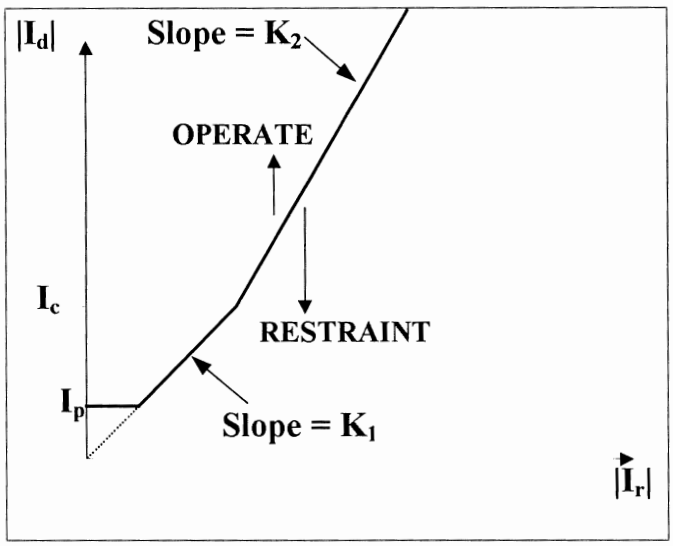

Figure (6- 3): Percentage differential protection characteristics with two slopes.

The relay will operate if the differential operating current Id satisfies one of the following conditions,

$$\begin{aligned} I_d &\geq K_1 \cdot I_r && \text{for } I_p \leq I_d < I_c \\ I_d &\geq K_2 \cdot \left(I_r - \frac{I_c}{K_1} \right) + I_c && \text{for } I_c \leq I_d \end{aligned} \qquad \text{..... (6-6)}$$

Three-phase transformer percentage differential protection follows the same principles outlined above. For a Y-Δ transformer, the line currents during normal operation on both sides have a phase difference between them. This must be accounted for before a differential relay can be connected. This usually accomplished by connection the CTs in the reverse connection (i.e. in Y on the Δ side of the transformer and in Δ on the Y side of the transformer). This is illustrated in figure (6-4). The same effect may be achieved through computation in a computer relay. From figure (6-4) the differential current phases are,

$$\begin{aligned} I_{da} &= i_a - i_A \\ I_{db} &= i_b - i_B \\ I_{dc} &= i_c - i_C \end{aligned} \qquad \text{..... (6-7)}$$

while the restraint current phases are,

$$I_{ra} = \frac{(i_a + i_A)}{2}$$

$$I_{rb} = \frac{(i_b + i_B)}{2} \qquad \text{..... (6-8)}$$

$$I_{rc} = \frac{(i_c + i_C)}{2}$$

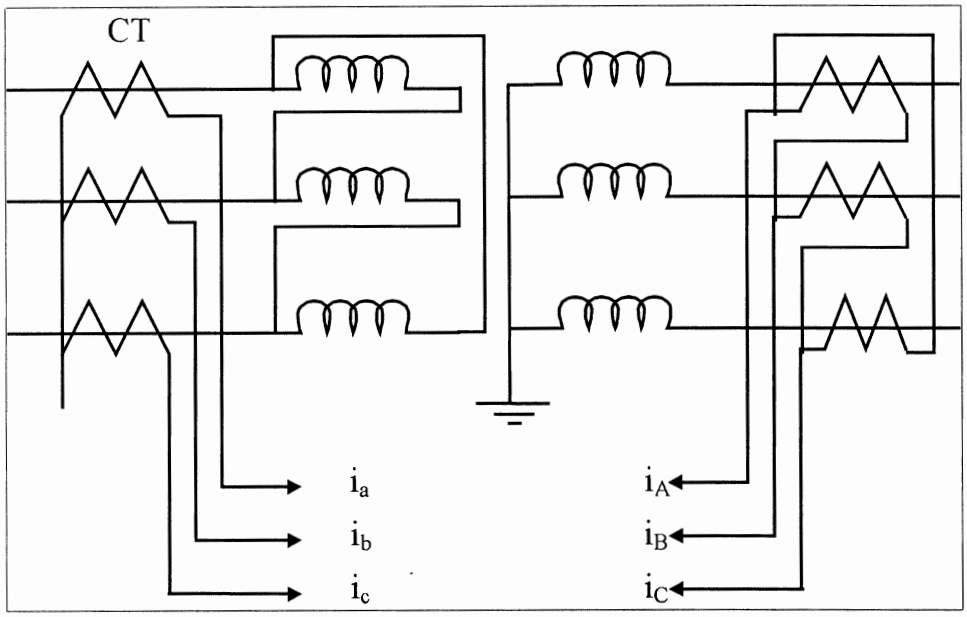

Figure (6- 4): A Y-Δ power transformer with CTs connections on its both sides for differential protection applications.

Another technique has been proposed to improve the ability of the percentage differential protection algorithm to detect external fault cases [6.10,6.16]. The idea is simply that the differential currents may appear during external faults due to CTs saturation. It has been proposed that during external fault cases those currents appear after (5-8) msec from the first impulse of the restraint current. This time lag could be use to insure the percentage differential protection algorithm decision in detecting external fault cases.

6-3: DIGITAL ALGORITHMS TO DISTINGUISH BETWEEN INTERNAL FAULT CURRENTS AND MAGNETIZING INRUSH CURRENTS

Using percentage differential protection techniques can detect the internal abnormal cases. Anyhow, internal abnormal cases are not necessary internal fault cases. They could be either an internal fault case, or an inrush current case or an overexcitation case. Any differential relay for power transformer protection has to distinguish between those cases and to initiate trip only for internal fault cases and to restraint for the other cases.

During energization of a transformer, abnormal currents may flow in the winding that is being energized. These are known as the magnetizing inrush currents, caused by the saturation of the transformer core for portions of cycles. Typical inrush currents are shown in figure (6-5). The inrush currents may be quite sever if there is residual in the core and it is of a polarity which takes the core further into saturation. The actual inrush currents depend on chance, as the relationship between the residual flux and the build up flux caused by energization, is random. The overexcitation phenomenon is produced when the transformer terminal voltages are increased suddenly of at least 10% of the rated value, or the operating frequency is decreased suddenly. However, the fact remains that, differential current may appear during energization of a transformer and due to an overexcitation phenomenon. It is then necessary to distinguish between those cases and internal fault cases.

The fact that, inrush currents are richer in harmonics than the fault currents has been used to design the harmonic restraint function. The second harmonic component of the differential current is used to detect an inrush current case, while the fifth harmonic component of the differential current is used to detect an overexcitation case. Almost all the conventional relays to protect power transformers use the harmonic restraint. With the application of the digital techniques in power transformer protection, many digital algorithm based the harmonic restraint have been proposed. Anyhow, they don't add any improvement on speed and accuracy. However, digital techniques allow applying another algorithms, which use the voltages as

supplementary signals to perform secure, and faster protection algorithms.

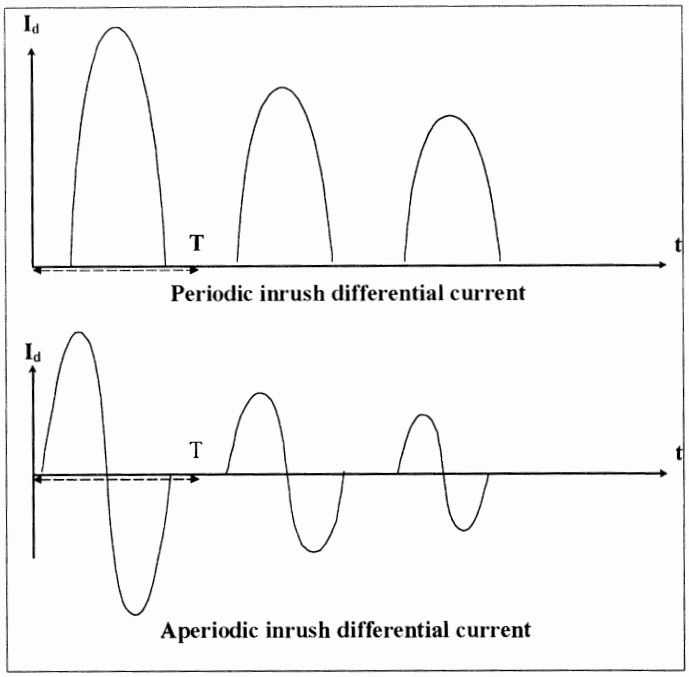

Figure (6- 5): Typical inrush currents.

6-3-A: DIGITAL DIFFERNTIAL ALGORITHMS BASED ON HARMINC RESTRAINT

In the area of digital differential protection of power transformers, two approaches have been proposed to estimate the harmonic components of the operating differential current to use them in the harmonic restraint protection algorithms. The first uses the digital filtering and the second depends correlating the differential currents samples with a pair of orthogonal functions. Anyhow, almost all of these algorithms still recognized as proposed algorithms waiting their practical applications.

6-3-A-1: USING OF DIGITAL FILTERS FOR SEPARATING THE HARMONIC COMPONENTS

In this section, we shall review some of the proposed digital algorithms using of digital filters for separating the harmonic components. Each of these algorithms has its limitations, which will be indicated separately.

(I)- Using of recursive band-pass filters

The recursive digital band-pass filters are used to obtain fundamental and second harmonic components of the differential current [6.2]. With sampling rate of 20 samples/cycle, the output of the 50 Hz and 100 Hz filters respectively are,

$$F_1(n) = 0.09\, i_n - 0.96\, i_{n-1} + 1.81\, F_1(n-1) - 0.905\, F_1(n-2) \quad \text{..... (6-9)}$$

$$F_2(n) = 0.04\, i_n - 0.045\, i_{n-1} + 1.58\, F_2(n-1) - 0.953\, F_2(n-2) \quad \text{.. (6-10)}$$

where, i_n is the n_{th} current sample. The outputs of the band-pass filter are rectified and smoothed using recursive digital low-pass filter to obtain unidirectional signals, which can be compared. The output of the low-pass filter is,

$$Y_n = 0.087\, X_n + 1.904\, Y_{n-1} - 0.913\, Y_{n-2} \quad \text{..... (6-11)}$$

where, X_n and Y_n are the n_{th} input and output samples.

The simplicity of this algorithm has its severe limitations. First, the digital filter coefficient values are severely affected by the input signals waveforms. Secondly, it takes about three cycles to indicate a fault case. The algorithm ignores the case of filtering the fifth harmonic components to detect the overexcitation cases, which may add more complexity and time.

(II)- Digital filters based on finite impulse response

Using finite impulse response approach [6.4] four finite impulse response digital filters are used for each phase with outputs of,

$$Y_1(n) = \sum_{m=n-N+1}^{n-\frac{N}{2}} \left[i_m - i_{m+\frac{N}{2}} \right] \quad \text{..... (6-12)}$$

$$Y_2(n) = \sum_{m=n-N+1}^{n-\frac{3N}{4}} \left[i_m - \left(i_{m+\frac{N}{4}} + i_{m+\frac{N}{2}} \right) + i_{m+\frac{3N}{4}} \right] \quad \text{..... (6-13)}$$

$$Y_3(n) = \sum_{m=n-N+1}^{n-\frac{3N}{4}} \left[i_m - i_{m+\frac{N}{4}} + i_{m+\frac{N}{2}} - i_{m+\frac{3N}{4}} \right] \quad \text{..... (6-14)}$$

$$Y_4(n) = \sum_{m=n-N+1}^{n-\frac{7N}{8}} \left[i_m - \left(i_{m+\frac{N}{8}} + i_{m+\frac{N}{4}} \right) + i_{m+\frac{3N}{8}} + i_{m+\frac{N}{2}} - \left(i_{m+\frac{5N}{8}} + i_{m+\frac{3N}{4}} \right) + i_{m+\frac{7N}{8}} \right] \quad \text{..... (6-15)}$$

where, in is the n_{th} differential current sample. Fundamental and second harmonic components of each phase are calculated respectively as,

$$F_1 = \sqrt{(Y_1(n))^2 + (Y_2(n))^2} \quad \text{..... (6-16)}$$

$$F_2 = \sqrt{(Y_3(n))^2 + (Y_4(n))^2} \quad \text{..... (6-17)}$$

The relay restraint if, $F2 > 0.25\ F_1$.

Besides the high number of the digital filters, the relay is of other limitations. This algorithm is of long time to detect internal faults. This time is more than one cycle and becomes of several cycles affected by dc components of the fault current and by CTs saturation. More complexity will be added if additional filters are added to estimate the fifth harmonic components.

(III)- Digital filters based on analyzing of pure sinusoidal waveforms

A derivation of Wedmore's superposition method of harmonic analysis, has been used to calculate the harmonic components of the differential currents signals [6.5]. The basic idea is that if a pure sine wave is divided into any number of equal parts and equivalent ordinates are added, then the sum of the ordinates will be zero. Hence, twice the second harmonic component of a differential current is filtered by summing the last sample with that half cycle before. The fifth harmonic component is the fifth the sum of samples at intervals of 1/5 of the fundamental frequency. This algorithm is only suitable for pure sine wave. Thus, dc component and higher harmonics than the fifth have to be removed. The higher harmonics are removed using filter circuits. Dc

components are removed by averaging the signal using the data of last cycle. With a sampling rate of 20 sample/cycle, the dc component of the n_{th} current sample is,

$$F_o(n) = \frac{S(n)}{20} = \frac{i_n + S(n-1) - i_{n-20}}{20} \quad \text{..... (6-18)}$$

Where, $S(n) = \sum_{n=1}^{20} i_n$. Then the corresponding differential current without dc component is,

$$i'(n) = i(n) - F_o(n) \quad \text{..... (6-19)}$$

The second and fifth harmonic components are calculated as,

$$F_2(n) = \frac{i'(n) + i'(n-10)}{2} \quad \text{..... (6-20)}$$

$$F_5(n) = \frac{i'(n) + i'(n-4) + i'(n-8) + i'(n-12) + i'(n-16)}{5} \quad \text{.... (6-21)}$$

As mentioned before, this algorithm is suitable only for currents of pure sine waveforms. This practically could not be achieved because of the distortion caused by CTs saturation. The operating times still more than one cycle.

(IV)- Digital filtering based on the weighting least square method

The differential current has been represented by the following equation [6.7],

$$i(t) = I_o \cdot e^{-A \cdot t} + \sum_{k=1}^{k} I_k \cdot \sin(k\omega t + \theta_k) \quad \text{..... (6-22)}$$

where, I_o and I_k are the dc and the k_{th} harmonic components respectively, and $\theta_k = k\ t_k$. If the time of the data window is smaller

than the time constant of the decaying dc component (i.e. 1/A), the equation (6-22) can be simplified to be,

$$i(t) = I_0 + I'_o t + I''_o t^2 + \sum_{k=1}^{k} \left| Is_k \cdot \sin(k\omega T) + Ic_k (k\omega T) \right| \quad \text{.... (6-23)}$$

which can be expressed in matrix form as,

$$[i(t)] = [A] \cdot [Y] \quad \text{..... (6-24)}$$

where,

$$[A] = \begin{bmatrix} 1 & t_1 & t_1^2 & \sin(\omega t_1) & \cos(\omega t_1) & \sin(\omega t_2) & . & . \\ t_k & t_k^2 & \sin(\omega t_k) & \cos(\omega t_k) & \sin(2\omega t_k) & \cos(2\omega t_k) & . & . \end{bmatrix} \quad \text{..... (6-25)}$$

and,

$$[Y] = \begin{bmatrix} I_o \\ I'_o \\ I''_o \\ Is_1 \sin(\theta_1) \\ Ic_1 \cos(\theta_1) \\ . \\ . \\ . \\ Is_k \sin(\theta_k) \\ Ic_k \cos(\theta_k) \end{bmatrix} \quad \text{..... (6-26)}$$

If the number of samples of the data window (N) is greater than the order of the model (i.e. k), then the least square solution of the last equation becomes;

$$[Y] = \left[\left(A^T \cdot A^{-1} \right) \cdot A^T \right] \cdot [i(t)] = [B] \cdot [i(t)] \quad \text{..... (6-27)}$$

where, $[A]^{-1}$ and $[A]^{T}$ are the inverse and transfer matrices of [A]. Using equation, all the unknown elements of [Y] can be calculated using the known elements of [B] and [i(t)].

In addition to the complex and high number of calculations used in this algorithm, it has other limitations. To apply this algorithm successfully, an appropriate weighting matrix is needed for every transformer. The speed and the accuracy of this algorithm depend on the number of samples per a cycle and the order of the model. The algorithm error increases with the high order of the model and the increasing of the dc component. CTs saturation has its effect on the accuracy of the algorithm.

In [6.18], this algorithm is developed to minimize the execution time by squaring the currents samples. Anyhow, this can be applied only if the harmonic distortion of the input signal does not exceed (10-15)% of the first harmonic. This assumption cannot be achieved practically since for example the second harmonic distortion in our today transformers normally reaches 40% of the fundamental.

(V)- Using of Kalman filters

A time varying Kalman filter has been used to separate the harmonics components of the differential currents [6.11, 6.13] using state-spaced observers with constant gains. A number of gains have to be precomputed and stored for this implementation. The following state-variable equations are for a signal having harmonic components up to the n_{th} order with samples z_k, at time t_k, (2n+1) samples per period,

$$x_{k+1} = [F] \cdot x_k$$
$$z_k = [H] \cdot x_k \qquad \text{..... (6-28)}$$

where, 2n+1-dimension state vector x_k is as follows,

$x_k(2i-1)$: real component of the i_{th} harmonic phasor.

$x_k(2i)$: imaginary component of the i_{th} harmonic phasor.

$x_k(2n+1)$: dc component.

The i_{th} element of x_k is represented by xk(i).

$$[F]=\begin{bmatrix} f(\omega T) & 0 & . & . & 0 & 0 \\ 0 & f(2\omega T) & . & . & 0 & 0 \\ . & . & . & . & . & 0 \\ . & . & . & . & . & . \\ 0 & 0 & . & . & f(n\omega T) & . \\ 0 & 0 & . & . & . & 1 \end{bmatrix}$$

T: sampling time.

$$f(\omega T)=\begin{bmatrix} \cos(i\omega t) & -\sin(i\omega t) \\ \sin(i\omega t) & \cos(i\omega t) \end{bmatrix} \quad , i = 1,2,3,...,n.$$

[H]: a $1\times(2n+1)$ matrix which gives the connection between the measurement (z_k) and the state vector x_k.

The sampled value of the signal is considered to be as the sum of the real components of the harmonic phasors and the dc component. Therefore, the matrix [H] is given by,

[H] = [1 0 1 0 1..... 0 1]

The harmonic components h_i (i.e., in rms. values) are given by,

$$h_i^2 = \frac{(x_k^2(2i-1)+x_k^2(2i))}{2} \qquad i = 1,...,n$$

$$h_o = x_k(2n+1) \qquad \text{..... (6-29)}$$

The sampling frequency should be at least twice the highest harmonics frequency in the signal.

The problem of estimating the present state of the signal model of equation (6-28) from output measurements z_k involves the design of standard state observers [6.13]. The observer state can be represented by,

$$\hat{x}_{k+1} = [F]\cdot\hat{x}_k + [M](z_k - [H]\cdot\hat{x}_k) \qquad \text{..... (6-30)}$$

where $\hat{x}_k$ denotes the estimate of the state vector x_k, and [M] is the observer gain matrix determined as,

$$[M]=[F]\cdot[P]\cdot[H]^{T}\cdot\left([R]+[H][P][H]^{T}\right)^{-1} \quad \text{..... (6-31)}$$

where, [P] is a stable steady-state solution of the Riccatti equation,

$$[P]_{k+1}=[F]\cdot[P]_{k}\cdot[F]^{T}+[Q]-[F]\cdot[P]_{k}\cdot[H]^{T}\cdot\left([R]+[H]\cdot[P]_{k}\cdot[H]^{T}\right)^{-1}\cdot[H]\cdot[P]_{k}\cdot[F]^{T} \quad \text{.(6-32)}$$

The subscripts (-1) and (T) in the last two equations denote the inverse and transpose of the matrix respectively. R and Q are symmetric weighting matrices to be chosen taking the relative importance of the individual components for the objective of differential protection into account.

The greatest limitation of using Kalman filtering is that it has assumed well enough the statistic properties of the signal occurring in reality. However, such exact forecasting is practically not possible and it is necessary to expect wider ranges of signal distortion so that the behavior of Kalman filter deteriorates quickly [6.18]. Besides, eleven-states Kalman filter has been proposed to filter up to the fifth harmonic components, however models of higher orders are required for complex signals such as inrush currents and distorted signals due to CTs saturation. In addition to that, the filter is of complex computation burden.

6-3-A-2: DIGITAL ALGORITHMS BASED ON FOURIER ANALYSIS

Fourier analysis has been based to estimate the harmonic components of the differential currents by correlating the differential currents signals with a pair of orthogonal signals. The orthogonal signals could be sin, cos. odd and even square waves of one cycle duration, etc. All the following algorithms calculate the Fourier coefficients in different ways. They all are of more than one cycle operation, which is somehow long time. In addition to that, all the presented approaches are not effective with distorted current signals due to CTs saturation. In this section, we shall review some of these algorithms in simplified mathematical analysis, since detailed mathematical analysis can be found in section 3-1 of chapter three.

(I)- Digital algorithms based on fourier transform

Using Fourier analysis approach [6.8], the n_{th} harmonic term beginning at the r_{th} sample is given as,

$$F_n(r) = \frac{1}{N} \sum_{k=r}^{r+N-1} i_k \, e^{-j \frac{2\pi kn}{N}} \qquad \text{..... (6-33)}$$

where, i_k is the k_{th} sample of the differential current signal, and N is the number of samples per a cycle. For N=12 samples/cycle, the last equation becomes,

$$F_n(r) = \frac{1}{12} \sum_{k=r}^{r+11} i_k \, e^{-j \frac{2\pi kn}{12}} \qquad \text{..... (6-34)}$$

After the next sample becomes available, the next set of harmonics can be computed by updating $F_n(r)$, viz. $F_n(r+1)$ can then be calculated easily as,

$$F_n(r+1) = F_n(r) + \tfrac{1}{12}\left[i_{r+12} - i_r\right] e^{-j \frac{2\pi nr}{12}} \qquad \text{..... (6-35)}$$

Real and imaginary parts of the nth harmonic components can be computed using an expression similar to equation (6-35), replacing the exponential term with $\cos(\frac{nr\pi}{6})$ and $\sin(\frac{nr\pi}{6})$ terms respectively,

$$\begin{aligned} F_{n(Rel.)}(r+1) &= F_{n(Rel.)}(r) + \tfrac{1}{12}\left[i_{r+12} - i_r\right]\cos(\tfrac{\pi nr}{6}) \\ F_{n(Im.)}(r+1) &= F_{n(Im.)}(r) + \tfrac{1}{12}\left[i_{r+12} - i_r\right]\sin(\tfrac{\pi nr}{6}) \end{aligned} \qquad \text{..... (6-36)}$$

The n_{th} harmonic component is calculated then as,

$$|F_n| = \sqrt{F_{n(Rel.)}^2 + F_{n(Im.)}^2} \qquad \text{..... (6-37)}$$

Trip takes place if one of the following conditions are satisfied,

$$|F_2| \le 0.3|F_1|$$
$$|F_5| \le 0.2|F_1| \qquad \text{..... (6-38)}$$

(II)- Digital algorithms based on the rectangular transform technique

Replacing the cos. and sin. terms of equation (6-34) with equivalent rectangular functions, we get the following equation [6.6],

$$S_n = \sum_{j=0}^{N-1} I_j \ \text{sgn}\left[\sin\left(\frac{2\pi nr}{N}\right)\right]$$
$$C_n = \sum_{j=0}^{N-1} I_j \ \text{sgn}\left[\cos\left(\frac{2\pi nr}{N}\right)\right] \qquad \text{..... (6-39)}$$

where,

$$\text{sgn}(x) = \begin{bmatrix} x/|x| & \text{for } x \neq 0 \\ 0 & \text{for } x = 0 \end{bmatrix}$$

For a band-limited signal, rectangular coefficients of equations (6-39)(i.e. S_n and C_n) are related to the Fourier sin. and cos. coefficients (i.e. F_{is} and F_{ic}) in such a way,

$$S_n = [A] \cdot F_{is}$$
$$C_n = [B] \cdot F_{ic} \qquad \text{..... (6-40)}$$

Thus, the Fourier coefficients are calculated then as,

$$F_{is} = [A]^{-1} \cdot S_n$$
$$F_{ic} = [B]^{-1} \cdot C_n \qquad \text{..... (6-41)}$$

where [A] and [B] are infinite sparse matrices, and $[A]^{-1}$ and $[B]^{-1}$ are their inverse matrices respectively defined as,

$$[A]^{-1},[B]^{-1} = \frac{\pi}{4}\begin{bmatrix} 1 & 0 & \pm\frac{1}{3} & 0 & \frac{1}{5} & 0 & \pm\frac{1}{7} & 0 & \frac{1}{9} & 0 & \pm\frac{1}{11} \\ & 1 & 0 & 0 & 0 & \pm\frac{1}{3} & 0 & 0 & 0 & \frac{1}{5} & 0 \\ & & 1 & 0 & 0 & 0 & 0 & 0 & \pm\frac{1}{3} & 0 & 0 \\ & & & 1 & & & & & & & \\ & & & & 1 & & & & & & \\ & & & & & 1 & & & & & \\ & & & & & & 1 & & & & \\ & & & & & & & 1 & & & \\ & & & & & & & & 1 & & \\ & & & & & & & & & 1 & \\ & & & & & & & & & & 1 \end{bmatrix} \quad \text{...(6-42)}$$

The minus sign is for $[A]^{-1}$ matrix and the plus sign is for $[B]^{-1}$. The Fourier coefficients of the fundamental, second, and fifth harmonic components are calculated as,

$$F_{1s} = S_1 - \frac{1}{3}S_3 - \frac{1}{5}S_5$$

$$F_{1c} = C_1 + \frac{1}{3}C_3 - \frac{1}{5}C_5$$

$$F_{2s} = S_2$$

$$F_{2c} = C_2$$

$$F_{5s} = S_5$$

$$F_{5c} = C_5$$

and the n_{th} harmonic can now be calculated as,

$$F_n = \frac{2}{N}\sqrt{(F_{ns})^2 + (F_{nc})^2} \qquad \text{..... (6-43)}$$

Trip takes place if one of the conditions of (6-38) are satisfied.

(III)- Digital algorithms based on Walsh and Haar functions

Walsh and Haar functions have been used in designing harmonic restraint algorithms [6.12, 6.26, and 6.27]. The Walsh expansion of the differential current signal i(t) in the interval [0,T] is defined as;

$$i(t) = \sum_{k=0}^{\infty} W_k \cdot Wal(k, \frac{t}{T}) \qquad \text{..... (6-44)}$$

where, Wal(k,t) is the Walsh function, T is the sampling time, and W_k is the Walsh coefficients that obtaining by correlating the samples of differential current i(t) with reference Walsh functions,

$$W_k = \frac{1}{T}\int_0^T i(t)\, Wal(k, \frac{t}{T})\, dt \qquad \text{..... (6-45)}$$

The relationship between Fourier and Walsh coefficients can be expressed in matrix form as;

$$[W] = [A] \cdot [F] \qquad \text{..... (6-46)}$$

Any element A_{kk} in [A] is the result of substituting the k_{th} sinusoid that appears in equation (6-34) for i(t) in equation (6-44). The Fourier coefficients F1, F2, F3, and F4 can be determined from the Walsh coefficients as;

$$F_1 = 0.9W_1 - 0.373W_5 - 0.074W_9$$
$$F_2 = 0.9W_2 + 0.373W_6 - 0.074W_{10}$$
$$F_3 = 0.9W_3 - 0.373W_{11}$$
$$F_4 = 0.9W_4 + 0.373W_{12}$$

The fundamental and second harmonic components are calculated as,

$$I_1 = \sqrt{(F_1)^2 + (F_2)^2}$$
$$I_2 = \sqrt{(F_3)^2 + (F_4)^2} \qquad \text{..... (6-47)}$$

The Haar function have three possible states 0, +A, and –A where ±A are functions of 2 and it may be expressed as Har(n,t). For a time interval 0<t<1, the Haar functions are given as,

$$\mathrm{Har}(0,t) = 1 \quad \text{for} \quad 0 \le t \le 1$$

$$\mathrm{Har}(1,t) = \begin{bmatrix} 1 & \text{for} \quad 0 \le t \le \frac{1}{2} \\ -1 & \text{for} \quad \frac{1}{2} \le t \le 1 \end{bmatrix} \qquad \text{..... (6-48)}$$

$$\mathrm{Har}(2^p + n, t) = \begin{bmatrix} \sqrt{2^p} & \text{for} \quad \frac{n}{2^p} \le t \le \frac{(n+1)/2}{2^p} \\ -\sqrt{2^p} & \text{for} \quad \frac{(n+1)/2}{2^p} \le t \le \frac{(n+1)}{2^p} \\ 0 & \text{otherwise} \end{bmatrix}$$

where, p=1,2,.. and n=0,1,2,…,(2^p-1). In terms of these functions the Haar expansion of i(t) in the interval (0,T) is defined as,

$$i(t) = \sum C_k \ \mathrm{Har}(k,t) \qquad \text{..... (6-49)}$$

where, C_k is the Haar coefficient which is obtained by correlating the samples of differential current i(t) with reference Haar functions,

$$C_k = \int_{t=0}^{1} i(t)\, \mathrm{Har}(k,t)\ dt \qquad \text{..... (6-50)}$$

The Fourier coefficients are then obtained as,

$$\left\{ \begin{aligned} F_1 &= 0.9C_1 + 0.1865(-C_4 + C_5 + C_6 - C_7) + \\ &\quad 0.089(-C_8 + C_{11} + C_{12} - C_7) + 0.037(-C_9 + C_{10} + C_{13} - C_{14}) \\ F_2 &= 0.6366(C_2 - C_3) + 0.1865(C_4 + C_5 - C_6 - C_7) + \\ &\quad 0.037(C_8 + C_{11} - C_{12} - C_{15}) + 0.089(C_9 + C_{10} - C_{13} - C_{14}) \\ F_3 &= 0.6366(C_2 + C_3) + 0.037(C_9 + C_{10} + C_{13} + C_{14} - \\ &\quad C_8 - C_{11} - C_{12} - C_{15}) \\ F_4 &= 0.6366(C_4 - C_5 + C_6 - C_7) + \\ &\quad 0.1318(C_8 + C_9 + C_{12} + C_{13} - C_{10} - C_{11} - C_{14} - C_{15}) \end{aligned} \right\} \qquad \text{.....(6-51)}$$

The fundamental and second harmonic components are calculated using equation (6-47). Trip takes place if one of the conditions of (6-38) is satisfied.

It is obvious that both theses algorithms don't include the calculations of the fifth harmonic components. Anyhow, including the calculations of the fifth harmonic components means adding more complexity to calculations burden of both of these algorithms and longer time of operation.

6-3-B: ERRORS OF HARMONIC RESTRAINT ALGORITHMS DUE CURRENT TRANSFORMER'S SATURATION

Using the amount of the differential currents harmonic components to distinguish between internal fault and magnetizing current cases becomes increasingly difficult. The non-pure sinusoidal waveshapes of the differential currents and their distortion caused by current transformers saturation, are the main factors which effect the differential currents harmonic components [6.10,6.28,6.45].

During severe internal fault cases, CTs saturation is expected in both steady state and transient state cases. This saturation may distort the differential currents waveshapes. The distorted currents contain substantial amount of higher harmonics. In figure (6-6), the level of particular harmonics (I_n) related to the fundamental harmonic (I_1) is shown. In the figure, (I_3) and (I_5) are the third and the fifth harmonic components respectively, and the coefficient (X) determines the

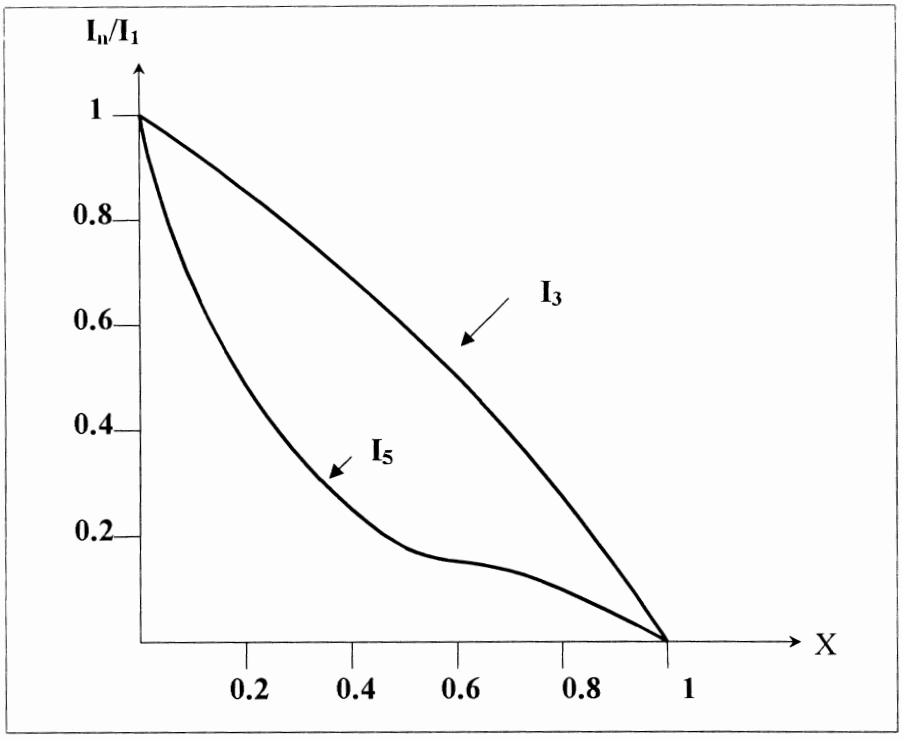

Figure (6- 6): Harmonics in distorted differential current due to CTs saturation.

relative level of saturation [6.45]. If X=0 it means the CT is fully saturated, while if X=1 it means that there is no saturation. The level (X) is calculated as,

$$X = 1.3\frac{V_k}{I_p \cdot Z_2} \qquad \text{.....(6-52)}$$

Where,

V_k : is the CT knee point voltage.

I_p : is the r.m.s primary current reduced to the secondary side of the CT.

Z_2 : is the total CT secondary burden including the winding, the wires, and the relay impedance.

With severe internal fault cases in which the fault current may reach 50 times or more than the rated current, CTs are saturated severely and (X) will be quite low. From figure (6-6), with such expected cases the distorted differential currents may contain

substantial high fifth harmonic frequency components up to 40% of the fundamental component or even high. This makes the relay to recognize the case as an overexcitation case. This is of great risk since the high fifth harmonic components may block the relay during such severe faults leading the transformer to damage.

CTs are likely to saturate during transient states when the faults current contains decaying dc components. Therefore, transient errors and distortion of differential currents may take place. In figure (6-7), second and fifth harmonic components related to the fundamental are shown as a function of the dc offset factor (A). The (A) factor is defined as the ratio of the dc component of a signal to the amplitude of the ac component. From figure (6-7) one can see that how high dc component may cause high second harmonic component. This means that with a fault current of high dc component, higher second harmonic components are expected and it may cause the relay to block until the dc component will decay to small values. This may cause a delay in the relay operation up to several cycles depending on the primary current decaying time constant.

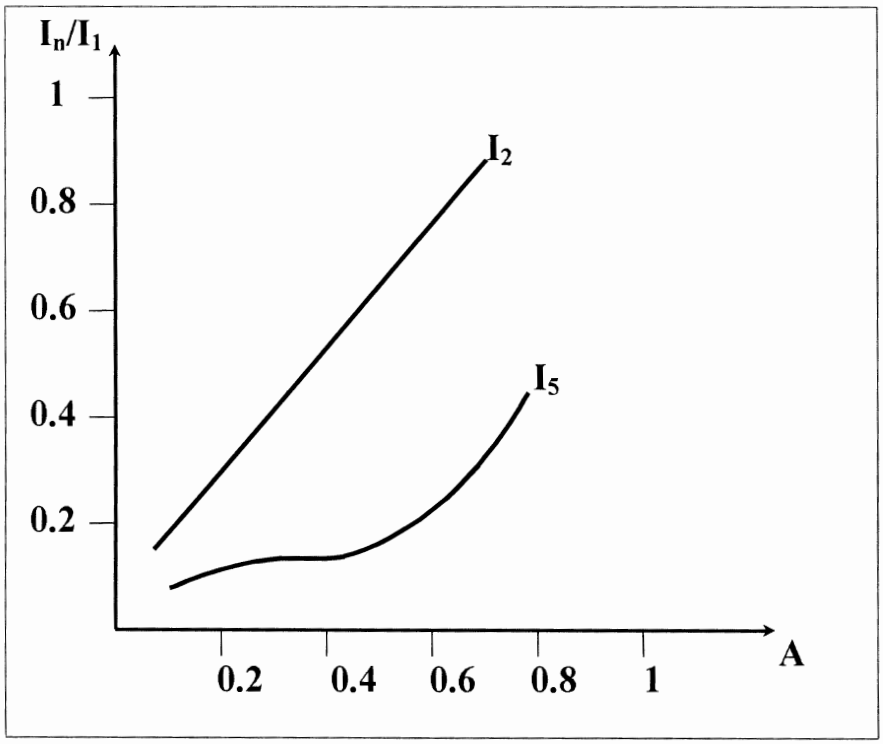

Figure (6- 7): Harmonics in distorted differential current with CT saturates at transient state.

It is well known that inrush currents are rich of second harmonic components. However, the minimal expected level of the second harmonic in inrush differential currents depends mainly on the highest residual fluxes in power transformer cores. Figure (6-8) shows the amount of the second harmonic related to the fundamental frequency component, as a function of the maximum expected residual flux density in the power transformer core (B_r). It is clear from the figure, how high residual flux density may cause inrush currents with low second harmonic components, which may cause the relay to consider the case as an internal fault case and maloperation takes place. This is one of big the problems of using the harmonic restraint differential protection schemes in our today's very huge power transformers. Those huge power transformers are usually designed with small core size to reduce the losses. This makes the residual flux density in the cores to be as high as (1.8) Tesla. With such residual flux density ranges, the second harmonic components may be less than 20% of the fundamental causing the relay to trip concerning the case as a internal case.

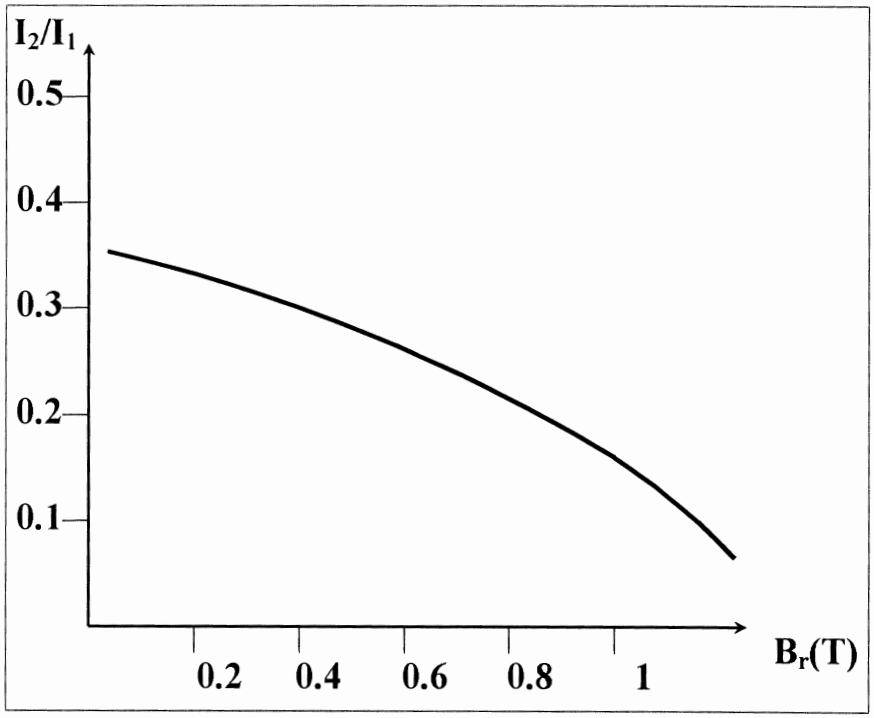

Figure (6- 8): Minimal expected second harmonic in inrush currents as a function of the residual flux density.

From the previous review, we can conclude that the security and selectivity of the harmonic restraint protection schemes are a mater of concern. It therefore important to think of new algorithms, which are faster and more secure. Recently new digital algorithms using the transformer voltage signals in addition to the current signals have been proposed. Those algorithms make use of the digital techniques abilities in creating new algorithms for calculation the transformer parameters. In general, those algorithms show high security and selectivity with an improved speed of operation. In the next section, some of those algorithms will be illustrated.

6-3-C: USING OF VOLTAGES AS SUPPLEMENTARY SIGNALS TO THE DIFFERENTIAL CURRENTS

6-3-C-1: DIGITAL ALGORITHM BASED ON THE TRANSFORMER FLUX BEHAVIOR

This algorithm has been designed and tested for three-phase transformer, based on the behavior of the mutual fluxes of the transformer windings [6.9]. The voltage at the terminal of any winding of the transformer and neglecting the winding resistance is calculated by,

$$e - L\frac{di}{dt} = \frac{d\phi}{dt} \qquad \text{..... (6-53)}$$

where,
e: is the voltage at the winding terminal.
L: is the winding leakage inductance.
i : is the current entering the winding.
ϕ : is the mutual flux of the winding.

Using the trapezoidal method of integration, the last equation can be expressed in digital form for the samples (n) and (n-1) as,

$$\phi_n - \phi_{n-1} = \frac{T}{2}(e_n + e_{n-1}) - L(i_n - i_{n-1})$$

where, T is the sampling time. Then, an expression for the flux (ϕ) can be given as,

$$\phi_n = \phi_{n-1} + \frac{T}{2}(e_n + e_{n-1}) - L(i_n - i_{n-1}) \qquad \text{..... (6-54)}$$

The last equation describes a procedure to calculate the mutual flux linkages of a transformer from its past history and the measured current and voltage samples at its terminal. Assuming that the flux computed in equation (6-54) represents the actual flux in the transformer, the samples of the differential current and the flux (i_{dk}, ϕ_k) will lie then on the open circuit magnetizing curve of the transformer as shown in figure (6-9-a). Simultaneously, the location of the (i_{dk}, ϕ_k) could be checked. A trip would be issued if (i_{dk}, ϕ_k) do not lie on the open circuit magnetizing curve.

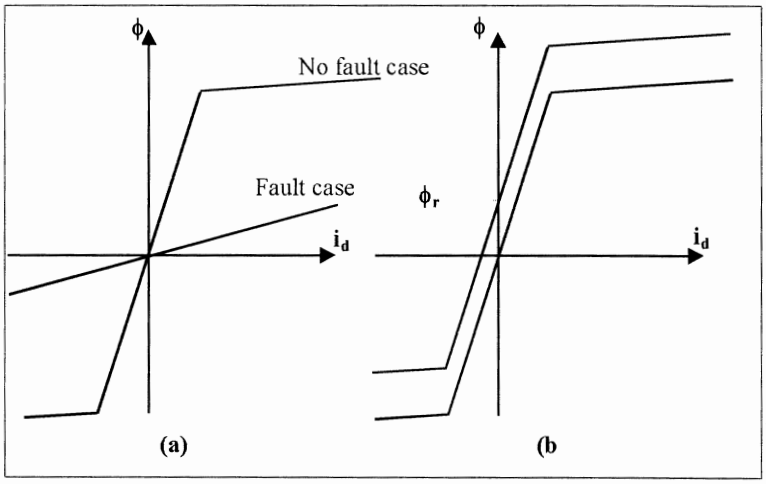

Figure (6- 9): a- Fault and no-fault region in (i,ϕ) plane. b- Effect of unknown residual flux (ϕ_r).

However, the last assumption could not be met practically since we neglect the effect of the residual flux in the transformer core. In the presence of the residual flux, the actual (i,ϕ) characteristics of the transformer may vary according to the curves shown in figure (6-9-b). Anyhow, this problem has been overcome by considering the slope ($d\phi/di$) rather than the flux (ϕ) in determining the restraining function. The derivative ($d\phi/di$) is immune to the error made by residual flux. From equation (6-54),

$$\left(\frac{d\phi}{di}\right)_n \cong \frac{\phi_n - \phi_{n-1}}{i_n - i_{n-1}} = \frac{T}{2}\left(\frac{e_n + e_{n-1}}{i_n - i_{n-1}}\right) - L \qquad \text{..... (6-55)}$$

In the ($d\phi/di$ – i) plane, there is a region which corresponds to a fault or saturated operation. Another region, sufficiently removed from the first, designates operation on the magnetizing curve in the unsaturated region. This is illustrated in figure (6-10). During an internal fault case, the differential samples and the ($d\phi/di$) samples remain continuously in region (1). While in the inrush current cases these samples alternate between the two regions. This behavior has been used to indicate the internal fault cases.

This algorithm is faster than the harmonic restraint algorithms and more secure. Anyhow, the most limitation of this algorithm is that it needs the phase quantities of the currents and voltages to run the algorithm, which cannot be always achieved particularly.

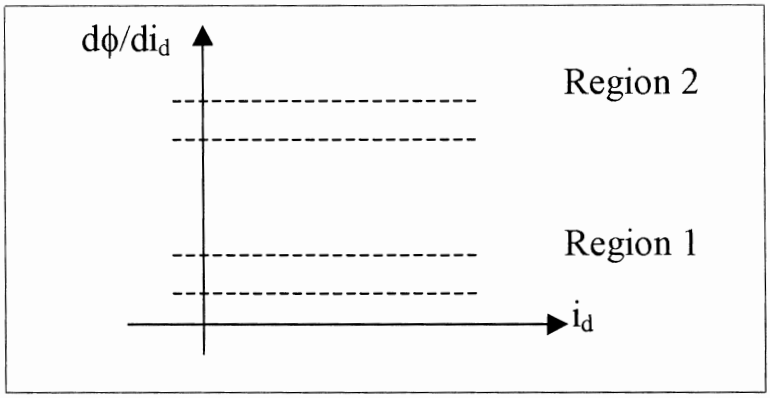

Figure (6- 10): Fault and non-fault regions in the ($d\phi/di$ – i) plane.

6-3-C-2: DIGITAL ALGORITHMS BASED ON THE COMPARISON OF THE TERMINALS VOLTAGE WITH THEIR ESTIMATED VALUES

The main idea of these algorithms is that each phase of a three-phase power transformer at no load can be represented as shown in figure (6-11) [6.14, 6.17]. From the figure, and neglecting the winding resistances,

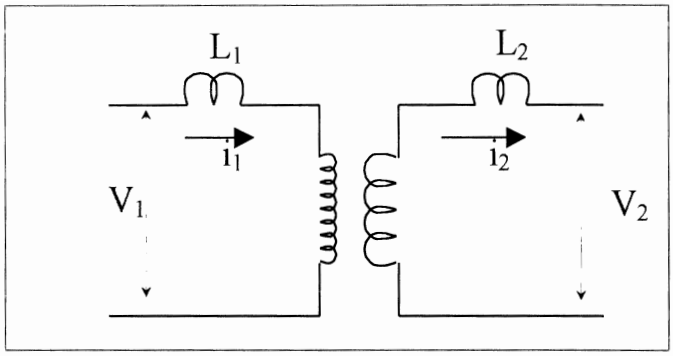

Figure (6- 11): Unloaded transformer circuit diagram.

the following equation is applied,

$$V_1 = L_1 \frac{di_1}{dt} + L_2 \frac{di_2}{dt} + V_2 \qquad \text{..... (6-56)}$$

where, subscripts 1 and 2 in the last equation relate to the primary and secondary voltages, currents, and inductances respectively. Using the trapezoidal method of integration [6.17], the last equation can be represented as,

$$V_{1(n)} + V_{1(n-1)} = 2\frac{L_1}{T}\left[i_{1(n)} - i_{1(n-1)}\right] + 2\frac{L_2}{T}\left[i_{2(n)} - i_{2(n-1)}\right] + V_{2(n)} + V_{2(n-1)}$$

or,

$$V_{1(n)} = 2\frac{L_1}{T}\left[i_{1(n)} - i_{1(n-1)}\right] + 2\frac{L_2}{T}\left[i_{2(n)} - i_{2(n-1)}\right] + V_{2(n)} + V_{2(n-1)} - V_{1(n-1)} \qquad \text{.... (6-57)}$$

From the last equation, a method to detect internal fault cases has been proposed. It is that the calculation results of the right hand side of the equation is nearly equal to the measured value of the voltage sample (i.e. $V_{1(n)}$) during normal healthy operation, however they are not during internal fault cases [6.17]. The most imitation of this algorithm that it needs the phase currents samples. These samples cannot be collected practically on the delta-connected sides of the transformer.

This algorithm has been modified to propose an expression, which does not contain phase quantities items [6.14]. Equation (6-57) can be rewritten for phases (a) and (b) of the Δ-Y transformer of figure (6-4) as,

$$Va_{1(n)} = 2\frac{L_1}{T}\left[ia_{1(n)} - ia_{1(n-1)}\right] + 2\frac{L_2}{T}\left[ia_{2(n)} - ia_{2(n-1)}\right] + Va_{2(n)} + Va_{2(n-1)} - Va_{1(n-1)} \quad \text{..... (6-58)}$$

$$Vb_{1(n)} = 2\frac{L_1}{T}\left[ib_{1(n)} - ib_{1(n-1)}\right] + 2\frac{L_2}{T}\left[ib_{2(n)} - ib_{2(n-1)}\right] + Vb_{2(n)} + Vb_{2(n-1)} - Vb_{1(n-1)} \quad \text{..... (6-59)}$$

Subtracting equation (6-59) from (6-58) we get,

$$\begin{aligned} Va_{1(n)} - Vb_{1(n)} = {} & 2\frac{L_1}{T}\left[ia_{1(n)} - ib_{1(n)}\right] + 2\frac{L_2}{T}\left[ia_{2(n)} - ib_{2(n)}\right] - \\ & 2\frac{L_1}{T}\left[ia_{1(n-1)} - ib_{1(n-1)}\right] - 2\frac{L_2}{T}\left[ia_{2(n-1)} - ib_{2(n-1)}\right] + \\ & \left[Va_{2(n)} - Vb_{2(n)}\right] + \left[Va_{2(n-1)} - Vb_{2(n-1)}\right] - \\ & \left[Va_{1(n-1)} - Vb_{1(n-1)}\right] \end{aligned} \quad \text{.... (6-60)}$$

It is clear from figure (6-12) that,

$$\begin{aligned} & (i_{a1} - i_{b1}) - (i_{a2} - i_{b2}) \equiv i_{a-b} - i_B \\ & V_{ab} = V_{a1} - V_{b1} \\ & V_{(a-b)} = V_{a2} - V_{b2} \end{aligned} \quad \text{..... (6-61)}$$

Where,

$i_{(a-b)}$ and i_B : are the lines currents of phase (b) of the differential currents phases through the current transformers.

V_{ab} : is the line-line voltage at delta side.

$V_{(a-b)}$: is the phase-phase voltage at star side.

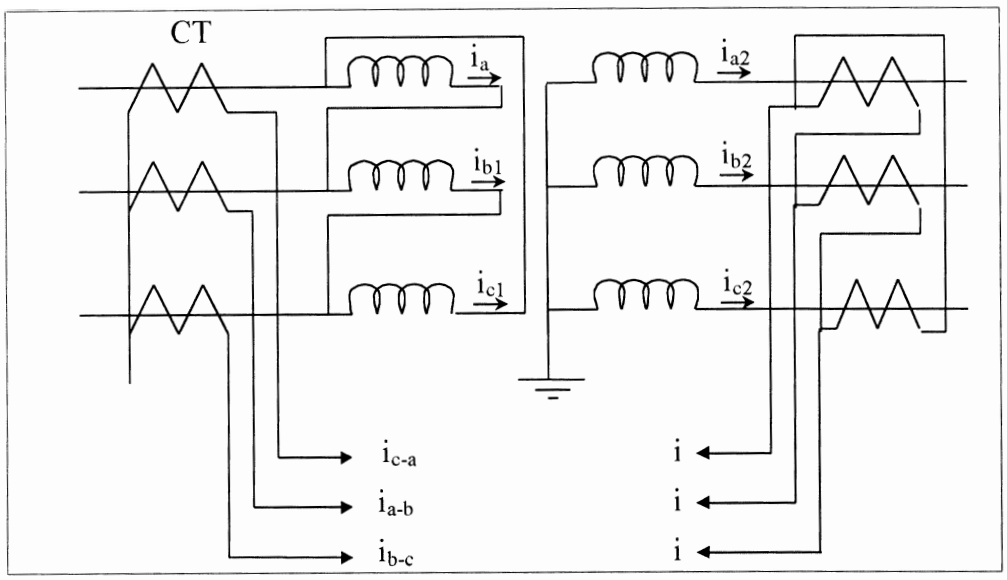

Figure (6- 12): Differential currents phases of a Δ-Y power transformer.

Substituting equation (6-61) in (6-60) we get,

$$V_{ab_{(n)}} = 2\frac{L_1}{T}\left[i_{(a-b)_{(n)}}\right] + 2\frac{L_2}{T}\left[i_{B_{(n)}}\right] - 2\frac{L_1}{T}\left[i_{(a-b)_{(n)}}\right] - 2\frac{L_2}{T}\left[i_{B_{(n)}}\right] + \left[V_{(a-b)_{(n)}}\right] + \left[V_{(a-b)_{(n)}}\right] - V_{ab_{(n-1)}} \quad \text{..... (6-63)}$$

The last equation uses the quantities, which are possible to collect. The same checking method to detect internal fault cases of the previous algorithm is used.

The most limitation of both those algorithms is that it can not detect all types of internal faults. For many internal fault types where the fault occurs at the end of one winding to earth, the both sides of equations (6-57) or (6-63) will be nearly equal and the restraining takes place instead of tripping is expected. In addition, the methods require both sides voltages, the matter which is costly to be satisfied practically.

6-3-C-3: DIGITAL ALGORITHM BASED ON THE INVERSE SHUNT INDUCTANCE OF THE TRANSFORMER

The Japanese introduced an algorithm which depends the behavior of what the called, the inverse shunt inductance of the transformer [6.29]. For a three-winding transformer that can be expressed as a six-terminal circuit, the following admittance equation can be obtained,

$$\begin{bmatrix} i_1 \\ i_2 \\ i_3 \end{bmatrix} = \begin{bmatrix} Y_{11} & Y_2 & Y_3 \\ Y_1 & Y_{22} & Y_3 \\ Y_1 & Y_2 & Y_{33} \end{bmatrix} \cdot \begin{bmatrix} \int v_1\, dt \\ \int v_2\, dt \\ \int v_3\, dt \end{bmatrix} \quad \text{..... (6-64)}$$

where,

i_1, i_2, and i_3 : are the primary, secondary and tertiary windings phase currents respectively.

V_1, V_2 , and V_3 : are the primary, secondary and tertiary windings phase voltages respectively.

Y_1, Y_2, and Y_3: are the primary, secondary and tertiary windings phase leakage admittance respectively.

Y_{11}, Y_{22}, and Y_{33}: are admittance calculated as,

$$Y_{11} = \frac{i_1 - \left(Y_2 \int V_2\, dt + Y_3 \int V_3\, dt\right)}{\int V_1\, dt}$$

$$Y_{22} = \frac{i_1 - \left(Y_1 \int V_1\, dt + Y_3 \int V_3\, dt\right)}{\int V_2\, dt} \quad \text{..... (6-65)}$$

$$Y_{33} = \frac{i_1 - \left(Y_1 \int V_1\, dt + Y_2 \int V_2\, dt\right)}{\int V_3\, dt}$$

The proposed shunt inverse inductance of the transformer windings are defined as,

$$\begin{aligned} Y_{01} &= Y_{11} + Y_2 + Y_3 \\ Y_{02} &= Y_{22} + Y_1 + Y_3 \\ Y_{03} &= Y_{33} + Y_1 + Y_2 \end{aligned} \quad \text{..... (6-66)}$$

It has been found that the values of the shunt inverse inductance of the transformer windings during internal fault cases are different from those during magnetizing inrush current cases. This has been taken to indicate internal fault cases. Tripping takes place if one of the following conditions comes true,

$$Y_{30} \leq 2 \text{ p.u.}$$
$$Y_{10} \leq 2 \text{ p.u.} \qquad \text{..... (6-67)}$$

The most limitation of this algorithm still its dependence on phase quantities of currents and voltages of all sides including the tertiary windings, which can not be achieved practically for all types of transformer.

6-3-C-4: DIGITAL ALGORITHM BASED ON THE ESTIMATED MAGNETIZING INDUCTANCES

The differential current waveforms of a three-phase Δ–Y power transformer are shown in figure (6-13). Studying those waveforms carefully, we can see that the magnetizing inrush currents have always, and each period, a comparatively long time span during which both the differential current and its first derivative are close to zero.

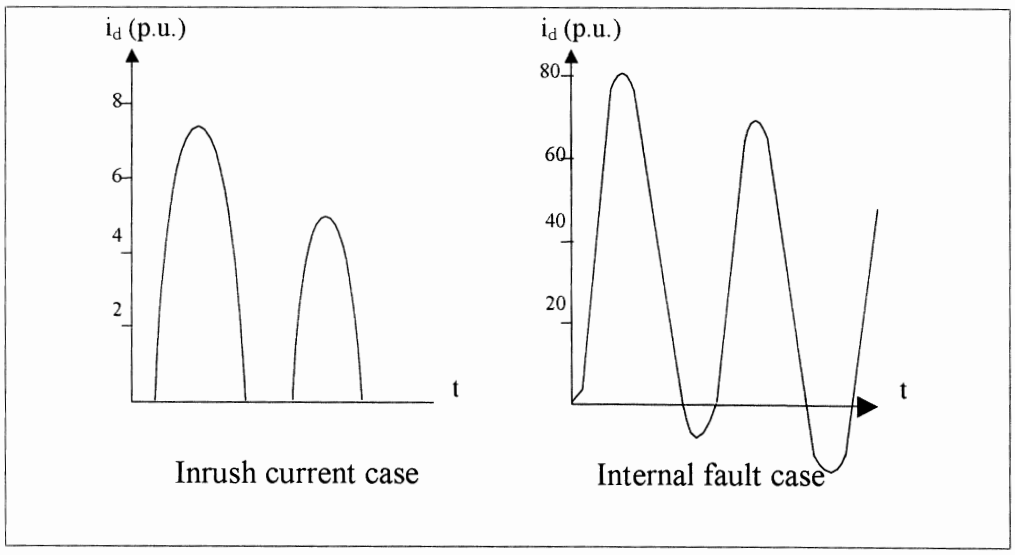

Figure (6- 13): Typical differential current waveforms.

This time span is not less than 1/6 of the cycle. Anyhow, those time spans do not exit in the internal faults differential currents, only and only if the magnetizing inductance of the current transformer has a low value close to zero. The non-linear nature of the transformer core magnetizing inductance stands behind that phenomenon. In magnetizing inrush current cases and during those times spans, the magnetizing inductances are of high values compared with their values during other times and during internal faults cases. This variation in the magnetizing inductance has been taken as an indicator to distinguish between internal faults and magnetizing current cases [6.30].

In this algorithm, each phase of the transformer differential current phases is modeled as a series R-L circuit, as shown in figure (6-14). The following equation can then be proposed for phase (a);

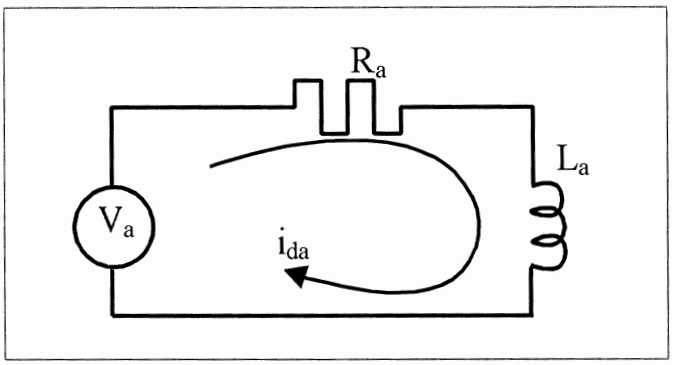

Figure (6- 14): Estimated R-L series circuit of a differential current.

$$V_a = R_a \cdot i_{da} + L_a \frac{d i_{da}}{d t}$$

or,

$$V_a = i_{da} \cdot R_a + L_a \cdot s i_{da} \qquad \text{..... (6-68)}$$

where;
s : is the symbol of differentiation.
V_a : is a voltage signal convenient to i_{da}.
i_{da} :is the phase(a) of the differential current phases .
L_a and R_a :are the non-linear inductance and resistance related to i_{da} and V_a.

Integrating the last differential equation, we get an expression to calculate the term (L). The values of (L) and hence its behavior, and of all differential current phases, are taken as the indicator to distinguish between internal fault and magnetizing current cases [6.30].

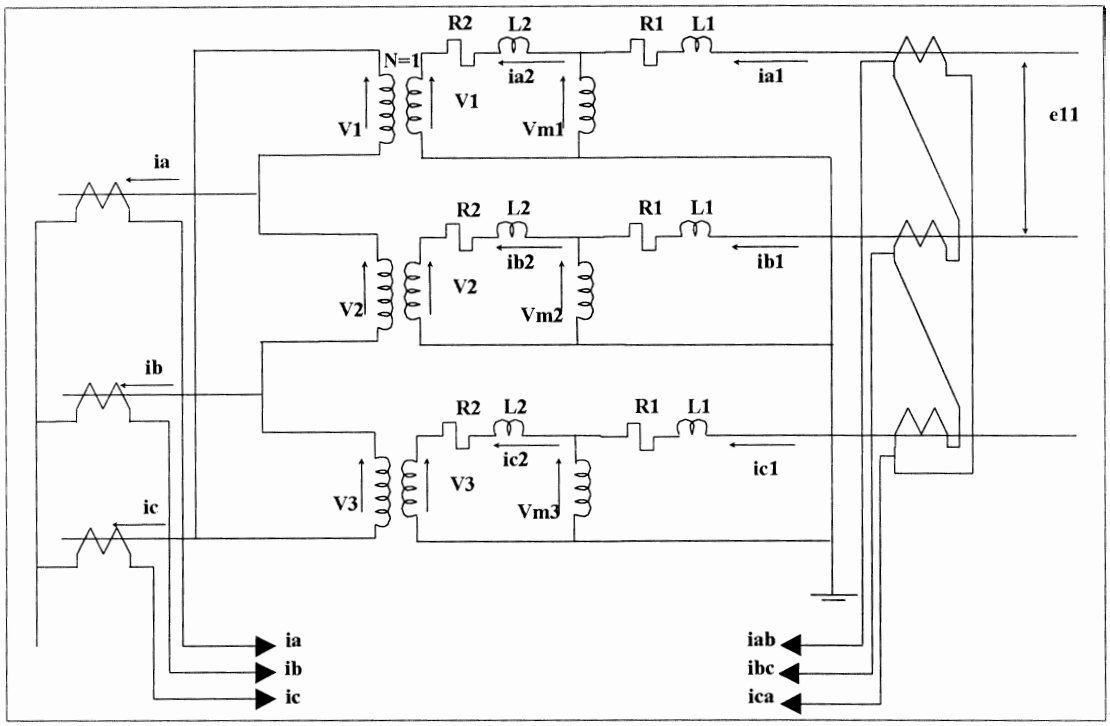

Figure (6- 15): Delta-Star power transformer equivalent circuit.

To define the proper voltage signals, which correspond to the differential currents phases, a Δ–Y connected power transformer equivalent circuit shown in figure (6-15), is analyzed. This circuit is selected, as it represents all the transformer connection performances. This equivalent circuit represents the transformer under switching-on case. The same circuit can be applied for internal fault cases replacing the magnetizing branch inductances with the corresponding fault impedances. The following must be define to analyze the equivalent circuit of figure (6-15) ;

L_1 and R_1: are the star side phase winding inductance and resistance respectively.

L_2 and R_2: are the delta side phase winding inductance and resistance respectively referred to the star side.

V_{m1}: is the voltage drop across phase (a) magnetizing branch inductances.

i_{m1} : is the magnetizing current of phase(a) of magnetizing branch inductances .

e_{11} : is the star side, phase (a) to phase (b) voltage. In another word, it is phase (a) of the line voltage at star side.

V_1: is the delta side phase (a) voltage referred to the star side.

The following considerations are taken in this analysis;

$$\begin{aligned} i_{ab} &= i_{a1} - i_{b1} \\ i_{bc} &= i_{b1} - i_{c1} \\ i_{ca} &= i_{c1} - i_{a1} \end{aligned} \qquad \text{..... (6-69)}$$

$$\begin{aligned} i_{a} &= i_{a2} - i_{b2} \\ i_{b} &= i_{b2} - i_{c2} \\ i_{c} &= i_{c2} - i_{a2} \end{aligned} \qquad \text{..... (6-70)}$$

The differential current phases i_{da}, i_{db}, and i_{dc} are calculated as the subtraction of the loading side current transformer's currents from the feeding side current transformer's currents. If the delta side is taken as the feeding side then;

$$\begin{aligned} i_{da} &= i_{a} - i_{ab} \\ i_{db} &= i_{b} - i_{bc} \\ i_{dc} &= i_{c} - i_{ca} \end{aligned} \qquad \text{..... (6-71)}$$

The through current phases i_{tha} , i_{thb} , and i_{thc} are calculated as the sum of the current transformer's currents coming from both sides ;

$$\begin{aligned} i_{tha} &= i_{a} + i_{ab} \\ i_{thb} &= i_{b} + i_{bc} \\ i_{thc} &= i_{c} + i_{ca} \end{aligned} \qquad \text{..... (6-72)}$$

The transformer is analyzed as it is fed from the delta side. The analysis is taken for one phase of the differential current phases and similar analysis can be applied for the other phases. Similar procedure can be followed if transformer is fed from the star side.

From the equivalent circuit of figure (6-15) , the phase voltages (V_1) and (V_2) at the delta side are expressed as ;

$$V_1 = V_{m1} + i_{a2} \cdot R_2 + s i_{a2} \cdot L_2 \quad \text{..... (6-73)}$$

$$V_2 = V_{m2} + i_{b2} \cdot R_2 + s i_{b2} \cdot L_2 \quad \text{..... (6-74)}$$

where ; (s) is the symbol of differentiation . The difference between those phase voltages is taken as;

$$V_1 - V_2 = V_{m1} - V_{m2} + (i_{a2} - i_{b2}) \cdot R_2 + s(i_{a2} - i_{b2}) \cdot L_2 \quad \text{..... (6-75)}$$

The differential (i_{da}) and through (i_{tha}) phase currents, which are related to phases (a) and (b), can be expressed respectively as;

$$i_{da} = (i_{a2} - i_{b2}) - (i_{a1} - i_{b1}) = i_{m1} - i_{m2} \quad \text{..... (6-76)}$$

$$i_{tha} = (i_{a2} - i_{b2}) + (i_{a1} - i_{b1}) \quad \text{..... (6-77)}$$

then;

$$\frac{i_{da} + i_{tha}}{2} = (i_{a2} - i_{b2}) \quad \text{..... (6-78)}$$

substituting the last equation in equation (6-75) we get ;

$$V_1 - V_2 = V_{m1} - V_{m2} + (i_{da} + i_{tha}) \frac{R_2}{2} + s(i_{da} + i_{tha}) \frac{L_2}{2} \quad \text{..... (6-79)}$$

The voltages V_{m1} and V_{m2} can be expressed as;

$$V_{m1} = \frac{d\Phi_1}{dt}$$

$$V_{m2} = \frac{d\Phi_2}{dt} \qquad \text{..... (6-80)}$$

where ; ϕ_1 and ϕ_2 are the core fluxes in branches (a) and (b) respectively . Hence,

$$V_{m1} - V_{m2} = \frac{d\Phi_1}{dt} - \frac{d\Phi_2}{dt} = \frac{d(\Phi_1 - \Phi_2)}{dt} \qquad \text{..... (6-81)}$$

The last equation remains unchanged if we multiply the right side by $d(i_{m1} - i_{m2})/d(i_{m1} - i_{m2})$ and it becomes;

$$V_{m1} - V_{m2} = \frac{d(\Phi_1 - \Phi_2)}{dt} \cdot \frac{d(i_{m1} - i_{m2})}{d(i_{m1} - i_{m2})} = \frac{d(i_{m1} - i_{m2})}{dt} \cdot \frac{d(\Phi_1 - \Phi_2)}{d(i_{m1} - i_{m2})} \qquad \text{..... (6-82)}$$

The term $[d(\Phi_1 - \Phi_2)/d(i_{m1} - i_{m2})]$ in equation (6-82) gives an expression of magnetizing inductance related to magnetizing branches of phase (a) and phase (b) of the transformer. In other meaning, it is related to phase (a) of the differential currents phases. That inductance has been defined as the estimated inductance (L_e) [6.30]. For phase (a) of the differential currents phases (i.e. i_{da}), the estimated inductance will be (L_{ea}). Making use of equation (6-76), the last equation can be modified to;

$$V_{m1} - V_{m2} = \frac{d i_{da}}{dt} \cdot L_{ea} \qquad \text{..... (6-83)}$$

Substituting equation (6-83) in equation (6-75) and rearranging the terms, we get;

$$V_1 - V_2 - \frac{R_2}{2} \cdot i_{tha} - s i_{tha} \cdot \frac{L_2}{2} = V_a = \frac{R_2}{2} \cdot i_{da} + s i_{da} \cdot \left(\frac{L_2}{2} + L_{ea} \right) \quad \text{.. (6-84)}$$

The last equation is nothing but equation (6-68) in which;

$$R_a = \frac{R_2}{2}$$

$$L_a = \frac{L_2}{2} + L_{ea}$$

$$V_a = V_1 - V_2 - C_a$$

where (C_a) is the correction voltage of phase (a) of the differential current phases. For the n_{th} phase and feeding the transformer from the delta side;

$$C_n = i_{thn} \frac{R_2}{2} + s i_{thn} \cdot \frac{L_2}{2} \quad \text{..... (6-85)}$$

Taking phase (a) of the differential current phases and integrating equation (6-84) using the trapezoidal method of integration, we get ;

$$V_{a(n)} + V_{a(n-1)} = E_{a(n)} + E_{a(n-1)} - i_{tha(n)} \cdot M_1 - i_{tha(n-1)} \cdot M_2 \quad \text{..... (6-86)}$$

where ;

n : is of the n_{th} sample.

$$E_a = V_1 - V_2$$

$$M_1 = \frac{R}{2} + \frac{L}{T}$$

$$M_2 = \frac{R}{2} - \frac{L}{T}$$

T: is the sampling time.

From equation (6-84), a digital expression to calculate the estimated inductance of phase (a) is derived as [6.30],

$$L_{ea(n)} = \frac{T}{2} \cdot \frac{\left(E_{a(n)} + E_{a(n-1)} \right) - M_1 \cdot i_{da(n)} - M_2 \cdot i_{da(n-1)}}{i_{da(n)} + i_{da(n-1)}} \quad \text{..... (6-87)}$$

The last equation describes the procedure of computing the estimated inductance value of the n_{th} sample of phase (a) of the differential current phases, using the measured samples of the differential currents, its related through currents, and its corresponding voltage signal sampling. All those quantities are practically available.

Figure (6-16) shows typical results of the absolute values of the estimated inductance (L_e) calculated using equation (6-87) and under many types of power transformer operation, with and without current transformer's saturation. From the figures, we can conclude the following;

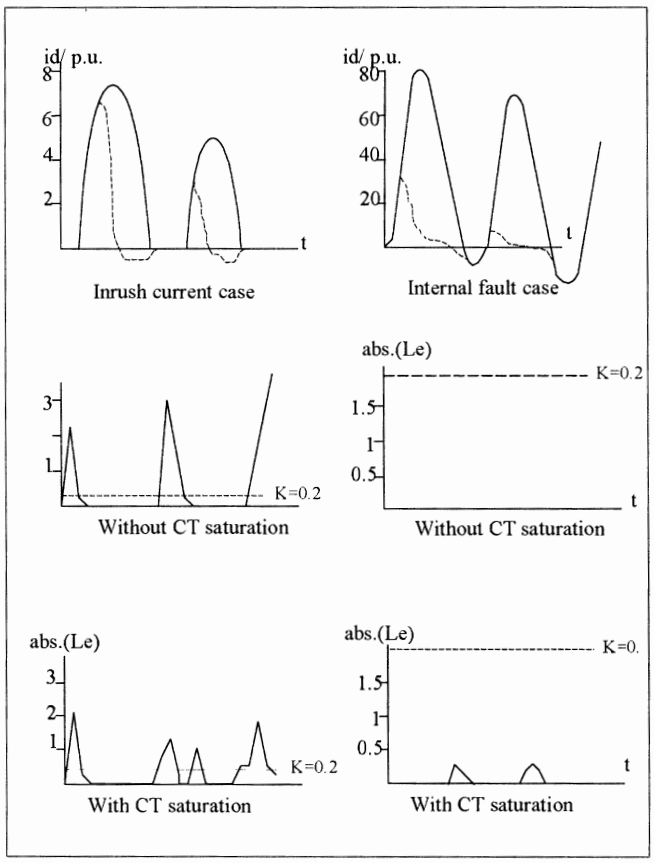

Figure (6- 16): Typical results of Le calculations during internal fault and magnetizing inrush current cases, with (—) and without (...) CT saturation.

1. L_e and during magnetizing inrush current and overexcitation cases, shows a great variation in magnitude. It shows high values during those time spans, in which both the differential currents and

their first derivatives are of low values close to zero, while it shows low values other times.

2. During internal fault cases, L_e shows low values close to zero and it is in general of constant values compared to the previous case.
3. Current transformer's saturation has no effect on the previous conclusions.

From the last conclusions, an algorithm for power transformer protection has been designed, based on the estimated inductances values and behavior [6.30].

In this algorithm, the values of (Le) are calculated just at the time of initiation of an internal abnormal case and in all phases, and then checked. The detected internal abnormal cases could be an internal fault, a magnetizing inrush current, or an overexcitation case.

Anyhow, we have to bear in mind that, recording the exact time of internal abnormal cases initiation which is necessary to begin the calculations of L_e, can not be achieved depending on differential current samples only. Using terminals voltage signals, we can detect the instant at which the abnormal case is initiated. A special technique is used to compare the feeding side line voltage signal's samples with their samples one cycle before, has been proposed [6.30]. In this technique the following condition is checked,

$$|E_a(n) - E_a(n-N)| > 0.01\, V_r \qquad \text{..... (6-88)}$$

where,

E_a: is the phase (a) of the line voltages measured at the feeding side.

N: is the number of samples per a cycle.

n : indicates the n_{th} sample.

V_r: is the rated voltage of the transformer.

If in any sample, the above condition is achieved into at lest two phases, a voltage difference is detected.

No calculations will take place until the percentage differential protection technique will indicate an internal abnormal case, so that

external fault cases are neglected. If the case is indicated as an internal case, the algorithm starts calculate (L_e) of all phases using the sample at which the voltage difference are detected and one sample after. The following conditions will be checked;

1- CONDITION No.1:

The low absolute values of the estimated inductance (L_e) in all phases, will indicate an internal faults case;

$$\begin{bmatrix} \text{IF} & |L_{ea}| < K \\ \text{AND} & |L_{eb}| < K \\ \text{AND} & |L_{ec}| < K \end{bmatrix} \Rightarrow \text{TRIP} \qquad \ldots\ldots\ldots\ldots\ldots\ldots\ldots\ldots \text{(6-89)}$$

2- CONDITION No.2:

IF the last condition is not achieved, then the test has to be completed for the reset of the cycle to indicate the behavior of the obsolete values of (L_e) in all the phases. If the condition [$|L_e| > K$] is achieved in one cycle for consecutive two samples of the differential currents and at least in two phases of the differential current phases, the case is considered as a magnetizing current case and RESET takes place,

$$\text{IF} \begin{bmatrix} L_{ea} > K \quad \text{AND} \quad L_{eb} > K \\ (\text{in one cycle and in two consecutive samples}) \end{bmatrix} \Rightarrow \text{RESET}$$

$$\text{OR} \begin{bmatrix} L_{eb} > K \quad \text{AND} \quad L_{ec} > K \\ (\text{in one cycle and in two consecutive samples}) \end{bmatrix} \Rightarrow \text{RESET} \qquad \ldots\ldots\ldots \text{(6-90)}$$

$$\text{OR} \begin{bmatrix} L_{ec} > K \quad \text{AND} \quad L_{ea} > K \\ (\text{in one cycle and in two consecutive samples}) \end{bmatrix} \Rightarrow \text{RESET}$$

Otherwise, TRIP takes place due to internal fault case.

The factor (K) in the last conditions are defined as the expected value of the inductance due to the transformer rated voltage and the minimum differential setting current (i_p) (i.e. defined in section 6-2)

enough to initiate the percentage differential protection technique to operate;

$$K = \frac{V_{rated}}{\omega \cdot i_p} \qquad \text{(6-91)}$$

where ;

V_{rated}: is the transformer feeding side rated phase voltage.

ω : is system fundamental angular frequency .

i_p : is the minimum threshold current.

The algorithm's tests (i.e., typical results shown in figure 6-16 with K=0.2) show that it is of high speed (i.e. (1/6 of the cycle) to detect most of internal fault cases. Other limited cases have been tripped within less than one cycle. The algorithm resets for all other cases successfully. Current transformers saturation has no effect on the algorithm doing [6.30].

REFERENCES

(6.1) G. D. ROCKEFELLER, " FAULT PROTECTION WITH A DIGITAL COMPUTER", IEEE TRANS. ON PAS VOL. PAS-88, NO. 4, APRIL 1969, PP. 434-464.

(6.2) J. A. SYKES, AND I. F. MORRISON, " A PROPOSED METHODE OF HARMONIC RESTRAINT DIFFERENTIAL PROTECTION OF TRANSFORMERS BY DIGITAL COMPUTER", IEEE, TRANS. ON PAS, VOL. PAS-91, 1972, PP. 1266-1273.

(6.3) C. H. ENVALL, AND J. R. LINDERS, " A THREE-PHASE DIFFERENTIAL RELAY FOR TRANSFORMER PROTECTION", IEEE TRANS. ON PAS, VOL. PAS-94, NO. 6, NOV. /DEC. 1975, PP. 1971-1980.

(6.4) R. R. LARESON, A. T. FLECHSIG, AND E. O. SCHWEITZER, " THE DESIGN AND TEST OF A DIGITAL RELAY FOR TRANSFORMER PROTECTION", IEEE TRANS. ON PAS, VOL. PAS-98, NO. 3, MAY/JUNE 1979, PP. 795-803.

(6.5) M. ILAR, BADEN, "A NEW TRANSFORMER DIFFERENTIAL RELAY PILOT WIRE RELAY FROM BROWN BOVERI", REV., 2-1981, PP. 70-78.

(6.6) M. A. RAHMAN, AND P. K. DASH, "FAST ALGORITHM FOR DIGITAL PROTECTION OF POWER TRANSFORMER, IEE PROC., VOL. 129, PT. C, NO. 2, MARCH 1982, PP. 79-85.

(6.7) M. A. RAHMAN, P. K. DASH, AND E. R. DOWNTON, "DIGITAL PROTECTION OF POWER TRANSFORMER BASED ON WEIGHTED LEAST SEQUARE ALGORITHM", IEEE, TRANS. ON PAS, VOL. PAS-101, NO. 11, NOV. 1982, PP. 4204-4209.

(6.8) J. S. THORP, AND A. G. PHADKE, "A MICROPROCESSOR BASED THREE-PHASE TRANSFORMER DIFFERENTIAL RELAY", IEEE, TRANS. ON PAS, VOL. PAS-101, NO. 2, FEB. 1982, PP. 426-432.

(6.9) J. S. THORP, AND A. G. PHADKE, "A NEW COMPUTER-BASED FLUX-RESTRAINT CURRENT-DIFFERENTIAL RELAY FOR POWER TRANSFORMER PROTECTION", IEEE TRANS. ON PAS, VOL. PAS-102, NO. 11, NOV. 1983, PP. 3624-3629.

(6.10) A. WISZNIEWSKI, " DIGITAL ALGORITHM FOR DIFFERENTIAL PROTECTION OF POWER TRANSFORMERS", NINTH SYSTEM COMPUTATION CONFERENCE. CASAIS, PORTUGAL, 30 AUG. – 4 SEPT. 1987, PROC. PP. 725-731.

(6.11) Y. MURTY, AND W. J. SMOLINSKI, "DESIGN AND IMPLEMENTATION OF A DIGITAL DIFFERENTIAL RELAY FOR A THREE-PHASE POWER TRANSFORMER BASED ON KALMAN FILTERING THEORY", IEEE, TRANS. ON POWER ELIVRY, VOL. 3, NO. 2, APRIL 1988, PP. 525-533.

(6.12) M. A. RAHMAN, AND B. JEYASURYA, "A STATE-OF-THE ART REVIEW OF TRANSFORMER PROTECTION ALGORITHM", IEEE, TRANS. ON POWER ELIVRY, VOL. 3, NO. 2, APRIL 1988, PP. 534-544.

(6.13) Y. MURTY, W. J. SMOLINSKI, AND S. SIVAKUMAR, " DESIGN OF A DIGITAL PROTECTION SCHEME FOR POWER TRANSFORMER USING OPTIMAL STATE OBSERVERS", IEE PROC. VOL. 135, PT. C. NO. 3, MAY 1988, PP. 224-230.

(6.14) YESRI Z. MOHAMMED, " VOLTAGES AS SUPPLEMENTARY SIGNALS IN POWER TRANSFORMER PROTECTION", SECOND INTER. SIMPOSIOM ON POWER SYSTEM ENGINEERING, WROCLAW, POLAND, JAN. 1989.

(6.15) P. MUDDITT, AND R. NIVEN, " DEVELOPMENTS IN TRANSFORMER PROTECTION", FOURTH INTER. CONF. ON DEVELOPMENTS IN POWER SYSTEM PROTECTION, UNIVERSITY OF EDINDURGH, U.K., APRIL 1989, PP. 61-65.

(6.16) M. MIKRUT, W. WINKLER, AND B. WITEK, " PERFORMANCE OF DIFFERENTIAL PROTECTION FOR THREE-WINDING POWER TRANSFORMERS DURING TRANSIENT CURRENT TRANSFORMERS SATURATION", ", FOURTH INTER. CONF. ON DEVELOPMENTS IN POWER SYSTEM PROTECTION, UNIVERSITY OF EDINDURGH, U.K., APRIL 1989, PP. 66-69.

(6.17) T. S. SIDHU, M. S. SACHEV, AND H. C. WOOD, "DETECTING TRANSFORMER WINDING FAULTS USING NON-LINEAR MODELS OF TRANSFORMERS", ", FOURTH INTER. CONF. ON DEVELOPMENTS IN POWER SYSTEM PROTECTION, UNIVERSITY OF EDINDURGH, U.K., APRIL 1989, PP. 70-74.

(6.18) B. GRCAR, D. DOLINAR, J. RITOJA, AND J. PIHLER, "SYSTEM ANALYSIS OF DIGITAL DIFFERENTIAL POWER TRANSFORMER PROTECTION", ", FOURTH INTER. CONF. ON DEVELOPMENTS IN POWER SYSTEM PROTECTION, UNIVERSITY OF EDINDURGH, U.K., APRIL 1989, PP. 220-224.

(6.19) P. LING AND A. BASAK, " A NEW DETECTION SCHEME FOR REALISATION OF MAGNETIZING INRUSH CURRENT IN TRANSFORMERS", FOURTH INTER. CONF. ON DEVELOPMENTS IN POWER SYSTEM PROTECTION, UNIVERSITY OF EDINDURGH, U.K., APRIL 1989, PP. 239-243.

(6.20) E. BADAWY, A. IBRAHIM, AND G. GIRGIS, "A NEW COMPUTER-BASED DIFFERENTIAL RELAY FOR POWER TRANSFORMER PROTECTION", 21ST UNIVERSITIES POWER ENGINEERING CONFERENCE, LONDON, U.K., 1986.

(6.21) B. DAKERS, "REYROLLE PROTECTION", POWER SYSTEM PROTECTION MANUAL, 1982.

(6.22) " DIGITAL PROTECTION TECHNIQUES AND SUBSTATIONS FUNCTIONS", REPORT BY WORKING GROUP 34.01 OF STUDY COMMITTEE 34, CIGRE, 16 MAY 1989.

(6.23) A. R. WARRIGTON, " PROTECTIVE RELAYS THEIR THEORY AND PRACTICE", BOOK, VOL. 1, CHAPMAN AND HALL, 1962.

(6.24) "POWER SYSTEM PROTECTION ", BOOK EDIT BY THE ELECTRICITY COUNCIL, VOL. 3, MCDONALDS, LONDON, 1969.

(6.25) A. C. FRANKLIN, " THE J AND P TRANSFORMER BOOK", BOOK, 11TH EDITION, BUTTERWORTHS, 1983.

(6.26) B. JEYASURYA, AND M. A. RAHMAN, " APPLICATION OF WALSH FUNCTIONS FOR MICROPROCESSOR-BASED TRANSFORMER PROTECTION", IEEE TRANS. ON ELECTROMAGNETIC COMPATABILITY, VOL. EMC-27, NO. 4, NOV. 1985, PP. 221-225.

(6.27) D. B. FAKRUDDIN, K. PARTHASARATHY, L. JENKINS, AND B. W. HOGG, " APPLICATION OF HAAR FUNCTIONS FOR TRANSMISSION LINE AND TRANSFORMER DIFFERENTAIL PROTECTION", ELECTRICITY POWER AND ENERGY SYSTEMS, VOL. 6, NO. 3, JULY 1984, PP. 169-180.

(6.28) W. WINKLER, Z. DAWID, AND P. SOWA, "INTERFERENCE OF HARMINICS IN DIFFERENTIAL PROTECTION SCHEMES CAUSED BY SATURATED CURRENT TRANSFORMERS", PROC. OF THE 21ST UPEC, IMPERIAL COLLEDGE, LONDON, 1986, PP. 146-149.

(6.29) K. INAGKI, M. HIGAKI, Y. MATSUI, K. KURITA, M. SUZUKI, K. YOSHIDA, AND T. MAEDA, " DIGITAL PROTECTION FOR POWER TRANSFORMERS BASED ON AN EQUIVALENT CIRCUIT COMPOSED OF INVERSE INDUCTANCE", IEEE TRANS. ON POWER DELIVARY, VOL. 3, NO.4, OCT. 1988.

(6.30) YESRI Z. MOHAMMAD, "NEW HIGH SPEED DIGITAL ALGORITHM FOR POWER TRANSFORMER PROTECTION"; ARAB CIGRE' 97; AMMAN; JORDAN; MAY 12-14, 1997.